

# Annals of the National Academy of Medical Sciences (India)



Volume 54, No. 4  
Oct-Dec, 2018  
ISSN 0379 - 038X (Print)  
ISSN 2454-5635 (Online)



# **Annals of the National Academy of Medical Sciences (India)**

-: A Quarterly Journal:-

## ***Editor-in-Chief***

Dr. Sanjeev Misra

## ***Associate Editors***

Dr. Kuldeep Singh  
Dr. K. K. Sharma  
Dr. Deep N. Srivastava

## **Editorial Board**

Dr. A.K. Jain	Dr. Ashish Wakhlu
Dr. Ashok Kumar Saxena	Dr. Gopal Nath
Dr. K.K. Deepak	Dr. M.V. Padma Srivastava
Dr. Pankaj Bhardwaj	Dr. Piyush Gupta
Dr. Praveen Sharma	Dr. R. Goswami
Dr. R.K. Chadda	Dr. Raj Kumar
Dr. Rajesh Kumar	Dr. Rajesh Malhotra
Dr. Sanjay Wadhwa	Dr. S.S. Yadav
Dr. Siddhartha Datta Gupta	Dr.(Ms) U.M. Thatte

## **Advisory Board**

Dr. B.K. Jain	Dr. C. Adithan
Dr. Jagat Ram	Dr. Kamal Buckshee
Dr.(Mrs.) Krishana Garg	Dr. Mukund S. Joshi
Dr. N.R. Jagannathan	Dr. P.K. Dave
Dr. Pratibha Singh	Dr. Prema Ramachandran
Dr. Randeep Guleria	Dr. Shridhar Dwivedi
Dr. Shridhar Sharma	Dr. Snehalata Deshmukh
Dr. T.D. Chugh	Dr. Yogesh K. Chawla

## ***International Advisor***

Dr. M.S. Boparai  
Dr. Soumya Swaminathan

## ***Emeritus Editor: Prof. J. S. Bajaj***

### **Annual Subscription Rates**

Inland	Rs. 1500.00
Foreign	\$ 40.00
	£ 30.00
	€ 30.00
Single Copy	Rs. 500.00

### **Correspondence**

*All correspondence concerning the Journal should be addressed to:*

#### **Honorary Secretary**

National Academy of Medical Sciences (India)  
NAMS House, Ansari Nagar,  
Mahatma Gandhi Marg, New Delhi- 110029  
Tel.: 011-26589289 Email: nams\_aca@yahoo.com  
Website: www.nams-india.in

## **ANAMS 54(4): 179-244, 2018**

### **CONTENTS**

Editorial <i>Dr. Kuldeep Singh, Dr. Sanjeev Misra</i>	i
The Current Status of Prostate Cancer <i>Mukund S. Joshi</i>	179
Role of Adipokines in Development of Metabolic Syndrome <i>Vani Gupta</i>	194
Anthropometric Study of Proximal Femur Geometry and Its Clinical Application <i>Ramchander Siwach</i>	203
Molecular and Functional Basis of Cystic Fibrosis in Indian Patients: Genetic, Diagnostic and Therapeutic Implications <i>Rajendra Prasad</i>	216
Phagocytes and the Leishmania Parasite: A Marriage of Convenience <i>Mitali Chatterjee</i>	231

## ***Editorial***

### **Ensuring Healthy Community: Tapping them Young**

It is a saying that “Health is Wealth” and no matter how much wealth one has, it loses its significance if one is not healthy enough to enjoy it. There are wide individual variations regarding health-seeking behaviors. With the launch of National Health Mission, it has been observed that the availability of facilities nearby has encouraged residents especially to avail those facilities which will result in minimization of transportation cost. Literacy and health status has a strong correlation with facilities effective utilization but varies on a regional scale with Kerala still at the top (1). While studying various health-seeking behaviors among pregnant women, Das and Sarkar found that doctors and para-medical staff were only consulted during complications. Lack of access to health care and pregnancy-related health information led their study participants to rely heavily on information and misconceptions about pregnancy gathered from elder women, friends, and mothers-in-law and husbands (2).

Children usually spend on an average 6-8 hours of a day in a school. Schools have a great responsibility in shaping their habits and healthy behavior apart from scholastics development. School educators are now concerned more than ever on observing marked lifestyle changes among children especially teenagers. Personal communication from a teacher revealed decreased activity among children to the extent that they demand to pick up vehicle to be at their doorsteps. Smartphone overuse is another concern resulting in poor concentration and sleepiness in classes. The good thing coming from schools is optimism and openness to change these attitudes through innovations towards positive behaviors. Policy changes like Right to Education (RTE) in 2009 have enhanced literacy levels for marginalized children, but they still lag behind educational goals. Both recognized (Government and Private) and unrecognized Alternative schools (owned by people showing passion for teaching) are willing to comply with the RTE Act. Unrecognized schools face challenges of closure and quality of education (3). The disadvantaged population prefers these schools because of proximity to their home or workplace and much lower fees than that charged by private schools. However, continuity of education for higher grades is harder since these schools are unable to provide Migration Certificates. Various NGOs and independent researchers have raised the plight of these schools at the various platform.

Adolescent health education issues have been discussed widely in the medical literature (4). The most important indicator of the health of a country is the Infant Mortality Rate (IMR). India has achieved a marked decline in IMR in the last few decades, but reduction below 30 is still a distant dream. The significant portion of IMR is due to Neonatal and Perinatal deaths. Improved neonatal and obstetric services have decelerated neonatal deaths, but a further reduction is highly dependent on maternal health and socio-cultural factors. There are still gaps in nutritional problems among pregnant women and adolescent girls despite various health programs. The health of both women and men is essential for reproductive health. Health care is sought only once a woman is pregnant. However, once pregnant it becomes too late for health interventions that should be initiated much before. Adolescent health education is one such initiative to improve the overall health of the community. Though results will not be immediately available but considering the synergistic effect with improving secular trends of education, such interventions are expected to have very high long term impact. Research from the West about reproductive health have shown favorable time trend results compared to a study in 2001 (5).

It has also been shown that children are more receptive to ideas and they can be molded readily into a persona society needs. For example, Tragler had shown that giving information about nutrition,

hygiene, immunization to children between 12-16 years not only leads to increased awareness but casts away misconceptions (6). Children can also be a carrier for changes in transmitting the current health information to their parents (7). Joyful methods are the most cost-effective in bringing about desired knowledge and behavior changes (8).

Howsoever easy it may sound but is not without challenges. An American study found that integrating health education efforts within core curricula classes can lead to favorable outcomes. However, it also cautioned that implementation barriers must be actively addressed by schools and program developers to improve program fidelity and maximize the sustainability of program gains (9). The challenge becomes enormous in the present era where parental- student focus moves towards demanding competitive examinations heavily reliant on cognitive skills as a student moves to 9<sup>th</sup> grade. In such a situation it will be determined mainly by the ingenuity of the teachers to incorporate such programs in their routine school schedule.

The role of physicians, curriculum planners, developmental pediatrician, educationists to come together to plan and implement an innovative health program, without compromising the school schedule, is need of the hour. This is the most crucial step. Many times teachers do have creative ideas to experiment with the students. However, rigidity of the schedule, regulatory issues and fear of controversy with some sensitive information often hold them back. The developmental pediatrician and educationists will be the best guide for preparing developmentally appropriate educational program coupled with scientifically proven authentic information from physicians. Teachers' role enhances manifold as they teach, acknowledge, demonstrate, model, provide feedback, encourage, provide assistance, ask questions and give directions to the students.

Though there are many theories behind the human brain and psychological development but most acceptable is that of Erikson's psycho-development theory which spans the whole life of an individual. Out of eight stages of development, stage 4 and five need to be considered while preparing educational activities and modules. Stage 4 focus on industry vs. inferiority where children between ages 5-11 need to cope with new social and academic demands. Success leads to a sense of competence. For a health education program to be effective child should be given the material in chunks and adequate time to be provided for every child to assimilate the information. Stage 5 focus on children between ages 12- 18 years where Teens need to develop a sense of self and personal identity. This adolescent stage is the period of turmoil and is also referred to as a hormonal stage. Significant changes in lifestyle can be implemented at this stage.

Martin and other using standard Cochrane procedure analyzed 18 randomized clinical trials (RCTs) and have shown that school and community-based physical activity interventions as part of obesity prevention or treatment programme can benefit executive functions of children with obesity or overweight specifically (10).

In India, school health promotion has been practiced for many years in the form of health check-ups, school health services, health education and as a life skills initiative. However, only recently it has been recognized to have immense potentials. The many States in India, mostly from the South, have implemented health programs in different forms. The National Health Policy 2017 while relying heavily on Universal Health Coverage emphasized investment and action in school health- by incorporating health education as part of the curriculum, promoting hygiene and safe health practices within the school environs and by acting as a site of primary health care. Taking a cue from the policy, Ministry of Health and Family Welfare (MoHFW) and Ministry of Human Resource Development (MHRD) joined hand under the Honorable Prime Minister Shri Narendra Modi's Ayushman Bharat initiative launched on April 14, 2018, at Bijapur, Chattishgarh to promote School Health Education.

(iii)

They were entrusted with designing a school health program targeting school children and adolescents. The program will integrate various existing initiatives including those by Rashtriya Kishore SwasthyaKaryakram (RKSK) in the Indian context to promote the holistic development of children and a healthy community.

National Academy of Medical Sciences (India) is committed to promoting public health, develop skilled human resources and validate various medical, scientific initiatives with its precious resources of expertise of its distinguished Fellows and young, energetic members. The Academy also felicitate the biomedical scientists in the country through awards, honors, orations at its annual conferences and through the dissemination of high-quality scientific knowledge and skills through Continuing Medical Education, Symposia and Workshops. The Academy supports activities which may assist a wide range of health care professionals to acquire contemporary skills and knowledge to provide the best practice evidence-based healthcare to ensure a healthy community. We wish readers A Happy New Year.

Kuldeep Singh

Sanjeev Misra

## References

1. Jana A, Basu R (2017). Examining the changing health care seeking behavior in the era of health sector reforms in India: evidences from the National Sample Surveys 2004 & 2014. *Glob Health Res Policy* **2**:6.
2. Das A, Sarkar M (2014). Pregnancy-related health information-seeking behaviors among rural pregnant women in India: validating the Wilson model in the Indian context. *Yale J Biol Med* **87**(3):251-262.
3. Sharma K, Ibrar M (2018). Why unrecognised Delhi schools are still trusted. Time of India Feb 10. Accessed at <https://timesofindia.indiatimes.com/home/education/news/why-unrecognised-schools-are-still-trusted/articleshow/62857015.cms>.
4. Sivagurunathan C, Umadevi R, Rama R, Gopalakrishnan S (2015). Adolescent health: present status and its related programmes in India. Are we in the right direction? *J Clin Diagn Res* **9**(3):LE01-LE06.
5. Breuner CC, Mattson G; Committee on Adolescence; Committee on Psychosocial Aspects of Child and Family Health (2016). Sexuality Education for Children and Adolescents. *Pediatrics* **138**(2). pii: e20161348.
6. Tragler A (1991). Health education in school children. *Indian Pediatr* **28**(5):541-544.
7. Bhore PD, Bhore CP, Powar S, Nade AL, Kartikeyan S, Chaturvedi RM (1992). Child-to-parent education: a pilot study. *Indian J Lepr* **64**(1):51-57.
8. Sedighi I, Nouri S, Sadrosadat T, Nemati R, Shahbazi M (2012). Can children enhance their family's health knowledge? An Infectious Disease Prevention Program. *Iran J Pediatr* **22**(4):493-498.
9. Rajan S, Roberts KJ, Guerra L, Pirsch M, Morrell E (2017). Integrating health education in core curriculum classrooms: successes, challenges, and implications for urban middle schools. *J Sch Health* **87**(12):949-957.
10. Martin A, Booth JN, Laird Y, Sproule J, Reilly JJ, Saunders DH (2018). Physical activity, diet and other behavioural interventions for improving cognition and school achievement in children and adolescents with obesity or overweight. *Cochrane Database Syst Rev* **3**:CD009728.

## The Current Status of Prostate Cancer\*

*Mukund S. Joshi*  
President, NAMS

### ABSTRACT

Prostate cancer (PC) is the commonest malignancy in men that causes significant morbidity and mortality. The incidence has quadrupled in the last three decades. This is predominantly due to its increased detection by excellent newer techniques like Prostate-specific antigen (PSA) evaluation, Transrectal ultrasonography (TRUS), Transrectal ultrasound-guided biopsy, Contrast enhanced ultrasound studies, Multiparametric (Mp) MRI (MpMRI) and Nuclear medicine. Its incidence shows a rise in India. With the availability of PSA and trans-rectal biopsy, nowadays the majority of prostate cancers (PC) are diagnosed at an asymptomatic early stage (T1). Most PC are adenocarcinomas while a small percentage are ductal carcinomas, mucinous carcinomas, signet ring cell carcinomas and small cell carcinomas. These variants have poor prognosis.

The anatomy of prostate will help us to further understand the basis of TRUS studies. The whole prostate can be divided into Transition Zone (TZ), Central Zone (CZ) and Peripheral Zone (PZ). This zonal anatomy of prostate is vital to understand the PC, since PC is predominantly seen as follows: TZ – 20%; CZ – 10%; and PZ – 70%.

PSA is an extremely valuable tool in the evaluation of PC. It is exclusively produced by the prostate and to a lesser extent by the seminal vesicles. It is present in all post-pubertal men and absent in women and men following radical prostatectomy. Though the PSA is a vital parameter to detect PC, it can also be elevated in: i) Benign prostrate hypertrophy; ii) Prostate inflammation; iii) Prostatic infarct; iv) Post-digital rectal examination; and v) Sexual activity. The normal value of PSA is 0-4 ng/mL. The two techniques that are available to assess PSA levels are polyclonal assay or monoclonal assay. The monoclonal assay is the most commonly used method the world over. The accepted PSA values are: <4ng/mL (normal); 4.0-10.00ng/mL (borderline) and >10 ng/mL (abnormal). Other than normal PSA values, there are other PSA parameters which are often useful in confirming the diagnosis of PC. These are: i) PSA density; ii) PSA velocity; iii) PSA doubling time; iv) Other markers like PCA3; and v) PC is associated with more protein bound PSA (less free PSA) than in BPH.

**Free PSA (FPSA)** can enhance the specificity of the total PSA value for detection of the PC while reducing the number of unnecessary biopsies.

Another new finding is that of levels of insulin like growth factor binding protein-2 (IGFBP-2) appear to be directly associated with the presence of PC.

---

\*ACADEMY ORATION delivered by Dr. Mukund S. Joshi, President, NAMS (India) during the NAMSCON 2018 held at the Mahatma Gandhi Medical College & Research Institute, Puducherry.

*Correspondence:* Dr. Mukund S. Joshi, 809, Harjivandas Estate, Dr. Ambedkar Road, Dadar, Maharashtra-400014. E-mail: drmukundjoshi@gmail.com.

**Prostate Biopsy:** Ultrasound guided biopsy of the prostate still remains the most important technique for the diagnosis of PC. Different biopsies which are used for diagnosis of PC are: Saturation Biopsy, MRI Guided Biopsy and Fusion Biopsy.

**Use of Gleason Score for grading the PC:** Gleason score is the grading system used to determine the aggressiveness of PC. This grading system can be used to choose appropriate treatment options. The tumour grades provide important information regarding how fast the cancer is likely to be growing and the likelihood of the cancer spreading to other parts of the body such as lymph nodes or bones. The pathologist assigns the grade of the tumour when he or she looks at the malignant cells under the microscope. The higher the Gleason grade, the more aggressive is the tumour.

**Histopathology:** Variants of usual acinar adenocarcinoma defined in 2004 by the WHO, include atrophic, pseudohyperplastic, foamy, colloid, signet ring, etc. Recently, variants not included in the 2004 WHO classification are microcystic adenocarcinoma, prostatic intraepithelial neoplasia – adenocarcinoma, large cell neuro endocrine carcinoma and pleomorphic giant cell carcinoma.

**Other diagnostic modalities for PC are** Colour Flow Imaging, Elastography, Contrast Enhanced Ultrasound (CEUS), MR Imaging of Prostate Malignancies. The MR Imaging consisting of the following:

**Prostate Imaging Reporting and Data System (PIRADS)** refers to a structured reporting scheme for evaluating the prostate for PC.

**T1-weighted** images are not helpful in differentiating different zones or detecting the lesion. However, invasion of neurovascular bundle, haemorrhage within the gland and loco-regional lymphadenopathy is better visualized on this sequence.

**DWI imaging** plays an important role in determining PIRADS score, predominantly in peripheral zone neoplasm. It utilizes proton diffusion properties in water to produce image contrast. Thus prostate malignancy appears bright (hyperintense) on DWI with corresponding low values on ADC map (dark-hypo intense). Of all functional MR imaging techniques, DW imaging is the most practical and simple in its use.

**Dynamic Contrast Scan** is considered positive if a suspected lesion/ nodule on T2-W or DWI image reveals earlier than normal or more than normal enhancement (hyper enhancement), as routinely seen in lesions with malignant etiology.

**MR Spectroscopy** reflects resonance frequencies that are unique for protons in different metabolites present at the sampled location. A change in the ratios of concentrations of these metabolites suggests abnormality within the tissue. Normal PZ has high concentration of citrate and polyamines and low concentration of choline and creatinine. A reversal of these, i.e. decrease in citrate peak due to altered metabolism and increase in choline and creatinine peaks in a suspected nodule on T2-W image may suggest malignancy. Recent studies reveal that MR spectroscopy is more specific and less sensitive than anatomic T2-W scan.

### **Current Modalities of Prostate Cancer Treatments**

There are a wide variety of treatments available for the management of prostate cancer. Radical prostatectomy, external beam radiation and radioactive prostate seed implant are potential cures for the prostate cancer. Hormone therapy may force the cancer into a prolonged remission but does not provide a cure unless it is combined with other treatments. The most commonly used treatments include the

following:

- Watchful Waiting (Active surveillance)
- Radical Prostatectomy (Robot assisted radical prostatectomy; Laparoscopic prostatectomy)
- Radiation Therapy (External beam radiation; Radioactive prostate seed implants)
- Hormone Therapy
- Combination of Therapies
- High Intensity Focused Ultrasound (HIFU) or Magnetic Resonance-guided Focussed Ultrasound Surgery (MRgFUS)
- Others (Cryotherapy; Photodynamic therapy)
- Metastatic Disease
  1. Hormonal therapy (orchidectomy)
  2. Anti androgens
  3. Luteinizing Hormone-releasing Hormone (LHRH) Agonists (Leuprolide; Goserelin; Triptorelin; Histrelin) – monthly to annual depot injection S.C. implants

Metastatic PC responds to androgen- ablation/deprivation therapy, which heralded the beginning of a new era PC therapy.

*Keywords:* Prostate cancer, transrectal ultrasonography, transrectal ultrasound-guided prostate biopsy, prostate-specific antigen (PSA), anti-androgen therapy of prostate cancer.

## **Introduction**

Prostate cancer is the commonest malignancy in men that causes significant morbidity and mortality. The incidence has quadrupled in the last three decades. This is predominantly due to excellent newer techniques like Prostate-specific antigen (PSA) evaluation, Transrectal ultrasonography (TRUS), Transrectal biopsy, contrast enhanced ultrasound studies, MpmMRI and nuclear medicine. Its incidence shows arise in India. It is the second leading site of cancer in Indian cities like Delhi, Kolkata and Pune. It is the 3<sup>rd</sup> leading site in cities like Mumbai and Bangalore. In India, it has an incidence rate of 3.9 per 1,00,000men and is responsible for 9% of cancer related mortality. Prostate imaging and interpretation is based on prostate imaging, reporting and data system. With the availability of PSA and trans-rectal biopsy, nowadays the majority of prostate cancers are diagnosed at an asymptomatic early stage (T1). Most cancers of the prostate are adenocarcinomas while a small percentage are ductal carcinomas, mucinous carcinomas, signet ring cell carcinomas and small cell carcinomas.

These variants have poor prognosis.

It is well said that the discovery which will cause the greatest impact on our field would be the development of accurate imaging of a tumour within the prostate. New biological markers such as PSA 3 are thought to be promising for positive biopsies that will once again cut down the unindicated number of biopsies.

***“PROSTATE CANCER IS CONSIDERED  
AS THE BIGGEST ENEMY OF A  
GENTLEMAN.”***

## **Anatomy of Prostate**

The anatomy of prostate and further discussions are based on transrectal ultrasound studies. A quick anatomical detail was thought necessary before I proceed further.

## ***Transition Zone (TZ)***

The transition zone in the earlier years of life contains approximately 5% of prostatic

glandular tissue. In the ageing prostate, the TZ shows marked hyperplasia and constitutes the majority of the overall prostatic glandular elements. It is located on both sides of the urethra. Prostatic calcification within the periurethral glands in the proximal urethra and verumontanum produce the typical 'Eiffel tower' effect. About 20% of prostatic cancers arise within the transition zone. These are embedded in the longitudinal smooth muscle of the proximal urethra, which is also known as the internal prostatic sphincter.

### ***Central Zone (CZ)***

The central zone is pyramidal in shape and consists of approximately 25% of glandular tissue. It is located near the base of the prostate. Its apex is at the verumontanum. Ducts from the CZ radiate from the base of the gland and terminate in the proximal urethra. The ejaculatory ducts pass through the CZ and terminate into the urethra at the verumontanum. The CZ is resistant to disease process and is the site of origin of 10% of all prostatic cancers.

### ***Peripheral Zone (PZ)***

The peripheral zone is the largest of the glandular zones, contains 70% of prostatic glandular tissue and surrounds the distal urethra. It occupies the posterolateral and apical regions of the prostate and extends anteriorly. The ducts of the PZ enter the distal urethra, distal to the verumontanum. The PZ is homogeneous in echotexture. About 70% of prostatic cancers originate in the PZ. The majority of these are located in close proximity of the prostatic capsule. They are separated from the central and transition zones by the surgical capsule.

### ***Anterior Fibromuscular Stroma (AFMS)***

The AFMS is non-glandular tissue, which forms the anterior surface of the prostate. It is situated anterior to the urethra and is composed of smooth muscle that is continuous

with the detrusor muscle fibers. It is thickest just distal to the verumontanum where it mainly consists of fibrous tissue. It becomes thinner as it reaches the apex of the prostate.

Over the years, TRUS has been very useful along with PSA findings in predicting prostate volume and detecting prostate cancer lesions. Currently, MRI finds its clinical applications in all aspects in prostate cancer evaluation (1).

This zonal anatomy is vital to understand since cancer is predominantly seen as follows:

1. TZ – 20%
2. CZ – 10%
3. PZ – 70%

### **Prostate-specific Antigen**

PSA is an extremely valuable tool in the evaluation of prostate cancers. It is exclusively produced by the prostate and to a lesser extent by the seminal vesicles. It is present in all post pubertal men and absent in women and men following radical prostatectomy.

PSA is a glycoprotein of low molecular weight (35,000 D) produced by the acinii and ducts of the prostate gland. It is the tumour marker currently used for early detection of prostate cancer. Disruption of normal prostatic architecture results in elevated serum PSA levels which otherwise is rather low. Prior to the availability of PSA, the detection of prostatic cancer was mainly based on DRE and serum acetate phosphate. With the availability of PSA testing, 32 to 35 % of patients with clinically significant prostatic cancer can be diagnosed before the disease is palpable. In more than 90% of patients, prostate cancer is diagnosed before symptoms occur.

Though the PSA is a vital parameter to detect prostate cancer, it can also be elevated in

1. Benign prostrate hypertrophy
2. Prostate inflammation

3. Prostatic infarct
4. Post digital rectal examination
5. Sexual activity

The normal value of PSA is 0-4 ng/cc. The two techniques that are available to assess PSA levels are polyclonal assay or monoclonal assay. The monoclonal assay is the most commonly used method the world over. The accepted PSA values are:

- <4ng/mL - normal
- 4.0-10.00ng/mL - borderline
- >10 ng/mL - abnormal

The importance of PSA values is vital in deciding the line of treatment for a given cancer. It also guides as to whether to perform a prostate biopsy or otherwise. The diagnosis of prostate biopsy is not specific or absolute with PSA studies. Normal PSA does not necessarily mean that the patient has no cancer.

Similarly, abnormal values are not definitive for the presence of prostate malignancy. Of the several new entities which are useful in the diagnosis of prostate cancer in a doubtful patient, free to total PSA ratio is being advocated and practiced often by several urologists. Normally PSA in the blood is partly free and partly protein bound, thus the ratio of 3:4 tends to be high in benign lesions while it is low in cancer. The necessity of using this parameter is to reduce the number of biopsies and to detect cancer with higher degree of confidence. No definitive cut off value has yet been accepted. In nutshell the accepted predicted values in different ages are as follows:

Age (years)	Normal range of PSA (ng/mL)
42-49	0.0 - 2.5
50-59	0.0 - 3.5
60-69	0.0 - 4.5
70-79	0.0 - 6.5

Other than normal PSA values, there are other PSA parameters which are often useful in

confirming the diagnosis of prostate cancer. These are

- PSA density
- PSA velocity
- PSA doubling time
- Other markers like PSA 3
- Prostate cancer is associated with more protein bound PSA (less free PSA) than in BPH.
  - i) F/T ratio is lower in patients with prostate cancer. This is of great value since it can improve the results of the test specificity. It is also of great value when total PSA is in the range of 4-10 Ng/CC.

In nutshell the importance of PSA as a diagnostic tool, which maybe summarised as:

- (a) Screening
- (b) Staging
- (c) Prognostic indicator
- (d) Surveillance in prostatic cancer.

The importance of PSA especially in patients who are asymptomatic are as follows:

PSA	Probability %
0.5	6.60
6-1	10
1.1-2	17
2.1-3	24
3.1-4	27
4-10	25-30
<10	42-64
>20	87

**Free (FPSA)** can enhance the specificity of the total PSA value for detection of the prostate cancer while reducing the number of unnecessary biopsies

Another new finding is that of levels of insulin like growth factor binding protein-2 (IGFBP- 2) appear to be directly associated with the presence of prostate cancer (2).

## Prostate Biopsy

Ultrasound guided biopsy of the prostate still remains the most important technique for the diagnosis of prostate cancer. A rising PSA or an elevated PSA remains to date the most vital technique to diagnose prostate cancer. The previously carried out sextant biopsy has now increased to a minimum of 12 core biopsy technique. This has improved the sensitivity of prostate cancer detection. Predominantly the samples are taken from the peripheral zone. Most workers do not take TZ biopsies as a routine. A TZ biopsy is undertaken in patients where the initial systematic sampling has been negative. The routine transition biopsy has a low yield of cancer ranging from 0.6 – 1.0%. The indications for trans-rectal biopsy of the prostate may be summarised (3) as:

- a. Abnormal DRE
- b. elevated or rising total PSA
- c. Previous negative biopsy but high clinical suspicion for prostate cancer
- d. Focal capsular bulge

## Prostate Evasive Anterior Tumours

A significant number of anteriorly located cancers are diagnosed relatively late. These are missed on trans-rectal biopsy, as the biopsies tend to be laterally directed focusing mainly on the PZ. These hidden cancers are located anterior to the urethra in the TZ (49%), anterior horns of PZ (36%) or both 8%). These tumours are suspected when high or increasing PSA levels are present despite repeatedly negative biopsies. These patients are often kept under close surveillance. MRI is now recommended to locate such cancers after adequate anterior and TZ biopsies have failed.

## Saturation Biopsies

Considering the difficulties in routine biopsies, there are many urologists who suggest and practice Saturation biopsies (24 to 40 cores). However, this technique has not been well

accepted, fallen out of repute and most urologists have come back to 10/12 core biopsies.

With the assistance of elastography, Doppler and contrast enhanced imaging, there is significant increase in the correct diagnosis of prostate cancers. As a result of the use of these modalities, the number of biopsies have also been reduced.

## MRI Guided Biopsy

MRI guided biopsy has a constant high cancer detection rate independent of the number of previous negative TRUS biopsies as well as the number of removed prostatic cores. Assuming that MRI guided biopsy provides an accurate diagnosis in a high proportion of patients while being less invasive than repeated TRUS guided biopsies, this technique is an attractive alternative diagnostic tool for the selected group of patients who have at least one negative prior TRUS guided biopsy with persistent suspicion of prostate cancer.

## Fusion Biopsy

MRI has a moderately high sensitivity and specificity for the detection of prostate cancer. Recently, a new technique has emerged which allows a pre-performed MRI to co-register to landmarks so that real time virtual ultrasound guided biopsies can be performed. Experience is limited but this is a very promising development that would overcome the limitations of TRUS in detecting cancer while retaining the flexibility and convenience of TRUS directed needle biopsy or ablative therapy (4, 5).

The technique allows multiplanar biopsy planning and Xu *et al* showed an accuracy of 2.4-1.2 mm in phantom and canine studies with a rate of 95.8 % with a significantly higher positivity rate than non-targeted cores. Further multicentre trials are necessary to evaluate this technique in cancer detection.

## Gleason Score

Gleason score is the grading system used to determine the aggressiveness of prostate cancer. This grading system can be used to choose appropriate treatment options.

The most commonly used grading system has two grades. Each patient's tumour is assigned two grades that represent the major and minor patterns of malignant glands seen under the microscope. Each of the two grades will range from 1-5, the two grades are then added together to give a Gleason score (which ranges from 2-10). A Gleason score of 2-5 represents a low grade malignancy. These tumours are usually slow growing and have a low likelihood of spreading and are rarely fatal. Tumours that have a Gleason score of 8-10 are high grade and are more likely to be fast growing and metastasize to lymph nodes or bones. Most patients have intermediate grade tumours or a Gleason score of 6 or 7. These are medium growing tumours and the prognosis is generally very good. The Gleason score strongly influences which staging test should be ordered and what treatment options should be considered.

The tumour grades provide important information regarding how fast the cancer is likely to be growing and the likelihood of the cancer spreading to other parts of the body such as lymph nodes or bones. The pathologist assigns the grade of the tumour when he or she looks at the malignant cells under the microscope. The higher the Gleason grade, the more aggressive is the tumour.

### *Importance of Gleason Score*

- Useful for predicting the behaviour of a prostate cancer
- PSA level
- Findings from rectal examination
- The number of biopsies core samples
- Is cancer found in one or both sides?
- Has the cancer spread outside the gland?

## *Prognostic Grade Grouping*

- Gleason Score 2 to 6 – Prognostic grade Group I/V
- Gleason Score 3+4=7– Prognostic grade Group II/V
- Gleason Score 4+3=7– Prognostic grade Grade III/V
- Gleason Score 8, Prognostic grade Grade IV/V
- Gleason Score 9-10– Prognostic grade Grade V/V

## Histopathology

Variants of usual acinar adenocarcinoma defined in 2004 by the WHO, include atrophic, pseudohyperplastic, foamy, colloid, signet ring etc. Recently, variants not included in the 2004 WHO classification are microcystic adenocarcinoma, prostatic intraepithelial neoplasia – adenocarcinoma, large cell neuro endocrine carcinoma and pleomorphic giant cell carcinoma (6).

## Colour Flow Imaging

The normal prostate gland has little but usually bilaterally symmetric flow. The neurovascular bundles are also well identified at the infero-lateral margins of the prostate. The neurovascular bundles, pericapsular and periurethral arteries show strong colour signals. In the initial stages, it was thought that colour flow signals especially with new machines with excellent software would solve the problem of detecting with certainty the problem of prostate cancer. However colour Doppler studies have no definite role to play in the diagnosis of prostate cancer. It has been realised that it has poor specificity with some malignancies being hypovascular while some benign lesions show increased vascularity. The commonly seen patterns in cancer of prostate colour-flow imaging are

1. Increased focal vascularity
2. Diffuse increased vascularity

3. Increased vascularity in the tissue surrounding the lesion.

Colour-flow imaging illustrates Macro-vascularity (Perfusion) thus its usefulness are

- Localisation of cancer
- Capsule penetration
- Locally advanced diseases
- Differentiates between fibrotic tissue and local recurrence.

### Elastography

This is an important new technique which depends on the stiffness of a given tissue. This really amounts to palpation of a given mass (Soft, Firm and Hard). The tumour can be imaged and quantified by measuring its strain under applied pressure (compression by transducer). Cancerous tissue reveals relatively increased stiffness as a result of increased cell density. In strain imaging, the images are obtained with and without manual compression of prostate. The degree of displacement (strain produced as a result) is used to generate an elastogram (color maps) in real time. Since a tumour is usually harder as compared to the surrounding tissue, it presents as a hypoechoic (black) area. This has been very useful especially in considering trans-rectal biopsies. The accuracy in detection of prostate cancer is about 80-85%.

In shear wave elastography technique, the shear waves are produced which travel at a right angle to the insonating beam. These travel faster in the stiffer tissues and thus provide a measure of tissue elasticity in quantitative terms. This technology is considered superior and more reproducible than strain imaging it has a high sensitivity and specificity. Shear wave elastography may also have better potential as this technique allows true quantification rather than strain, a surrogate index of stiffness. Shear wave elasticity helps in reducing the number of biopsies.

To summarise, Elastography is useful in

- Detection of prostate cancer
- Useful for targeted biopsy
- Staging of prostate cancer (presence or absence of extra capsular disease) (7)

### Contrast Enhanced Ultrasound

Angiogenesis is known to be essential for tumour growth and invasion, in a pathology specimen. Prostate tumours show increased microvascular density as compared with the normal parenchyma. Thus, an imaging investigation that allows quantification of blood flow in these micro vessels provides an opportunity to significantly increase the detection and characterisation of a prostatic cancer (8).

This is quite essential especially since the technological advances have shown significant false negative rates today. As a result it has been observed that newer biopsy techniques and technological advances have initiated further newer techniques to detect prostate cancer at high rates. With experience, it has been observed that with newer biopsy techniques, a significant number of false negative rates have regressed (9).

With the use of ultrasound contrast agents the number of unnecessary biopsies has decreased and also their morbidity.

Ultrasound contrast techniques allow imaging of vessels down to 50 to 100 micrometers in diameter. One of the greatest advantages is that these contrast agents are always intra-vascular and do not extravasate beyond the lumen of blood vessels. Thus there are hardly any side effects. Of the many indices that have been studied, the time-peak enhancement is the most predictive parameter for the localisation of the malignant lesion in the prostate which is 80% correctly diagnosed. Recently targeted microbubbles are under development and will certainly improve the sensitivity of certain specific markers. An important use of these contrasts is to utilise the

microbubbles for targeted biopsies. Though this has improved the sensitivity of detection of prostate cancer, it still does not avoid systemic biopsies. In short, further improvements are needed in increasing the sensitivity and specificity of these contrast agents.

Contrast agents are microbubbles of gas in an encapsulated cell. These are blood pool agents which remain confined to the vascular lumen until they disintegrate.

Tumour growth induces neovascularity and increased microvascular density, thus induces altered perfusion patterns that improve cancer detection. Practically, the increased density (rapid uptake) is followed by a quick wash out – CLASSICAL OF CANCER. As mentioned above, cancers have increased microvasculature. These agents enhance the area of cancer outlining the lesion in comparison to the surrounding normal tissue. Contrast enhanced targeted biopsy is one of the greatest advantages of the contrast agents.

In conclusion, the new contrast specific ultrasound techniques show promising results. One of the downsides of CEUS is the subjective interpretation by the investigators. The most important pattern which correlates with the presence of prostate cancer takes place within seconds of injection. This often makes the diagnosis of prostate cancer difficult. Much as a large group of workers believe that there is a significant increase in cancer detection rate using CEUS targeted biopsies compared to random biopsies, many scientists have reservation of the value of CEUS in this observation (10).

Microbubbles will soon be studied for quantification in prostate cancer. Similarly, they can also be used to transport certain substances. Ultrasound assisted drug delivery is being studied with great interest and will be an important usage of this very useful newer technology (11).

## MR Imaging in Prostate Malignancies

Prostate cancer is the most common malignancy in men. In recent years, prostate cancer is commonly detected early, hence imaging plays an important role in locating and delineating the extent of the disease. MRI is very useful in evaluating primary tumour, metastasis and recurrence. MRI allows detection of extracapsular spread of the disease, seminal vesicle invasion and simultaneous screening of regional lymph nodes and pelvic bones (12).

A multiparametric MR imaging prostate examination consists of T1- and T2-weighted imaging combined with one or more functional MR imaging techniques (dynamic contrast agent-enhanced MR imaging, diffusion-weighted (DW) imaging, and hydrogen 1 MR spectroscopic imaging) (13).

**T2-weighted** MR imaging is the workhorse of prostate MR imaging. T2-weighted images have high spatial resolution and, thus, can clearly differentiate the normal intermediate to high signal intensity peripheral zone from the low-signal-intensity central and transition zones in young male subjects. A neoplastic lesion is hypo intense on T2-W scan.

**T1-weighted** images are not helpful in differentiating different zones or detecting the lesion. However invasion of neurovascular bundle, haemorrhage within the gland and loco regional lymphadenopathy is better visualized on this sequence.

**DWI imaging** plays an important role in determining PIRADS score, predominantly in peripheral zone neoplasm. It utilizes proton diffusion properties in water to produce image contrast. Thus prostate malignancy appears bright (hyper intense) on DWI with corresponding low values on ADC map (dark-hypo intense). Of all functional MR imaging techniques, DW imaging is the most practical and simple in its use.

**Dynamic contrast scan** is considered positive if a suspected lesion/ nodule on T2-W or DWI image reveals earlier than normal or more than normal enhancement (hyper enhancement), as routinely seen in lesions with malignant etiology.

**MR spectroscopy** reflects resonance frequencies that are unique for protons in different metabolites present at the sampled location. A change in the ratios of concentrations of these metabolites suggests abnormality within the tissue. Normal peripheral zone has high concentration of citrate and polyamines and low concentration of choline and creatinine. A reversal of these i.e. decrease in citrate peak due to altered metabolism and increase in choline and creatinine peaks in a suspected nodule on T2-W image may suggest malignancy. Recent studies reveal that MR spectroscopy is more specific and less sensitive than anatomic T2-W scan.

**PI-RADS (Prostate Imaging Reporting and Data System)** refers to a structured reporting scheme for evaluating the prostate for prostate cancer (14). Categories of its scoring are given below (Table 1,2,3):

- PI-RADS 1: very low (clinically significant cancer is highly unlikely to be present)
- PI-RADS 2: low (clinically significant cancer is unlikely to be present)
- PI-RADS 3: intermediate (the presence of clinically significant cancer is equivocal)
- PI-RADS 4: high (clinically significant cancer is likely to be present)
- PI-RADS 5: very high (clinically significant cancer is highly likely to be present)

The PI-RADS score for peripheral gland lesion is predominantly acquired by DWI scan and for the central gland lesion is predominantly acquired by T2W scan.

PI-RADS scoring system is a standard subset of MR scan of prostate to grade the risk of malignancy.

**Table 1: Details of the PI-RADS scoring system**

Score	Peripheral Zone (PZ)	Transition Zone (TZ)
1	Uniform hyper intense signal intensity ( Normal )	Homogeneous intermediate signal intensity ( Normal )
2	Linear or wedge shaped hypo intensity or diffuse mild hypo intensity, usually indistinct margin	Circumscribed hypo intense or heterogeneous encapsulated nodule(s) (BPH)
3	Heterogeneous signal intensity or non-circumscribed, rounded, moderate hypo intensity	Heterogeneous signal intensity with obscured margins
4	Circumscribed, homogeneous moderate hypo intense focus/mass confined to prostate and <1.5 cm in greatest dimension	Lenticular or non -circumscribed, homogeneous, moderately hypo intense, and <1.5 cm in greatest dimension
5	Same as 4, but ≥ 1.5 cm in greatest dimension or definite extraprostatic extension/invasive behaviour	Same as 4, but ≥ 1.5 cm in greatest dimension or definite extraprostatic extension/invasive behaviour

**Table 2: PI-RADS scoring for peripheral gland lesions**

DWI	T2W	DCE	PI-RADS score
1	Any	Any	1
2	Any	Any	2
3	Any	-	3
		+	4
4	Any	Any	4
5	Any	Any	5

**Table 3: PI-RADS scoring for central gland lesions**

T2W	DWI	DCE	PI-RADS score
1	Any	Any	1
2	Any	Any	2
3	≤4	Any	3
	5	Any	4
4	Any	Any	4
5	Any	Any	5

**Table 4: Details of PI-RADS v2 scoring system**

Score	Peripheral Zone (PZ) OR Transition Zone (TZ)
1	No abnormality on ADC and high b-value DWI
2	Indistinct hypo intense on ADC
3	Focal mild-moderate hypo intense on ADC and iso-mildly hyper intense on high b-value DWI
4	Focal markedly hypo intense on ADC and markedly hyper intense on high b-value DWI; <1.5 cm in greatest dimension
5	Same as 4 but >1.5 cm in greatest dimension or definite extraprostatic extension

The original PI-RADS score was annotated, revised and published as the second version, **PI-RADS v2**, by a steering committee comprising the joint efforts of the American College of Radiology (ACR), European Society of Urogenital Radiology (ESUR), and

AdMeTech Foundation (Table 4).

**MR guided biopsy** is a promising tool in patients with one or more previous negative systematic random biopsy sessions. Transrectal MR-guided biopsy improves prostate cancer

detection; however, its availability is limited, and examination times are long. MR guidance of prostate biopsy may improve determination of the true pre-treatment Gleason score (15).

In conclusion, although reported accuracies of different components of multiparametric MR imaging techniques are inconsistent, in general the addition of multiparametric MR imaging techniques to T2-weighted MR imaging improves accuracy for both localization and local staging of prostate cancer.

Of all clinical indications for multiparametric MR imaging of the prostate, localization is the most important. Accurate localization of prostate cancer results in more accurate prostate cancer staging and MR guidance of prostate biopsy and therapy. MRI is also very helpful in determining recurrence of malignancy and restaging of prostate cancer. PIRADS v2 is the current standard method for evaluating pre-treatment prostate lesions and determining the risk of malignancy.

### **Role of Prostate Specific Membrane Antigen (PSMA)**

PSMA is a transmembrane glycoprotein with enzymatic properties which is expressed hundred to thousand-fold in prostate cancer. It is present very weakly in normal prostatic tissue and gets even more expressed in androgen resistant prostate cancer.

It can be imaged by Nuclear medicine techniques using <sup>68</sup>Ga-PSMA or <sup>18</sup>F-PSMA which are PET tracers. It has high sensitivity and specificity for imaging prostate cancer.

Over 90% of prostate cancers express PSMA. Expression may be low in low grade cancers or cancers which have undergone neuroendocrine differentiation.

PSMA PET-CT scan is becoming the diagnostic test of choice as a "one stop shop" in

the prostate cancer imaging (16). It has a role in:

1. Initial diagnosis of prostate cancer
2. Detection of recurrence after prostatectomy or radiation therapy in a patient with rising PSA (biochemical recurrence)
3. Follow-up response to chemotherapy or radiation therapy

In the initial diagnosis of prostate cancer in a symptomatic or asymptomatic patient with elevated PSA, PSMA PET-CT performs as well as a multiparametric MRI (MpMRI) which currently is considered the test of choice. There is a 97% concordance between PSMA PET-CT and MpMRI in this setting. The advantage of MpMRI is its ability to show involvement of the neurovascular bundle, which is difficult to detect on PSMA PET-CT due to inferior spatial resolution. However, PSMA PET-CT outperforms MRI and CT in N and M staging.

Over 80% of lymph nodal metastases in prostate cancer occur in nodes less than 8 mm. CT and MRI depend on size criteria for diagnosing metastases, hence would not detect all the lymph nodal metastases. PSMA PET-CT can detect nodal involvement in as small as 3 mm node (17).

In the setting of biochemical recurrence after radical prostatectomy and radiation therapy, PSMA PET-CT has great sensitivity of 60% for detection of recurrence site compared to almost zero with other modalities. At PSA levels < 2 ng/mL, the detection sensitivity is greater than 97%. PSMA PET-CT also identifies patients, who would be suitable for <sup>177</sup>lutium – PSMA therapy for refractory metastatic prostate cancer.

### **An Overview of Prostate Cancer Treatments**

There are a wide variety of treatments available for the management of prostate cancer. Radical prostatectomy, external beam radiation and radioactive prostate seed implant are

potential cures for the prostate cancer. Hormone therapy may force the cancer into a prolonged remission but does not provide a cure unless it is combined with other treatments. The most commonly used treatments include the following:

- Radical prostatectomy
  - Robot assisted radical prostatectomy
  - Laparoscopic prostatectomy
  - External beam radiation
  - Radioactive prostate seed implants
  - Hormone therapy
  - Watchful waiting
  - Combination of therapies
  - High intensity focussed ultrasound (HIFU)-guided thermal ablation
  - Others-cryotherapy, photodynamic therapy
  - Metastatic disease
1. Hormonal therapy (orchidectomy)
  2. Anti androgens
  3. LHR analogs (ZOLODEX, LUPRON)

Metastatic Prostate cancer responds to androgen ablation therapy, which heralded the beginning of a new era prostate cancer therapy (18).

Medical castration with oral androgens became the first effective systematic treatment for any cancer and to date the androgen ablation remains the most generally useful prostate cancer therapy.

### **High Intensity Focussed Ultrasound (HIFU) Guided Thermal Ablation**

or

### **Magnetic Resonance Guided Focussed Ultrasound Surgery (MRgFUS) for CA Prostate**

#### ***Principle and Rationale***

Traditionally accepted methods for treatment of Carcinoma prostate have been either radical surgery, radiotherapy or

brachytherapy. We see that the focus of therapy has been whole-gland therapy for disease that might very well be focal. With more widespread screening of healthy asymptomatic men by serum PSA, there has been a paradigm shift in recent years where lower grades and more focal disease are being picked up at an earlier stage. All of these patients do not necessarily require surgery or radical treatment and in fact, if it weren't for PSA screening, most of these patients would have lived the natural course of their lives without the disease manifesting or metastasizing. Thus, just as in breast cancer, a less radical method of treatment, i.e. lumpectomy was required to deal with lower grades of cancer caught in the early stages, a need was felt for non-invasive focal gland therapies for early stage low grade, localised prostate cancer. This is where High Intensity Focussed Ultrasound (HIFU) or Magnetic Resonance Guided Focussed Ultrasound Surgery (MRgFUS) for prostate cancer comes into picture (19).

#### ***Technique and Procedure***

MRgFUS is a thermal tissue ablation technique that works non-invasively. In HIFU the high intensity ultrasound waves focussed on a small focal point in the tissue, generate heat by tissue vibration effects to raise the local temperature upto 70-80°C. This causes thermal coagulation, tissue necrosis and heat shock. The coupled MRI scanner allows accurate targeting of the ultrasound beam by depicting detailed 3D anatomy of the gland. It also helps in monitoring the efficacy of thermal ablation by measuring real time temperatures achieved in the tissue by using real-time MR thermometry.

#### ***Selection Criteria***

Currently accepted patient selection criteria for surgery by MRgFUS for prostate cancer are as follows :

- 1) Age between 55 and 75 years,
- 2) PSA < 10,
- 3) Gleason Score , 7 (3+4),

- 4) cIIC& cT2a stage tumors,
- 5) Maximum of two lesions in the most recent mapping biopsy with each cancer site < 10mm in length,
- 6) Prostate Gland size < 60mL,
- 7) No prior TURP,
- 8) PSA density < 0.15,
- 9) No extra capsular spread, No calcification in beam path & tumor < 15mm.

Patients on medications that could affect PSA values were accepted if those medications were discontinued for at least 3months prior to the treatment.

## Results

Several reviews and published experience have shown urinary retention & dysuria, erectile dysfunction and urinary incontinence in a small number. Biopsy proven recurrence rates have also been studied and range from 1-20% for the entire prostate gland and 1-10% for the treated lobe. Erectile dysfunction is another complication that has been observed.

A number of urologists have reported negative biopsies of treated lobes in about 80% of patients.

In a carefully selected cohort of patients with localised prostate cancer of lower Gleason Grade, MRgFUS is a non-invasive technique that provides reasonable cure rates with significantly lower incidence of side effects like incontinence & erectile dysfunction as compared to conventional methods.

## Acoustic Radiation Force Impulse (ARFI) Imaging of Prostate

ARFI is a novel elasticity imaging technique to detect abnormalities inside the prostate. This technique has been extensively used in liver pathologies. ARFI imaging uses

high intensity focused acoustic beams to mechanically excite or push tissue and ultrasonic correlation based methods to monitor the tissue displacement response. The results suggest ARFI imaging is a promising new tool for providing image guidance for targeted prostate needle biopsies and focal therapy. This will however need further trials.

## Conclusion

Detection of prostate cancer at an early stage is a boon for men. From DRE and transrectal ultrasound, we have progressed significantly in the detection and treatment of prostate cancer. Unfortunately the incidence of prostate cancer has significantly increased. It is believed that this is because of early detection of prostate cancer at T1 stage, unlike previously seen cancers at T2 stage. Whether it is colour Doppler, elastography, HIFU or otherwise, there is significantly better localization of prostate cancer leading to better technique of prostate biopsy. A lot of attention has been drawn to the use of contrast enhanced ultrasound for definitely improved delineation of prostate cancer and also for follow up post treatment of these lesions. The addition of Mp MRI and PSMA-PET and the availability of HIFU have been invaluable in both detection and treatment of prostate cancer. Much as has been tried as anterior tumours are often missed on the available imaging techniques. With all these advances, TRUS and PSA will still remain the basic available modalities in spite of their limitations.

## References

1. Taneja SS (2004). Imaging in the diagnosis and management of prostate cancer. *Rev Urol* 6(3):101-113.
2. Shariat SF, Canto EI, Kattan MW, Slawin KM (2004). Beyond prostate-specific antigen: new serological biomarkers for

- improved diagnosis and management of prostate cancer. *Rev Urol* **6**(2):58-72.
3. Norberg M, Egevad L, Holmberg L, Sparen P, Norlen BJ, Busch C (1997). The sextant protocol for ultrasound-guided core biopsies of the prostate underestimates the presence of cancer. *Urology* **50**:562-566.
  4. Krucker J, Xu S, Venkatesan A, *et al* (2011). Clinical utility of real-time fusion guidance for biopsy and ablation. *JVIR* **22**(4):515-524.
  5. Vourganti S, Rastinehad A, Yerram N, *et al* (2012). Multiparametric magnetic resonance imaging and ultrasound fusion biopsy detects prostate cancer patients with prior negative TRUS biopsies. *J Urol* **188**(6):2152-2157.
  6. Humphrey PA (2012). Histological variants of prostatic carcinoma and their significance. *Histopathology* **60**(1):59-74.
  7. Miyagawa T, Tsutsumi M, Matsumura T, *et al* (2009). Real-time elastography for the diagnosis of prostate cancer: evaluation of elastographic moving images. *Japanese J Clin Oncol* **39**(6):394-398.
  8. Cornelis F, Bras YL, Rigou G, Correas JM, Grenier N (2014). Contrast enhanced ultrasound in prostate cancer. In: *Image Guided Prostate Cancer Treatments*. Bard RL, Futterer J, Sperling D, eds. New York: Springer-Verlag, 47-54.
  9. Konig K, Scheipers U, Pesavento A, *et al* (2005). Initial experiences with real-time elastography-guided biopsies of the prostate. *JUrol* **174**:115-117.
  10. Taverna G, Morandi G, Seveso M, *et al* (2011). Color doppler and microbubble contrast agent ultrasonography do not improve cancer detection rate in transrectal systemic prostate biopsies. *BJU Intl* **108**:1723-1727.
  11. Smeenge M, Misch M, Laguna MP, *et al* (2013). Contrast-enhanced ultrasonography. In: *Current Clinical Urology. Imaging and Focal Therapy of Early Prostate Cancer*. Polascik TJ, ed. Totowa, NJ: Humana Press, 155-164.
  12. Choi YJ, Kim JK, Kim N, Kim KW, Choi EK, Cho KS (2007). Functional MR imaging of prostate cancer. *Radiographics* **27**:63-75.
  13. Hoeks CM, Barentsz JO, Hambroek T, *et al* (2011). Prostate cancer: multiparametric MR imaging for detection, localisation and staging. *Radiology* **261**:46-66.
  14. Weinreb JC, Barentsz JO, Choyke PL, *et al* (2016). PI-RADS prostate imaging – reporting and data system: 2015, version 2. *Eur Urol* **69**(1):16-40.
  15. Roethke M, Anastasiadis AG, Lichy M, *et al* (2012). MRI-guided prostate biopsy detects clinically significant cancer: analysis of a cohort of 100 patients after previous negative TRUS biopsy. *World J Urol* **30**:213-218.
  16. Kallur KG, Ramchandra PG, Rajkumar K, *et al* (2017). Clinical utility of gallium 68 PSMA PET/CT scan for prostate cancer. *Indian J Nucl Med* **32**(2):110-117.
  17. Budaus L, Leyh-Bannurah SR, Salomon G, *et al* (2016). Initial Experience of (68) Ga-PSMA PET/CT imaging in high-risk prostate cancer patients prior to radical prostatectomy. *Eur Urol* **69**(3):392-396.
  18. Huggins C, Stevens RC Jr, Hodges CV (1941). Studies On Prostate Cancer II. The effects of castration on advanced carcinoma of the prostate gland. *Arch Surg* **43**:209-223.
  19. Blana A, Walter B, Rogenhofer S, Wieland WF (2004). High-intensity focused ultrasound for the treatment of localised prostate cancer: 5-year experience. *Urology* **63**(2): 297-300.

## Role of Adipokines in Development of Metabolic Syndrome

*Vani Gupta*

Department of Physiology,  
King George's Medical University, Lucknow,  
Uttar Pradesh, India.

### ABSTRACT

Visceral adipose tissue releases a variety of adipokines which together determine a comprehensive cardiometabolic risk profile. Estrogen deficiency leads to central fat deposition in postmenopausal women. However, premenopausal women are also running high risk of central obesity owing to unhealthy lifestyles, making them prone to development of metabolic syndrome which leads to infertility, polycystic ovary syndrome (PCOS), insulin resistance, and type 2 diabetes (T2D).

Premenopausal women with (n=30) and without (n=30) central obesity were studied. Metabolic risk factors and circulatory adipokines were measured. Insulin resistance was calculated by homeostasis model assessment (HOMA-IR). Adipokines' gene polymorphisms were studied by polymerase chain reaction and mRNA expression of leptin, adiponectin, resistin, and interleukin-6 (IL-6). Tumour necrosis factor- $\alpha$  (TNF- $\alpha$ ), acylation stimulating protein (ASP) receptor gene (C5L2) were done by real time-polymerase chain reaction in visceral (VAT) and subcutaneous (SAT) adipose tissues was also obtained.

Significant high circulating leptin, IL-6, TNF- $\alpha$ , resistin and their VAT mRNA expression and significant low circulating adiponectin and VAT mRNA expression were found in women with metabolic syndrome, irrespective of their menopausal status. Carriers of mutant genotype of TNF- $\alpha$  308 AA, IL-6 174 CC, resistin 420 GG, leptin 2549 AA, adiponectin 276 TT and C5L2 698 CT had significant association with metabolic syndrome. Conclusively changes in fat distribution modulate the secretion profile of adipokines, therefore elevated circulating leptin, IL-6, TNF- $\alpha$ , ASP, resistin, and low adiponectin may serve as surrogate markers for metabolic syndrome and related morbidities in women with central obesity.

*Keywords:* Central obesity, visceral adipose tissue, subcutaneous adipose tissue, mRNA, adipokines, insulin resistance, metabolic syndrome.

### Introduction

Postmenopausal women are more prone for central obesity attributed to hormonal

changes occurring during menopausal transition and in postmenopausal period; but recent studies have shown that adult premenopausal women also carry equal risk of central obesity and are

---

*Correspondence:* Dr. Vani Gupta, Professor, Department of Physiology, King George's Medical University, Lucknow, Uttar Pradesh, India. Email: vaniphysiology@gmail.com.

DR. J.S. BAJAJ ORATION delivered during the NAMSCON 2018 held at the Mahatma Gandhi Medical College & Research Institute, Puducherry.

prone for development of metabolic syndrome which leads to infertility, polycystic ovary syndrome (PCOS), adiposity, insulin resistance, diabetes and endocrinological problems. Females generally have a characteristic gynecoid type of fat distribution, with adipose tissue prominently developing in the subcutaneous depots around the hips and thighs. Female hormones make it easier to convert fat into food. Estrogen deficiency is responsible for centralization of fat deposition, i.e. visceral fat deposition or abdominal fat deposition, which is characterised as increased adipose tissue surrounding the intra-abdominal organs; this fat enhances metabolic dysfunction predisposing to type 2 diabetes mellitus (T2DM), the metabolic syndrome, and cardiovascular diseases. Visceral adipose tissue (VAT) also determines a comprehensive cardiovascular risk profile and increases the susceptibility to ischemic heart disease and arterial hypertension (1-3). VAT releases different bioactive molecules and hormones, such as adiponectin, leptin, tumour necrosis factor, resistin and interleukin-6 (IL-6), and acylation stimulating protein (ASP). Among these hormones, adiponectin and leptin are of particular significance owing to their involvement in the regulation of energy homeostasis, neuroendocrine function, haematopoiesis, angiogenesis, and reproduction (4). Circulating adiponectin is inversely correlated with the amount of VAT (5) while decreased concentrations of adiponectin are associated with T2D, elevated glucose levels, hypertension, cardiovascular disease and certain malignancies (5, 6). Leptin, released primarily from adipocytes and its expression, is directly related to the lipid content of the cells (7), its greater expression being found in the subcutaneous tissue (SAT) compared to VAT (8). Leptin increases with obesity (9) and its circulating levels are closely associated with all indices of adiposity. Consequently, it may be important to measure VAT mRNA expression of adiponectin and leptin along with their circulating level to better understand the pathogenesis of central obesity (VAT) related disorders in premenopausal women. Visceral

obesity is associated with poor prognosis, metabolic disturbances, and degree of pathology in several chronic diseases.

## **Methods**

This is a cross-sectional case control study. A total of 60 women (30 women with central obesity and 30 women without central obesity) age matched (22-39 years) were recruited at K.G. Medical University Lucknow, India who underwent elective abdominal surgery for gall bladder stone, hysterectomy or bariatric surgery. VAT was obtained during the surgery. During surgery neither specific standard diet nor any hormonal therapy were given to the patient, which ensured and ruled out the effect of hormone or diet on fat deposition. All tissue samples were stored in RNA later (Sigma – Aldrich) for the stability of RNA. This study is approved by Institutional Ethics Committee. Subjects were classified as premenopausal women with central obesity having waist hip ratio (WHR)  $> 0.85$  as per WHO guidelines for Asians. Premenopausal women without central obesity having  $WHR < 0.85$  served as controls. WHR is a good marker for central / visceral obesity (waist circumference was measured at the narrowest point superior to the hip and divided by the circumference of the hip measured at its greatest gluteal protuberance). Height (Ht.), weight (Wt.), waist circumference (WC) and hip circumference (HC) were measured. Body mass index (BMI) was calculated as weight (in kilograms) divided by height (in meter) square. Informed consent was obtained from each participant.

## **Laboratory Measurements**

Fasting blood samples for biochemical parameters were obtained in the morning after their admission to the hospital for surgery. Plasma glucose concentration was determined by glucose-peroxidase method (Merck) using semi automated glucose analyser (Microlab 300, Merck). Leptin (Diagnostics Biochem Canada Inc., Cat. No. CAN-L-4260, Version 6.0,

London, Ontario, Canada) and adiponectin (Human Adiponectin Cat. No. DRP300, R&D System Inc., Oxford, UK) were measured by enzyme linked immunosorbent assay. Plasma insulin concentration was determined using immuno radiometric assay (IRMA) (Immunotech). Insulin resistance was calculated by homeostatic model assessment index (HOMA Index) (10) using following formula:

$$\text{HOMA-IR} = \frac{\text{fasting insulin } (\mu\text{U/mL}) \times \text{fasting glucose (mM)}}{22.5}$$

If HOMA-IR  $\geq$  3.16 Insulin resistance  
 If HOMA-IR  $\leq$  3.16 Non Insulin resistance

### **RNA Extraction**

Total RNA was isolated from adipose tissue (30 mg of visceral fat / omental fat) with the RNA easy mini kit (Qiagen, USA) according to the manufacturer protocol. RNA was measured by spectrophotometric method at 260 and 280 nm while RNA integrity was checked by visual inspection of the two ribosomal RNAs 18s and 28s on agrose gel.

### **Measurement of Leptin and Adiponectin by Real-time PCR**

One-steps real-time reverse transcriptase (RT)-PCR is a sensitive method for quantification of specific mRNAs. In this approach, the RT as well as the PCR reaction was run together on the light cycler platform using quanti tect SYBR green RT-PCR kit (Qiagen, Hilden, Germany, CAT No.204243). SYBR green is a dye that binds to double but not single stranded DNA is used in quantitative PCR reactions. The reagents used were contained within the Light Cycler 2x Quantitect SYBR Green RT- PCR master mix which includes Hot Star Taq DNA polymerase, Quantitect SYBR Green RT-PCR Buffer, NTP mix, SYBR Green I, 5 mM MgCl<sub>2</sub> and quantitect RT mix which include omniscrypt reverse transcriptase and sensiscrypt reverse transcriptase.

All real-time reactions were performed in a Roche light cycler according to the

manufacturer's instructions. Total 30 ng RNA was used for PCR to analyze the gene expression of adiponectin, leptin and  $\beta$ -actin. The primer for PCR amplification of adiponectin F 5'GTGATGGCAGAGATGGCAC3' R 5'GCCTTGTCTTCTTGAAGAG3' leptin F5'GCTGTGCCCCATCCAAAAGT3, R 5'ACTGCCAGTGTCTGGTCCAT3 and  $\beta$ -actin F-5' GTGGCATCCACGAAACTA CTT 3' R 5' GGA CTCTGATACTCTGCT TG3' synthesized by (Agile Life Science Technology India). The annealing temperatures of gene is (Reverse transcription) 50°C for 30 min, (initial denaturation) 95°C for 15 min followed by 40 cycles of 94°C, 15 sec, (adiponectin is 52°C and for leptin and  $\beta$ -actin is 59°C), 30 sec and 72°C, 30 sec for denaturation, annealing, extension steps respectively done by light cycler 480 (Roche, real-time thermal cycler) the prepared reaction components were done in 96 well PCR plate. The reaction was set according to the standard protocol recommended by Qiagen. PCR reactions were carried out in total volume of 25  $\mu$ l. Expression of  $\beta$ -actin was used to normalized adiponectin and leptin expression values. There was no difference in glyceraldehyde -3-phosphatedehydrogenase or  $\beta$ -actin expression between women with central obesity or without central obesity.

### **Statistical Analysis**

Data were expressed as mean  $\pm$  SD. Anthropometric measurement, biochemical parameter and VAT adiponectin and leptin mRNA expression of two independent groups were compared by Student t test. Correlation was done to access association of VAT leptin and adiponectin mRNA expression with WHR and HOMA-IR, considering WHR and HOMA-IR an independent variable and VAT mRNA expression of leptin and adiponectin, the dependent variable. A two sided ( $\alpha=2$ )  $p<0.05$  was considered statistically significant.

### **Result**

Table 1 shows hormonal profile of premenopausal women with central obesity and

without central obesity. Serum FSH, LH, free testosterone, estradiol, DHEA and TSH were significantly high ( $p < 0.05$ ) in premenopausal women with central obesity than without central obesity while serum estradiol was significantly low in women with central obesity. The basic characters, viz. physical (age, weight, height, waist circumference, hip circumference, BMI, waist to hip ratio) and biochemical parameters (glucose, insulin, HOMA-IR) are shown in Table 2; weight, WC, BMI, WHR, insulin, glucose, HOMA-IR were significantly ( $p < 0.05$ ) higher in premenopausal women with central obesity than without central obesity. The VAT adiponectin and leptin mRNA expression of premenopausal women with central obesity and women without central obesity shown in Table 3 and Fig. 1 (a, b), VAT leptin mRNA expression Fig. 1 (a) was high in premenopausal women with central obesity than without central obesity ( $0.66 \pm 0.19$  vs.  $0.28 \pm 0.12$ ). VAT adiponectin mRNA expression [Fig. 1(b)] was significantly low in premenopausal women with central obesity ( $0.57 \pm 0.16$  vs.  $0.87 \pm 0.21$ ). Mean circulating level of leptin [Fig. 2(a)] was also high ( $31.6 \pm 14.21$  vs.  $22.53 \pm 11.04$ ) and adiponectin level [Fig. 2(b)] was low ( $7.6 \pm 2.4$  vs.  $11.72 \pm 3.53$ ) in premenopausal women with central obesity than without central obesity.

The correlations of VAT leptin and adiponectin mRNA expression of

premenopausal women having central obesity with their WHR and insulin resistance (HOMA-IR) are shown in Table 4. The VAT leptin mRNA expression was positively correlated with WHR ( $R=0.61$ ,  $p < 0.001$ ) and insulin resistance, i.e. HOMA-IR ( $R=0.72$ ,  $p < 0.001$ ). However, VAT adiponectin mRNA expression was negatively correlated with WHR ( $R=-0.76$ ,  $p < 0.001$ ) and insulin resistance HOMA-IR, i.e. ( $R=-0.59$ ,  $p < 0.002$ ). Premenopausal women without central obesity have positive correlation of VAT leptin mRNA with WHR ( $R=0.24$ ,  $p=0.13$ ) and HOMA-IR ( $R=0.06$ ,  $p=0.71$ ) but not significant. Adiponectin VAT mRNA level have negative correlation with WHR ( $R=-0.15$ ,  $p=0.23$ ) and HOMA-IR ( $R=-0.09$ ,  $p=0.43$ ) but not significant in premenopausal women without central obesity.

## Discussion

This study was undertaken to evaluate mRNA expression of adiponectin and leptin of VAT and their circulatory levels in premenopausal women with central obesity and without central obesity. Correlation of mRNA expression and circulatory level of both adipokines with WHR and insulin resistance, i.e. HOMA-IR were also observed. Observations of the present study show that premenopausal women with central obesity have significantly

**Table 1: Hormonal levels in premenopausal women with and without central obesity**

Hormone Level	Premenopausal Women WHR <0.85 (n= 30)	Premenopausal women WHR >0.85 (n=30)	p-value
FSH (mIU/ml)	6.30± 2.90	22.10± 6.50	<0.001*
LH (IU/ml)	5.60±1.35	18.65± 4.25	<0.001*
F-Testosterone (ng/dl)	57.35±18.70	72.28±11.85	0.004*
Estradiol (pg/ml)	111.25±94.12	35.05±15.82	<0.001*
TSH (µIU/ml)	1.42±0.78	1.78±0.80	<0.001*
SHBG (nmol/l)	44.15±14.55	46.02±21.80	0.548
DHEA (µg /dl)	111.45±18.45	167.30±25.20	<0.001*

Data are as mean ± SD

\*P < 0.05 = significant

**Table 2: Comparison of metabolic risk markers and circulatory adipokines in premenopausal women with and without central obesity**

Variables	Premenopausal Women with central obesity n = 30	Premenopausal Women without central obesity n=30	P-Value
Age (yr)	28±4.10	26±5.80	0.12
Weight (kg)	62.68±12.45	52±9.50	<0.0001*
Height (cm)	151.57±7.07	153±6.76	0.10
BMI (kg/m <sup>2</sup> )	27.33±5.57	22.21±3.72	<0.0001*
WC (cm)	83.14±14.71	70±8.91	<0.0001*
WHR	94.96±11.18	85±7.89	<0.0001*
HC (cm)	0.87±0.06	0.82±0.04	0.0002*
Glucose (mg/dl)	125.62±21.66	93±10.15	<0.0001*
Insulin (μU/ml)	11.67±5.77	9.36±4.00	0.008*
HOMA-IR	3.73±2.15	2.18±1.04	0.0003*
Leptin (pg/ml)	31.6 ± 14.21	22.53 ± 11.04	<0.0001*
Adiponectin (pg/ml)	7.6 ± 2.4	11.72 ± 3.53	<0.002*

Data are as mean ± SD \*P < 0.05 = significant ; BMI: Body mass index; WC: Waist circumference; HC: Hip circumference ; WHR: Waist Hip Ratio; HOMA - IR: homeostatic model assessment for insulin resistance.

**Table 3: Relative VAT mRNA expression of insulin leptin and adiponectin of premenopausal women with and without central obesity**

Adipokines	Visceral adipose tissue (VAT)		P-value
	Premenopausal women with central obesity (n= 30)	Premenopausal women without central obesity (n= 30)	
Leptin	0.66 ± 0.19	0.28 ± 0.12	0.001*
Adiponectin	0.57 ± 0.16	0.87 ± 0.21	<0.001*

Data are as mean ± SD

\*P < 0.05 = significant

**Table 4: Correlation (Pearson r) of Leptin and Adiponectin VAT mRNA expression with WHR and HOMA-IR (insulin resistance) in premenopausal women with central obesity**

Variables	Leptin VAT m-RNA (r-value)	P-value	Adiponectin VAT m-RNA (r-value)	P-value
WHR	0.61	<0.001*	-0.78	<0.0001*
HOMA-IR	0.72	<0.0001*	- 0.59	<0.002*

\*P < 0.05 = significant; WHR: Waist hip ratio; HOMA-IR: Homeostatic model assessment for insulin resistance.

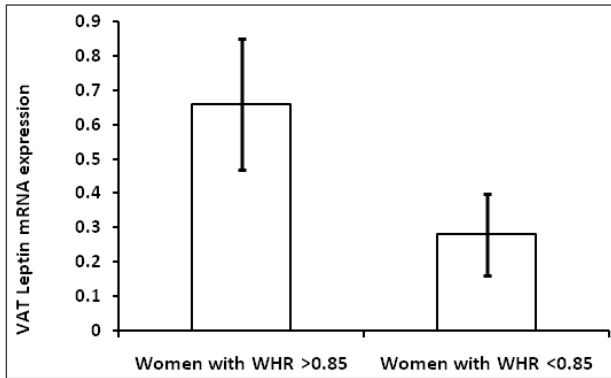


**Fig. 1(a):** VAT Leptin mRNA expression in women with central obesity and without central obesity.

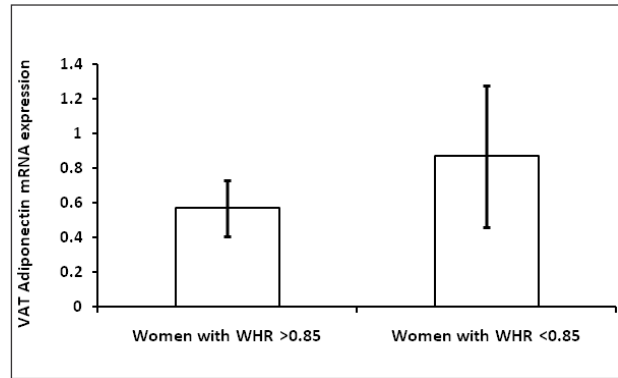


**Fig. 1(b):** VAT Adiponectin mRNA expression in women with central obesity and women without central obesity.

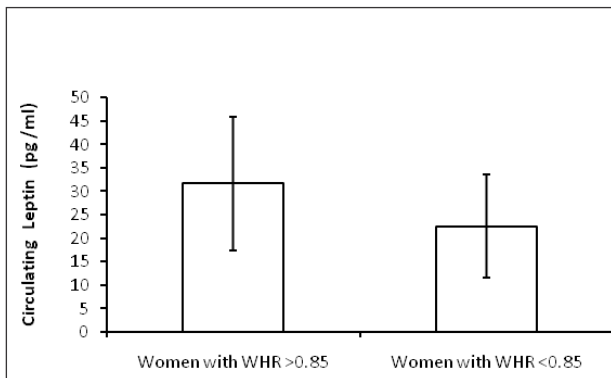


**Fig. 2(a):** Circulating leptin (pg/ml) level in women with central obesity and women without central obesity.

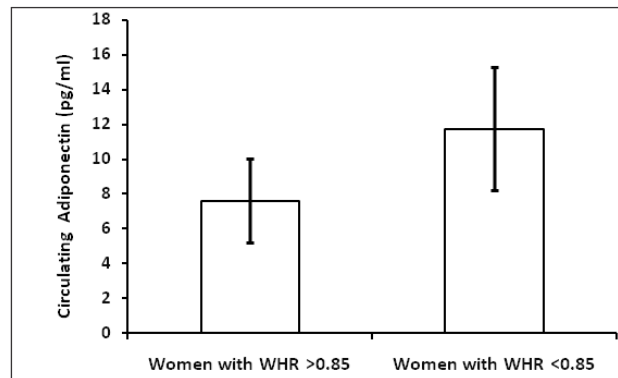


**Fig. 2(b):** Circulating adiponectin (pg/ml) level in women with central obesity and women without central obesity.

higher serum level of FSH, LH, free testosterone, TSH and DHEA while significantly low estradiol as compared to women without central obesity. These observations suggest hyperandrogenemia and low circulating estrogen in premenopausal women with central obesity responsible for centralization of fat. They also had significant high WC, WHR and BMI than women without central obesity. These observations were in concordance with other studies (11, 12) which have concluded that WC yields a better correlation values with all the metabolic risk factors indicating that WHR may be a better index for abdominal obesity / central obesity due to high visceral adipose tissue than BMI in Asian Indians. The observation shows that significant higher plasma glucose and plasma insulin and HOMA- IR were found in

women with central obesity suggesting the presence of insulin resistance. Insulin hormone regulates virtually all aspects of adipocytes functioning. Insulin increases the uptake of fatty acids by stimulating lipoprotein lipase activity in adipose tissue. There is increasing evidence supporting the fact that by the time glucose intolerance or fasting hyperglycemia set in appreciable  $\beta$ -cell destruction may have already occurred (13).

In the present study, circulating level and VAT mRNA expression of adiponectin level was found to be significantly lower in women with central obesity as compared to women without central obesity and low adiponectin VAT mRNA level in women with central obesity is strongly associated with HOMA-IR and WHR. Our

results are in concordance with other studies showed lower concentration of adiponectin is associated with WHR (14) and insulin resistance (15), as well as lower adiponectin mRNA expression in the VAT of type 2 diabetic patients (16). Further, the findings of the present study are also consistent with other study which showed significantly lower adiponectin gene expression and protein content in VAT of obese as compared to non-obese (17). Low adiponectin levels are more strongly associated with the amount of visceral fat than subcutaneous fat (18). Adiponectin have profound protective role in obesity. Several studies suggest that the decreased concentration of adiponectin in obesity, leads to the development of metabolic syndrome (19). *In vivo* and *in vitro* studies have demonstrated that adiponectin enhances insulin sensitivity, increases fatty acid oxidation, glucose uptake, suppresses hepatic glucose production (20) and has protective antiangiogenic effect.

These studies strongly indicate that adiponectin acts on multiple tissues to enhance insulin sensitivity thus, referred to as an insulin sensitizer. A recent study showed that adiponectin enhances insulin-stimulated IRS-1 tyrosine phosphorylation and Akt phosphorylation (21). This study further revealed that activation of the serine / threonine kinase 11/AMP-activated protein kinase (AMPK)/TSC1/2 pathway alleviates the p70S6 kinase-mediated negative regulation of insulin signalling, providing a mechanism by which adiponectin increases insulin sensitivity in cells.

Leptin produced by adipose tissue acts as a satiety hormone, is a major regulator of body weight and food intake and deficiency in leptin leads to obesity. However, in the present study circulatory leptin and its VAT mRNA expression level was found to be significantly higher in women with central obesity which may be due to leptin resistance, showing negative association with adiponectin also (22). Like adiponectin, leptin also modulates several metabolic processes including glucose regulation and fatty

acid breakdown. We observed significantly higher VAT leptin mRNA expression and its association with WHR in women with central obesity. Other studies showed that high leptin mRNA level was found in subcutaneous fat compared to VAT (23).

Our study also shows that high circulating leptin is significantly associated with HOMA- IR. This indicates that leptin resistance runs hand in hand with insulin resistance (12). In mice that became obese after being fed a high-fat diet, leptin concentration was increased, and this increase was accompanied by an increased expression of SOCS-3 (suppressor-of-cytokine-signaling), a potent inhibitor of leptin signaling (24).

The mRNA expression of leptin in adipose tissue is strongly associated with fat mass in obesity. Thus, leptin appears as a real marker of adipose tissue mass in humans where the subcutaneous fraction represents about 80% of total fat (25). Although, the principal biological effect of leptin in the central nervous system is control of food intake and energy expenditure. There is a significant relationship between leptinaemia and the chronic sub-inflammatory state in obesity.

Leptin pathways act in concert with insulin to control glucose and lipids, aside from regulating food intake and metabolic rate, linking this hormone to IR and T2D. Leptin can act through some of the components of the insulin signalling cascade, such as insulin receptor substrate (IRS)-1 and IRS-2, mitogen-activated protein kinase (MAPK) and phosphatidylinositol 3-kinase (PI3-kinase), suggesting that there are cross-talk between insulin and leptin signalling pathways (26). However, some schools of thought suggests that association of leptin with insulin resistance in T2D and obesity may be through its regulation of the deposition of fat in insulin responsive tissues, rather than through effects on insulin signalling. The role of high leptin in obesity associated IR is still controversial (27).

## Conclusion

Changes in fat distribution lead to a modification of the secretion profile of adipokines especially leptin and adiponectin, the two adipokines play important role in energy homeostasis of adipose tissue. High circulatory level and VAT mRNA expression of leptin and its positive correlation with HOMA-IR suggest that central obesity is a leptin-resistant state might be induced by insulin resistance. Low circulating level and mRNA expression of adiponectin and its negative correlation with HOMA-IR suggest its protective role. So circulatory leptin and adiponectin may serve as surrogate markers for development of insulin resistance and related morbidities in premenopausal women with central obesity.

## Acknowledgement

We would like to acknowledge faculty, residents of Surgery and Obstetrics & Gynaecology Deptt. of King George's Medical University, Lucknow and participants of this study for providing sample. This study was funded by Indian Council Medical Research (ICMR) No. 5/7/270/08-RHN, New Delhi, India. There is no conflict of interest and no financial disclosure.

## References

1. Fox CS, Massaro JM, Hoffmann U, *et al* (2007). Abdominal visceral and subcutaneous adipose tissue compartments: association with metabolic risk factors in the Framingham Heart Study. *Circulation* **116**: 39-48.
2. Lamarche B, Lemieux S, Dagenais GR, Després JP (1998). Visceral obesity and the risk of ischaemic heart disease: insights from the Quebec Cardiovascular Study. *Growth Horm IGF Res* **8**: 1-8.
3. Onat A, Avci GŞ, Barlan MM, Uyarel H, Uzunlar B, Sansoy V (2004). Measures of abdominal obesity assessed for visceral adiposity and relation to coronary risk. *Intl J Obes Relat Metab Disord* **8**: 1018-1025.
4. Blüher M, Mantzoros CS (2015). From leptin to other adipokines in health and disease: facts and expectations at the beginning of the 21st century. *Metabolism* **64**: 131-145.
5. Pinthus JH, Kleinmann N, Tisdale B, *et al* (2008). Lower plasma adiponectin levels are associated with larger tumor size and metastasis in clear-cell carcinoma of the kidney. *Eur Urol* **54**: 866-873.
6. Ritchie SA, Connell JM (2007). The link between abdominal obesity, metabolic syndrome and cardiovascular disease. *Nutr Metab Cardiovasc Dis* **17**: 319-326.
7. Zhang Y, Guo KY, Diaz PA, Heo M, Leibel RL (2002). Determinants of leptin gene expression in fat depots of lean mice. *Am J Physiol Regul Integr Comp Physiol* **282**: R226-R234.
8. Van Harmelen V, Reynisdottir S, Eriksson P, *et al* (1998). Leptin secretion from subcutaneous and visceral adipose tissue in women. *Diabetes* **6**: 913-917.
9. Pina T, Genre F, Lopez-Mejias R, *et al* (2015). Relationship of Leptin with adiposity and inflammation and resistin with disease severity in psoriatic patients undergoing anti-TNF-alpha therapy. *J Eur Acad Dermatol Venereol* **29**: 1995-2001.
10. Keskin M, Kurtoglu S, Kendirci M, Atabek ME, Yazici C (2005). Homeostasis model assessment is more reliable than the fasting glucose/insulin ratio and quantitative insulin sensitivity check index for assessing insulin resistance among obese children and adolescents. *Pediatrics* **4**: 500-503.
11. Misra A, Wasir JS, Pandey RM (2005). An evaluation of candidate definitions of the metabolic syndrome in adult Asian Indians. *Diabetes Care* **28**: 398-403.

12. Gupta A, Gupta V, Singh AK, *et al* (2011). Interleukin-6 G-174C gene polymorphism and serum resistin levels in North Indian women: potential risk of metabolic syndrome. *Hum Exp Toxicol* **30**: 1445-1453.
13. Ferrannini E (1997). Insulin resistance is central to the burden of diabetes. *Diab Metab Res Rev* **13**: 81-86.
14. Rashiti P, Elezi S, Behluli I, Mucaj S (2016). Relationship of plasma adiponectin and waist-hip ratio with coronary artery disease. *Med Arch* **6**: 413-418.
15. Chung CP, Long AG, Solus JF, *et al* (2009). Adipocytokines in systemic lupus erythematosus: relationship to inflammation, insulin resistance and coronary atherosclerosis. *Lupus* **9**: 799-806.
16. Statnick MA, Beavers LS, Conner LJ, *et al* (2000). Decreased expression of apM1 in omental and subcutaneous adipose tissue of humans with type 2 diabetes. *Intl J Exp Diabetes Res* **1**: 81-88.
17. Kovacova Z, Tencerova M, Roussel B, *et al* (2012). The impact of obesity on secretion of adiponectin multimeric isoforms differs in visceral and subcutaneous adipose tissue. *Intl J Obes* **36**: 1360-1365.
18. Kishida K, Kim KK, Funahashi T, Matsuzawa Y, Kang HC, Shimomura I (2011). Relationships between circulating adiponectin levels and fat distribution in obese subjects. *J Atheroscler Thromb* **18**: 592-595.
19. Bik W, Ostrowski J, Baranowska-Bik A, *et al* (2010). Adipokines and genetic factors in overweight or obese but metabolically healthy Polish women. *Neuro Endocrinol Lett* **4**: 497-506.
20. Wu X, Motoshima H, Mahadev K, *et al* (2003). Involvement of AMP-activated protein kinase in glucose uptake stimulated by the globular domain of adiponectin in primary rat adipocytes. *Diabetes* **52**: 1355-1363.
21. Wang J, Li H, Franco OH, Yu Z, Liu Y, Lin X (2008). Adiponectin and metabolic syndrome in middle aged and elderly Chinese. *Obesity* **1**: 172-178.
22. Baranowska B, Wolinska-Witort E, Martynska M, Chmielowska M, Baranowska-Bik A (2005). Plasma orexin A, orexin B, leptin, neuropeptide Y (NPY) and insulin in obese women. *Neuro Endocrinol Lett* **4**: 293-296.
23. Hube F, Lietz U, Igel M, *et al* (1996). Difference in leptin mRNA levels between omental and subcutaneous abdominal adipose tissue from obese humans. *Horm Metab Res* **28**(12): 690-693.
24. Munzberg H, Myers MG Jr (2005). Molecular and anatomical determinants of central leptin resistance. *Nat Neurosci* **8**: 566-570.
25. Vidal H, Auboeuf, D, De Vos, *et al* (1996). The expression of ob gene is not acutely regulated by insulin and fasting in human abdominal subcutaneous adipose tissue. *J Clin Invest* **98**:251-255.
26. Szanto, I, Kahn CR (2000). Selective interaction between leptin and insulin signaling pathways in a hepatic cell line. *Proc Natl Acad Sci* **97**: 2355-2360.
27. Hennige AM, Stefan N, Kapp K, *et al* (2006). Leptin down-regulates insulin action through phosphorylation of serine-318 in insulin receptor substrate 1. *FASEB J* **20**: 1206-1208.

# **Anthropometric Study of Proximal Femur Geometry and Its Clinical Application**

*Ramchander Siwach*  
Department of Orthopaedics,  
Pt. B.D. Sharma PGIMS,  
Rohtak, Haryana, India.

## **ABSTRACT**

The implants for fixation of proximal femur fractures and joint replacements have been designed taking into consideration of the anthropometry of the western population which vary from other ethnic groups. The present study aimed to study the morphology of the upper end of femur in relation to its various diameters and angles and compare the external and internal geometry of proximal femur as obtained from radiographs, with actual measurements on cadaveric specimens in Indian population. Seventy five pairs (150 bones) of cadaveric femora were studied morphologically and radiologically using standardized techniques to obtain various anthropometrics measurements. These values were compared with those reported in the literature for Hong Kong Chinese, Caucasian, Chinese and Western populations. Data were found to be quite different from them. It is proposed that implants designed for Western populations should be used judiciously and future implants be designed to match the morphology of the Indian bones.

*Keywords:* Anthropometry, proximal femur, cadaveric, Indian population.

## **Introduction**

Operations on the proximal femur are one of the commonest in orthopaedic surgical practice. The aim of these operations is to remove pathology and restore anatomy to the normal, as far as possible. The implants for fixation of proximal femur fractures and joint replacements have been designed taking into consideration of the anthropometry of the western population which vary from other ethnic groups (1, 2). The standard commercially available marketed prostheses sometimes may not be the best fit to all subjects because of the large anatomic variation among different

populations (2). The osteological parameters of the proximal femur are very important for the design of suitably sized prostheses of total hip replacement (THR), especially for cementless implantation (3). Orthopaedic surgeons always stress the need for a proper implant-patient match in hip joint replacements to avoid post-operative complication of mismatch which may affect the outcome of the operation (2).

Whereas what is normal has been standardized for Caucasians and Chinese (4-6), data for Indians are lacking. Since build, physique, habits and genetic make up vary markedly in different ethnic groups, it is possible

---

*Correspondence:* Dr. Ramchander Siwach, Senior Professor and Head, Department of Orthopaedics, Pt. B.D. Sharma PGIMS, Rohtak, Haryana, India. Email : rcsiwach.bps@gmail.com.

COL. SANGHAM LAL MEMORIAL ORATION delivered during the NAMSCON 2018 held at the Mahatma Gandhi Medical College & Research Institute, Puducherry.

that anthropometric dimensions described as normal for proximal end femur for Westerners might be quite different from those encountered amongst Indians. The present study was conducted with aim to remove the lacuna of information about proximal femoral geometry in Indian people and evaluate its impact on implant design. The present study aimed to investigate the morphology of the upper end of femur in relation to its various diameters and angles and compare the external and internal geometry of proximal femur as obtained from radiographs, with actual measurements on cadaveric specimens. The clinical application of the various geometric data, with the implants available, for osteosynthesis of the upper end of the femur and hip arthroplasty was also studied.

### Materials and Methods

The study was conducted on 150 adult cadaveric femora (Fig. 1). Specimens that showed osseous pathology or previous fractures were excluded from the study. With the help of forensic expert these 150 adult cadaveric femora were differentiated into male and female femora, and their approximate age was determined. We did study on femora of adult group (age approximately between 20-80 years). Roentgenograms of 75 pairs of near identical specimen were taken in antero-posterior and lateral views using a precise standardized technique.

The specimens were placed directly over the cassette so the magnification would be



**Fig. 1: Cadaveric femora of 150 adults.**

insignificant. The distance between the X-ray source and the film was 1.2 m and the beam was centered on the lesser trochanter with the femur lying in neutral rotation. For lateral view without moving the femur, the X-ray source was rotated through 90° in the vertical plane, the distance between the source and the film remaining the same. Then the femur was kept on a sponge of the 2 feet length, 10" breadth and 8" height; the X-ray cassette was kept touching the femur, with one technician holding the cassette after wearing a lead apron. But on these lateral views the whole neck profile was not clear due to superimposition of greater trochanter. So to avoid this problem we kept the femur directly on the cassette in frog leg view position holding the condyles of the femur. In this view the neck profile of femur was clear.

### Morphological Study

The standard extracortical and endosteal dimensions were determined by direct measurement of cadaveric specimens. These measurements were done with the help of vernier caliper and goniometer (Fig. 2). With the help of vernier caliper we measured femoral head diameter, femoral head length, effective neck length, femoral neck diameter and canal width 20 mm above lesser trochanter, at level of lesser trochanter and 20 mm below lesser trochanter. With the help of goniometer neck shaft angle and angle of anteversion were measured.

- a) *Femoral head diameter*: The distance between the two extreme points of head was measured.
- b) *Femoral head length*: Radius of femoral head is not equal superiorly and inferiorly due to its placement (Fig. 3):
  - (i) Maximum femoral head length - From the center of the femoral head to the periphery of femoral head along the articular cartilage border where it is maximum (superior);
  - (ii) Minimum femoral head length - From the center of femoral head to the periphery of

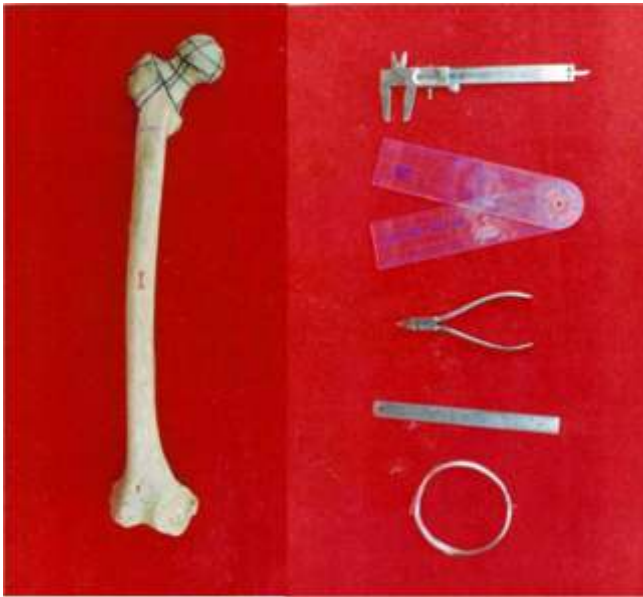


**Fig. 2: Showing various extra cortical dimensions in cadaveric femur and instruments used for various measurements.**



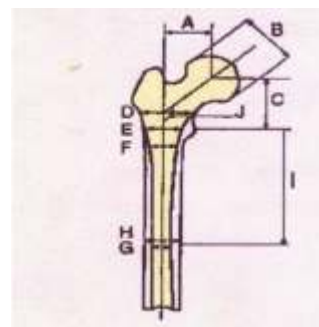
**Fig. 3: Showing femoral head length in superior and inferior quadrant in cadaveric femur.**



**Fig. 4: Showing variations in angles of anteversion in cadaveric femur.**



Reference axis system  
 O: Center of the lesser trochanter (origin of the axis system)  
 X: Horizontal axis through O on anteroposterior view  
 Y: Horizontal axis through O on lateral view  
 Z: Vertical axis through O on the anteroposterior and lateral Views.



A: Femoral head offset  
 B: Femoral head diameter  
 C: Femoral head position  
 D: Canal width, 20 mm above the lesser trochanter  
 E: Canal width, at the level of the lesser trochanter  
 F: Canal width, 20 mm below the lesser trochanter  
 G: Endosteal width, at the isthmus  
 H: Extracortical width, at the isthmus  
 I: Isthmus position  
 J: Neck-shaft angle (degrees).

Anatomical characteristics in millimeters measured on the anteroposterior radiograph

**Fig. 5: Anatomical representation and radiographic measurement on femoral radiographs.**

femoral head along the articular cartilage border where it is minimum (inferior).

- c) *Effective neck length*: (i) Maximum effective neck length - The length of neck where it is maximum was measured along the calcar (inferior); (ii) Minimum effective neck length - The length of neck where it is minimum was measured (superior).
- d) *Neck diameter*: (i) Anteroposterior neck diameter - The distance between the two extreme points in middle of neck from the center point of intertrochanteric line to base of head in anteroposterior plane was measured; (ii) Superoinferior neck diameter - The distance between the two extreme points in middle of neck in superoinferior plane was measured (sagittal plane).

- e) *Canal width, 20 mm above lesser trochanter*: It was marked with a sketch pen 20 mm above and parallel to the horizontal axis passing through the center of lesser trochanter.
- f) *Canal width at level of lesser trochanter*: A horizontal line was drawn through the center of lesser trochanter on anterior side.
- g) *Extracortical width 20 mm below lesser trochanter*: It was marked with a sketch pen 20 mm below and parallel to the horizontal axis passing through the center of lesser trochanter.
- h) *Neck shaft angle*: Center of head of femur was marked. Then mid point of the neck was marked by measuring the width of the narrowest portion of the neck and dividing by two. The line from center of the head of femur through the center of the neck was drawn. A line through the centre of the diaphysis of the femur was drawn. These two lines intersected each other. The angle between the two was measured.
- i) *Angle of anteversion*: The center of the neck between its anterior and posterior surfaces was determined at two different points on the neck, as viewed from above. A line was drawn connecting these two points (Fig. 4). The femur was placed on a smooth level, horizontal surface so that it rested on three points, namely, the posterior aspect of the two femoral condyles and the posterior aspect of the greater trochanter. The goniometer was placed on the block of wood on which femur was rested. One arm of goniometer was opened and rotated till it was corresponding to the line connecting 2 center points marked on the neck of femur. The angle thus formed was read directly from goniometer, the eye kept on a level with the axis of the neck.

### **Radiological Study**

A center point was marked at the level of isthmus. Second point was marked at the center

of femur 3 cm above isthmus and third point was marked at the center of femur 3 cm below isthmus, a line connecting these 3 points was drawn and extended upwards and downwards.

With the help of scale we measured femoral head offset, femoral head diameter, femoral head position, neck diameter, canal width 20 mm above lesser trochanter, canal width at level of lesser trochanter, canal width 20 mm below lesser trochanter, endosteal width at the isthmus and extracortical width at the isthmus and isthmus position.

- a) *Femoral head offset*: The distance between the center of head of femur and vertical axis drawn on femur.
- b) *Femoral head diameter*: Two points were marked at the maximum distance on the head and the distance between the two was measured.
- c) *Femoral head position*: It is the distance between the center of head and the horizontal line drawn through center of lesser trochanter.
- d) *Neck diameter*: The width of the narrowest portion of the neck was measured.
- e) *Canal width, 20 mm above lesser trochanter*: Two points were marked 20 mm above the lesser trochanter at maximum intracortical area and the distance between them was measured.
- f) *Canal width at level of lesser trochanter*: Two points were marked at the level of lesser trochanter at maximum intracortical area and the distance between them was measured.
- g) *Canal width 20 mm below lesser trochanter*: Two points were marked 20 mm below the lesser trochanter at maximum intracortical area and the distance between them was measured.
- h) *Endosteal width at the isthmus*: The narrowest portion of the medullary canal is

called isthmus. Two points were marked at this level at maximum intracortical area and the distance between them was measured.

- i) *Extracortical width at the isthmus*: Two points were marked at the above level at the maximum extracortical area and the distance between them was measured.
- j) *Isthmus position*: The distance between the isthmus and the center of lesser trochanter was measured.
- k) *Neck shaft angle*: Center of head was marked. The mid point of the neck was located by measuring the width of the narrowest portion of the neck and dividing by two. The line connecting the center of head of femur through the center of the neck was drawn and extended to meet the vertical axis marked on femur. The angle formed between these two lines was measured by goniometer.
- l) *Canal flare index (CFI)*: It is defined as the ratio of the intracortical width of the femur at a point 20 mm proximal to the lesser trochanter to that at the medullary isthmus, allowing us to classify the femur into three general shapes: Normal, Stove pipe and Champagne flute.

Various anatomical representation and radiological measurement parameters are well depicted in Fig. 5.

### **Clinical Correlation**

The implants used for osteosynthesis and arthroplasty were inserted in these bones, as described in their respective operative steps. The operations performed were dynamic hip screw, dynamic condylar screw, cancellous screws, and blade plate both 95° and 130°, for osteosynthesis, and femoral endoprosthesis for arthroplasty. In the cases of femoral arthroplasty the china clay was used as cement to assess the cement mantle. After performing operations these bones were examined morphologically as well as radiologically as described above.

The comparison was done of both radiological and morphological measurements of lengths, diameters and angles. These parameters were correlated with the lengths, diameter and angles of standard implants available in the market for fixation of fracture trochanter, fracture neck femur and arthroplasty of hip. The standardization of the implants have been done taking into account that the present parameters of implants are acceptable in western bone mass, the percentage of volume occupied by these implants in western bone was compared, by the percentage of volume occupied by these implants in our femoral bone. And taking these as standard, modifications in implants size will be suggested in accordance to the anthropometric study of our race femora.

### **Results**

Table 1 shows the average values of the morphological parameters studied, their standard deviation, minimum and maximum values and Table 2 shows the radiological aspect of all the morphological measurements. Table 3 shows comparison with Western and Asian (Chinese and Caucasians in Hong Kong). The volume of implants in the femoral head was calculated using  $d^2/4 \times l$  where d is diameter of femoral head and l is length of implant [ $l = 2/3 d - 10$  mm (subchondral bone left)]. Table 4 depicts the percentage of femoral head volume occupied by various implants in different populations. Cross-sectional area of femoral neck is calculated by Formula  $p d^2/4$  (d = diameter). Table 5 represents the percentage of cross-sectional area of neck  $p d^2/4$  occupied by various implants in different populations.

### **Discussion**

There are considerable variations in the femoral geometry of populations across different geographical locations and ethnic groups (3). Implants for fixation of proximal femur fractures have been designed taking into consideration of the anthropometry of the western population which varies from those of other ethnic groups (1). Similarly the standard

**Table 1: Morphological measurements**

Dimensions	No.	Average	Minimum (mm)	Maximum (mm)	Standard deviation (mm)
Femoral head diameter	150	43.95	35.4	50.0	3.06
Femoral head length					
Maximum (superiorly)	150	36.9	24.4	49.2	4.11
Minimum (inferiorly)		25.5	16.0	36.5	4.26
Effective neck length					
Maximum (superiorly)	150	37.23	26.5	50.5	4.65
Minimum (inferiorly)		22.69	16.3	39.2	3.65
Neck diameter					
Anteroposterior	150	24.90	18.7	34.4	2.94
Superoinferior		31.87	23.3	40.9	2.91
Extracortical width, 20mm above lesser trochanter	150	50.24	39.7	63	4.81
Extracortical width at level of lesser trochanter	150	40.44	29.8	52.6	4.67
Extracortical width 20mm below lesser trochanter	150	30.70	22.1	36.6	3.13
Neck shaft angle (°)	150	123.5°	114°	136°	4.34
Angle of anteversion (°)	150	13.68°	0°	36°	7.92

**Table 2: Radiological measurements**

Dimensions	No.	Average	Minimum (mm)	Maximum (mm)	Standard deviation (mm)
Femoral head offset	75	38	29	47	5.52
Femoral head diameter	75	43.53	38	49	3.40
Femoral head position	75	50.15	41	62	4.80
Neck diameter	75	29.5	24	35	3.19
Canal width, 20 mm above lesser trochanter	75	43.5	33	53	4.37
Canal width at level of lesser trochanter	75	23.8	18	30	3.20
Canal width 20 mm below lesser trochanter	75	16.57	12	21	1.99
Endosteal width at the isthmus	75	10.11	6	15	1.90
Extracortical width at the isthmus	75	24.42	20	30	2.54
Isthmus position	75	112.92	87	128	10.58
Neck shaft angle (°)	75	123°	118°	140°	4.29

**Table 3: Comparison of measurements with other groups**

Average Dimensions	Present study (Indian)	Western (6,7)	Caucasian (5)	Hongkong (Chinese) (5)
Femoral head offset	38	43	–	–
Femoral head diameter	43.53	46.1	46	45
Femoral head volume (mm <sup>3</sup> )	29618.55	34181.41	30744.48	26782.67
Length of implant in femoral head (mm)	19.3	20.73	19.67	18.33
Femoral head position	50.15	51.6	–	–
Neck diameter	29.5	–	33	31
Canal width, 20mm above lesser trochanter	43.5	45.4	–	–
Canal width at level of lesser trochanter	23.8	29.4	–	–
Canal width 20mm below lesser trochanter	16.57	20.9	–	–
Endosteal width at the isthmus	10.11	12.3	–	–
Extracortical width at the isthmus	24.42	–	–	–
Isthmus position	112.92	113.4	–	–
Neck shaft angle (°)	123°	124.7°	136°	135°
Angle of anteversion (°)	13.68°	–	7°	14°
Cross-sectional area of femoral neck (mm <sup>2</sup> )	633	–	778.92	660.12

**Table 4: Percentage of femoral head volume occupied by various implants in different races**

Different studies	3 Cancellous screws	3 Acinis screws	2 Garden screws	DHS	Blade plates
Western	6.03	6.99	6.88	7.44	4.39
Caucasian	6.37	7.38	7.26	7.85	4.64
Asian (Hongkong Chinese)	6.81	7.89	7.76	8.39	4.96
Indian	6.24	7.24	7.11	7.69	4.55
Our study	6.48	7.52	7.39	7.99	4.72

**Table 5: Percentage of cross sectional area of neck occupied by various implants**

Different studies	3 Cancellous screws	3 Acinis screws	2 Garden screws	DHS	Blade plates
Caucasian	12.77	14.81	14.56	15.75	9.31
Asian (Hongkong Chinese)	15.07	17.48	17.18	18.58	10.98
Our study	15.72	18.23	17.92	19.38	11.45

commercially available marketed prostheses sometimes may not be the best fit to Indian patients because of the large anatomic variation (7). So the present study aimed to report proximal femoral geometry in Indian population and evaluate its impact on implant design.

In our ethnic race on radiological measurement average femoral head offset was 38 mm as compared to 43 mm in western literature. Similarly femoral head diameter in present study was 43.53 mm as compared to 46.1 mm in western literature. This shows that our skeleton is smaller than the western one. So in consideration of clinical importance of this parameter we shall have to think of smaller implants for osteosynthesis and may be a smaller size of endoprosthesis in few of our bones, especially in females. This dimension is also of clinical significance in acetabular cup size and the number of screws to be used in osteosynthesis of fracture neck of femur. In our set up smaller acetabular cup and lesser number of screws and smaller implants as DHS, DCS and blade plates need to be designed. As there is difference between the size and shape of the proximal femur of our race and western race with respect to canal width at different levels, hence the implants made according to western race do not fit accurately in our bones. There has to be a close match between the dimensions of the femur and the implant prosthesis. Similarly on radiological measurement the average intramedullary width of isthmus in our race was 10.11 mm (maximum being 15 mm and minimum being 6 mm) as compared to 12.3 mm in western literature (maximum being 18.5 and minimum being 8 mm). There is marked difference between the two races in this parameter. This parameter is of immense importance in choosing the right size of the stem of endoprosthesis and the diameter of intramedullary nails because this parameter is much less in our race as compared to western race. On radiological measurement in our race average neck shaft angle was  $123^\circ$  (maximum being  $140^\circ$  and minimum being  $118^\circ$ ). In western literature average neck shaft angle was

$124.7^\circ$ , maximum being  $154.5^\circ$  and minimum being  $105.7^\circ$ . In Caucasian male average is  $136^\circ$  with maximum being  $161^\circ$  and minimum  $120^\circ$ . In Caucasian female average is  $133^\circ$  with maximum being  $145^\circ$  and minimum  $115^\circ$ . This dimension is of significance in angled implants such DCS, DHS, blade plate. This angle being lesser in our race, we should prefer implants of lesser angle to avoid their superior cut through in the femoral head and neck. On radiological measurement femoral head position average was 50.15 mm in the present study as compared to 51.6 mm in western population. There is no significant difference between the two, probably because there is not much difference between neck shaft angle of our and western race.

The percentage of cross-sectional area of neck occupied by three cancellous screws of 6.5 mm in the neck is 12.77% in Caucasian as compared to 15.72% in our study. Therefore, the volume of bone mass replaced by metal is more in our patients as compared to counterpart in west. The percentage of femoral head volume occupied by three cancellous screws is 6.48% in our study as compared to 6.37% and 6.03%, in Caucasian and western, respectively. So, the chances of union reduce when 3 lag screws of 6.5 mm diameter each are inserted in the already compromised head and neck of the femur, especially in females. Therefore, it is advisable to put only two screws in place of three. In case we need to put 3 cancellous screws, one should be put as a cantilever along the superior border of the neck, which will hold only in the trochanter and the head. If we reduce the thread diameter of cancellous screws to 6.0 mm then, the percentage of femoral head volume occupied by three cancellous screws in our race becomes 5.52% which is nearly ideal for our race. The main hold of the screw threads is in the head of the femur. The head length is more in the superior part, the average is 36.9 mm as compared to the inferior part where the average is 25.5 mm. The cancellous screws are available in 16 mm and 32 mm thread length. Considering these parameters the screw thread, especially the 32 mm thread length, will not cross the fractured

site in subcapital and transcervical fracture neck of the femur which is the prime requisite for union. Regarding the 16 mm thread length, it will cross the fracture site in subcapital and transcervical fracture neck femur in normal head which has reasonably adequate head length superiorly. In the central and superior area there is otherwise ample space available for a good hold. Therefore, in adults, subcapital and transcervical fractures, the 32 mm thread length, 6.5 mm or 7 mm cancellous screws should preferably not be used. The 16 mm thread length hold is good if they are passed through the center of the neck or in the superior quadrant. In the inferior area the head length is small and if the 5-10 mm subchondral area is left, as recommended the chances of the threaded portion crossing the fracture site is minimal even with 16 mm threaded screws. Therefore, accuracy is of prime importance regarding the length of the screws as the margin of error is less.

The percentage of femoral head volume occupied by DHS is 7.99%, 7.69%, 8.39%, 7.85% and 7.44% in present study, Indian counterpart, Asian, Caucasian and western studies, respectively. Similarly percentage of cross-sectional area of neck occupied by DHS in our study is 19.38%, Asians 18.58% and Caucasian 15.75%. The compression of bone in the head and replacement of bone mass by metal produces a tamponade effect in head which has a large bearing on nonunion and avascular necrosis; which are the key complications of fracture neck of femur. Secondly, there are two kinds of barrels in DHS, long and short ones with length of 38 mm and 25 mm respectively, with the outer diameter of 12.6 mm each. So while using this kind of barrel, one has to be considerate in accordance with the fracture line, otherwise the barrel will be longer. This will further occupy more space upto the longer portion along with the neck length and will not allow the controlled collapse. In our study the average neck length is 32 mm and only the short barrel should be used, because in using a long barrel there is always a danger of barrel crossing the fracture site, thereby preventing

compression at the fracture site and controlled collapse thereafter. Thirdly the thread length of the DHS screw is 22 mm, with the outer diameter of 12.5 mm, and shaft diameter of 8 mm. To put the 12.5 mm screw we have to tap for 12.5 mm which takes out a lot of bone mass both from the neck and the head. The head length in our series varies from 25.5 mm to 36.9 mm and for proper purchase of DHS screw 5-10 mm subchondral bone is to be left, resulting thereby that screw thread which is 22 mm in DHS will not cross the fracture site in subcapital fractures. Lastly in our study, the neck shaft angle was found to be 123° (average radiologically), though ranging from 118° to 140°. DHS is available in angles starting from 135° to 150° at the difference of 5°. From the above information it appears that the 135° angle is more and hence chances of the superior cut through of the implant are more. Otherwise one has to make the entry point at such a level on the lateral side of trochanteric area so that the tip of screw lies in the center or posteroinferior quadrant of the head. To achieve this valgus osteotomy will be needed simultaneously for a better approximation of femoral shaft with the plate, and thereby achieving an undesirable overall coxa valga in comparison to contralateral hip which may result in limb length discrepancy and avascular necrosis of head of femur. We conclude that for the Indian patients, the implant size should be reduced to 11.5 mm in place of 12.5 mm, then the cross-sectional area occupied in the neck will be 16.40% and the percentage of femoral head volume occupied will reduce to 6.76%, which are within the desirable limits. This should be done even with compromising the strength of the implant, to have better biology, which is the key factor for union and vascularity. The threaded portion should also be reduced from 22 mm to 15 mm, and the implant should also be available in 120°, 125° and 130° in accordance with our patients requirement. Also we should always procure the X-rays of both the hips to achieve same neck shaft angle preoperatively as it varies from person to person. Regarding the diameter and thread length parameters, same is true with DCS screw but its angle is acceptable.

In the present study, the CFI varies from 2.75 to 8.5. Depending on the CFI, the shape of the medullary canal, the normal canal type is 50%, champagne-fluted canal type in 38.46% and stovepipe canal type in 7.69%, and in a few cases do not fit in any of the types described above. The implants available are in variable lengths, ranging from 126 mm to 174 mm, with distal width ranging from 7 mm to 11 mm and anteroposterior thickness ranging from 6 mm to 8.5 mm. Our isthmus position ranges from 87 mm to 128 mm (average 112.92 mm) and the endosteal diameter at the level of isthmus varies from 6 mm to 15 mm (average 10.11 mm). Therefore, in the Indian patients only smaller prostheses are used, and in case of thin and lean patients (especially of younger age group) even CDH implants are good enough. At a distance of 20 mm above the lesser trochanter, the anteroposterior canal width was found to differ by 45.4%, when compared with a French population which can affect the mechanical stability of femoral stem (8). We recommend endoprosthesis having length ranging from 100 mm to 150 mm, distal width from 6 mm to 11 mm and anteroposterior thickness from 5.5 mm to 8 mm. The incidence of intraoperative complications like splintering and fractures ranges from 4% to 21% (9-11). These are due to over-sized implants available that have been manufactured basically with western parameters. Most femoral stems are designed to extend to the isthmus of medullary canal, so that the component is stable and there is a 2 mm cement mantle around it. Therefore, only smaller sized implant, both in length as well as in thickness, with straight and polished stem, are preferred. To achieve these conditions the manufacturers should reduce the geometric measurements of endoprosthesis but at the same time should not compromise on strength of implant. Another important point in total hip arthroplasty is restoration of original position of the center of head along with the limb length equality and the restoration of the original balance of abductors (6). For this purpose femoral components are available in a long range of neck lengths for each separate stem size.

To have a good muscle balance and limb length, the head offset is an essential component. There are various implants available with variable offsets ranging from 32.8 mm to 50 mm. In our study the head offset ranges from 29 mm to 47 mm (average 38 mm), hence in our patients 37.5 mm to 44 mm head offsets are suitable. So the clinical result of the above observations made in relation to the medullary canal geometry is, that the implant needs to be designed on the basis of anthropometric data available, along with other factors like age, sex and the environment, etc. This will minimise the preoperative and postoperative complications involved in total hip arthroplasty, although for a perfect match each implant needs to be customised.

Some other authors have also reported the assessment of geometry of proximal femur in Indian population and have suggested modifications in implants. Pathrot *et al* (1) advocated certain modifications in the presently available short cephalomedullary nail designs for them to better fit the anatomy of our subset of population: (a) two nails of 125° and 135°; (b) the medio-lateral angle at the level of 65 mm from the tip of the nail; (c) two femoral neck screw placements (35 and 45 mm from the tip of the nail); and (d) five different sizes of distal width for better fit in canal (9-13 mm). Maji *et al* also found variations in the morphology of the proximal femur between the Indian population and that of other countries, and advocated the need for standardizing THR implant sizes for the Indian population, especially for cementless implantation (3). Rawal *et al* observed a difference of 16.8% in the femoral head offset between Indian and Swiss populations, which can affect soft tissue tension and range of motion (7). Maheshwari *et al* also reported that when compared with the Western data, the femoral neck anteversion values were 3-12 degrees lower and the combined anteversion values were 3-5 degrees lower in Indian adults (11). The acetabulum anteversion values were comparable, but were skewed towards the higher side (11). But Saikia *et al* observed that the neck shaft angle and the femoral neck anteversion in

**Table 6: Our recommendations for implant dimensions**

<b>Implants</b>	<b>Presently available dimensions</b>	<b>Our recommendations</b>
Cancellous screw	Thread diameter 6.5 mm	Thread diameter 6 mm
	Thread length 16 mm, 32 mm	Thread length 16 mm
Acinis screw (cannulated)	Thread diameter 7 mm	Thread diameter 6.5 mm
	Thread length 16 mm, 32 mm	Thread length 16 mm
Garden screw	Thread diameter 8.5 mm	Thread diameter 8 mm
DHS screw	Thread diameter 12.5 mm	Thread diameter 11.5 mm
	Thread length 22 mm	Thread length 15 mm
	Barrel short and long	Barrel short
	Angles 135° to 150° (at difference of 5°)	Angles 120° to 150° (at difference of 5°)
Blade plate	‘U’ profile 6.5x16 mm	‘U’ profile 6.5x12.5 mm
	Angles 95° and 130°	Angles 95°, 120°, 125° and 130°
Gamma nail	Standard Gamma nail	Modified by Leung <i>et al</i> <sup>1</sup>
	Mediolateral angle-10°	Mediolateral angle 4°
	Length 200 mm	Length 180 mm
	Diameter of distal shaft 12 mm, 14 mm and 16 mm	Diameter of distal shaft 11 mm and 12 mm
	and 12 mm	This modified nail is also suitable to our race femora
Endoprosthesis	Length 126 mm to 174 mm	Length 100 mm to 150 mm
	Distal width 7 mm to 11 mm	Distal width 6 mm to 11 mm
	Anteroposterior thickness 6 mm to 8.5 mm	Anteroposterior thickness 5.5 mm to 8 mm
	Modularity up to 10 mm	Modularity up to 15 mm
	Head offset 32.8 mm to 50 mm	Head offset 37.5 mm to 44 mm
	Stem type – -Banana shape -Straight -Rough and grooved -Flat back -Rounded -Rectangular cross section -Trapezoidal and diamond shaped	Stem type – Polished, straight and trapped collarless stem is preferred.

individuals of North eastern region of India was 5-6 degrees more than the western literature (12).

Anthropometric studies for proximal femur in ethnic groups other than western population have reported significant differences. Pi *et al* reported that Chinese proximal femoral parameters are significantly different from Westerners (13). Compared with Westerners, the offset was smaller, while the neck shaft angle was significantly larger in Chinese population (13). Most parameters of the proximal femoral medullary cavity diameter were significantly smaller in Chinese population than those in Westerners (13). Atilla *et al* reported osteometry of the femora in Turkish individuals (14). They observed diverse features of femoral geometry in Turkish individuals compared to Western populations and advocated that these differences should be taken into account in the design and development of hip prostheses (14).

The observations in the present study have profound implications. Not only are western implants large in size, their angles, and orientations and thread length also mismatch Indian femora. Implants designed for western skeletons occupy much more space in the Indian femoral head and neck. A certain subset of Indian femora does not have any implant available to them as they are too small. Furthermore, a shorter neck length implies that the threads of cancellous or Garden screws used to fix neck fractures may not cross the fracture site thereby failing to provide compression and thus defeating the whole purpose of the surgery. If too much bone is replaced by metal a tamponade effect can ensue that may cause avascularity of femoral head, consequently resulting in nonunion of neck fractures and/or AVN. Since our heads are smaller, the threads of screws often fail to cross the fracture of neck of femur especially if the fracture is sub capital and the screw placement in the inferior quadrant of head. This means we must have screws with shorter thread lengths. In thin built and short individuals the neck may not have space enough to occupy the three 6.5 mm screws recommended for

fixation of neck fractures. A smaller neck shaft angle implies that a DHS inserted through the classical entry portal using angled guide will either go into the superior quadrant or pull the fracture in valgus both of which are undesirable. We probably require DHS with smaller angles. Our recommendations for different implants are shown in Table 6.

The implications of the study on arthroplasty operations cannot be overemphasized as these are designed to reproduce the normal anatomy as far as possible. Orthopaedic surgeons always stress the need for a proper implant-patient match in hip joint replacements, in particular, for a cementless femoral stem (7). The complications of mismatch are aseptic loosening, improper load distribution, and discomfort (7). The clinical symptoms are due to the bone implant mismatch, which result in micromotion. There are studies, which highlight that these micromotions should be reduced to 14 micra or less, to prevent osteolysis and aseptic loosening (5). We agree with Roy *et al* that improved knowledge of the morphology of the proximal femora will assist the surgeon in restoring the geometry of the proximal femur during total hip arthroplasty and the data could be used as a guideline to design a more suitable implant for Eastern Indian population (2).

## References

1. Pathrot D, Ul Haq R, Aggarwal AN, Nagar M, Bhatt S (2016). Assessment of the geometry of proximal femur for short cephalomedullary nail placement : an observational study in dry femora and living subjects. *Indian J Orthop* **50**(3): 269-276.
2. Roy S, Kundu R, Medda S, Gupta A, Nanrah BK (2014). Evaluation of proximal femoral geometry in plain anterior-posterior radiograph in Eastern-Indian population. *J Clin Diagn Res* **8**(9): AC01-AC03.
3. Maji PK, Roychowdhury A, Datta D

- (2012). Investigating the morphology of the proximal femur of the Indian population towards designing more suitable THR implants. *J Long Term Eff Med Implants* **22**(1): 49-64.
4. Hoaglund FT, Low WD (1980). Anatomy of the femoral neck and head, with comparative data from Caucasians and HongKong. *Chinese Clin Orthop* **152**: 10-16.
  5. Reddy VS, Moorthy GVS, Reddy SG (1999). Do we need a special design of femoral component of total hip prosthesis in our patients? *Indian J Orthop* **33**(4): 282-284.
  6. Noble C, Jerry W, Alexander BS, *et al* (1988). The anatomical basis of femoral component design. *Clin Orthop Rel Res* **235**: 148-164.
  7. Rawal B, Ribeiro R, Malhotra R, Bhatnagar N (2012). Anthropometric measurements to design best-fit femoral stem for the Indian population. *Indian J Orthop* **46**(1): 46-53.
  8. Bombelli R, Santore RF (1984). Cementless isoelastic total hip prosthesis: preliminary report on the first 215 consecutive cases. In: *The Cementless Fixation of Hip Endoprosthesis*. Morscher E, ed. New York: Springer-Verlag, 243.
  9. Engelhardt A (1984). Casual histogenesis and biomechanical discoveries as a basis for cementless fixation of hip endoprosthesis. In: *The Cementless Fixation of Hip Endoprosthesis*. Morscher E, ed. New York: Springer-Verlag.
  10. Zweymuller K (1986). A cementless titanium hip endoprosthesis system based on press-fit fixation: basic research and clinical results. *Instr Course Lect* **35**: 203-225.
  11. Maheshwari AV, Zlowodzki MP, Siram G, Jain AK (2010). Femoral neck anteversion, acetabular anteversion and combined anteversion in the normal Indian adult population: a computed tomographic study. *Indian J Orthop* **44**(3): 277-282.
  12. Saikia KC, Bhuyan SK, Rongphar R (2008). Anthropometric study of the hip joint in northeastern region population with computed tomography scan. *Indian J Orthop* **42**(3): 260-266.
  13. Pi Y, Zhao Y, Wang W, He Z, Mao X (2013). Measurement of proximal femoral morphology and analysis of 500 cases in Hunan Province. *Zhong Nan Da Xue Xue Bao Yi Xue Ban* **38**(9): 925-930.
  14. Atilla B, Oznur A, Cağlar O, Tokgözoğlu M, Alpaslan M (2007). Osteometry of the femora in Turkish individuals: a morphometric study in 114 cadaveric femora as an anatomic basis of femoral component design. *Acta Orthop Traumatol Turc* **41**(1): 64-68.

## **Molecular and Functional Basis of Cystic Fibrosis in Indian Patients: Genetic, Diagnostic and Therapeutic Implications**

*Rajendra Prasad*  
Department of Biochemistry,  
Postgraduate Institute of Medical Education and Research,  
Chandigarh, India.

### **ABSTRACT**

Cystic fibrosis (CF, MIM#219700) is a common autosomal recessive disorder among Caucasians, which was considered as rare disease for Indian population. CF is caused due to presence of mutations in the cystic fibrosis transmembrane conductance regulator (*CFTR*) gene. In this study, we established a spectrum of mutations from both classical CF as well as from infertile male patients with congenital absence of vas deferens (CAVD). In Indian classical CF patients, we reported 14 previously known and eight novel mutations, viz. 3986-3987 delC, 876-6 del4, 1792 InsA, L69H, S158N, Q493L, 1530L and E1329Q. The frequency of *delta 508* was found to be 27%. Absolute linkage between *delta 508* and *KM19-GATT TUB9-M470V-T854T* haplotype predicts a relatively recent appearance of *delta 508* mutations in Indian population. The *CFTR* gene analysis in CAVD infertile males documented 13 different *CFTR* gene mutations and 1 intronic variant that led to aberrant splicing. *P.Phe 508 del* (n= 16) and *p.Arg 117 His* (n=4) were among the common severe forms of *CFTR* mutations identified. The *IVS-8-T5* allele (mild form of mutations) was formed with an allele frequency of 28.3%. Eight novel mutations were also found in the *CFTR* gene from our patient cohort. We also investigated whether genetic modifiers, viz. transforming growth factor (TGF- $\beta$ ) and endothelial receptor type A (EDNRA) of CF lung disease also predispose to CAVD in association with *CFTR* mutations, which were associated with the CAVD phenotype.

Functional characterization of identified 11 novel *CFTR* gene mutations disclosed that a significant reduction in channel activity for L69H and S549N mutants in *CFTR* expressing cells was observed whereas impaired *CFTR* protein maturation was noticed only in L69H substitute *CFTR*. *CFTR* correctors (*VX809*) rescued the defect due to L69H mutation, which is evidenced from detection of C band in L69H mutant expressing cells pre-treated with *VX809*. The chloride channel activity in S549N and L69H mutant *CFTR* was also restored in presence of *CFTR* potentiators *VX770*.

Above findings confirms heterogeneity of *CFTR* mutations in Indian classical and non-classical CF patients. They may help in developing a strategy to develop counseling and therapeutic approach for CF patients in India.

*Keywords:* Cystic fibrosis, genetic mutation, *CFTR*.

---

*Correspondence:* Dr. Rajendra Prasad, Former Professor & Head, Department of Biochemistry, Postgraduate Institute of Medical Education and Research, Chandigarh-160012. Mob: +91-9417401134. Email : fateh1977@yahoo.com.

DR. V.R. KHANOLKAR ORATION delivered during the NAMSCON 2018 held at the Mahatma Gandhi Medical College & Research Institute, Puducherry.

## Introduction

Cystic fibrosis (CF MIM#219700) is the most common lethal autosomal recessive monogenic disease in Caucasian population with an average prevalence of one in 2500 live birth with carrier frequency 1 in 25 individuals (1). Notwithstanding, CF is still thought to be very rare in Indian population (2). However, published reports indicate that CF is probably far more common in people of Indian origin than previously thought but is underdiagnosed or missed in majority of cases. Dr. Bhakoo reported first case of CF in 1968 from PGIMER, Chandigarh (3). Later, we estimated the relative frequencies of various genetic disorders, which were found, with 7.56% frequency (4). The mutations in the CF transmembrane conductance regulator gene (*CFTR* or *ABC C7*; MIM # 602421), which are responsible for both classic and non-classic presentation of the disease (CAVD, MIM # 22180) (5, 6). The *CFTR* gene was identified and cloned about two decades ago (7, 8). The *CFTR* gene is located on the long arm of chromosome 7 (region q31 – q32) encompassing 250 kb and comprising 27 exons (7-9). It encodes a trans-membrane

protein of 1480- amino acids that function as a CAMP- regulated chloride channel in exocrine epithelia (10). Hydropathy plot analysis disclosed that *CFTR* protein composed of two motifs, each containing a membrane spanning domain (MSD) that is composed of six transmembrane helices and nucleotide binding domain (NBD) that contains sequence predicted to interact with ATP (II). MSD-NBD motifs are linked by a unique domain termed as regulatory domain (R) that contains multiple phosphorylation sites and many charged amino acids. The carbonyl terminal, consisting of threonine, arginine, and leucine (TRL) which is anchored through a PDZ type – binding interaction with the cytoskeleton (11, 12) (Fig. 1).

More than 2000 sequence variants have been identified in the *CFTR* gene (<http://www.genet.sickkids.on.ca/fchrome.html>) and many of them have been implicated in a variety of *CFTR* related pathologic conditions such as respiratory distress, pancreatic insufficiency, meconium ileus and congenital absence of the vas deferens (CAVD) (13). *Delta 508F* is the most common *CFTR* mutation

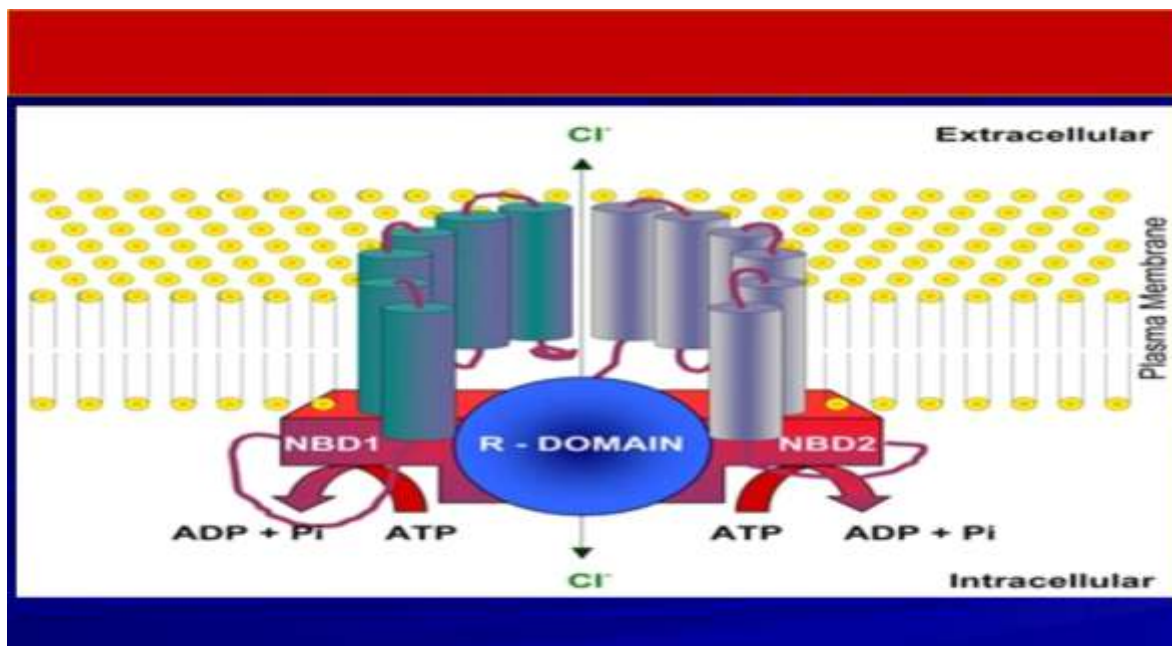


**Fig.1: Hypothesized structure of CFTR showing proposed structure of CFTR protein.**

worldwide, which is present upto 92% of patients with CF. However, this frequency varies among countries and ethnic groups (<http://www.cftrscience.com>). All these mutations are classified into six classes based on the mechanism of the disruption of CFTR (14) and the absence of the CFTR protein at the apical plasma membrane which include defective protein synthesis, impaired protein maturation leading to protein degradation, defective regulation of CFTR channel activity, altered ionic selectivity and conductance, lowered CFTR mRNA amount and decreased protein stability.

CAVD is characterized as an isolated urogenital form of CF which is associated with normal spermatogenesis, but absence of sperm in the ejaculate due to lack of vas deferens (15). More than 95% of males with CF are infertile due to obstructive azoospermia caused by absent, atrophic or fibrotic Wolffian duct structure (16). The *p. Phe 508 del*, *p. Arg 117H* is and *T5 allele* were identified as most common CFTR mutations in caucasians associated with CAVD phenotype (16, 17). Despite advances in understanding the pathophysiology of CF, there are still many inexplicable differences in its clinical association with CAVD. The role of intensifying the severity of classical CF is well established (17, 18). Transforming growth factor (TGF  $\beta$ ), codon 10 polymorphism (rs180470) and codon 25 polymorphism (rs1800471) as well as endothelial receptor type-A (*EDNRA*) gene polymorphism have been previously established in enhancing the severity of classical CF (17, 19). Molecularly, established mutations including preferentially novel and rare mutations is urgently needed for functional characterization at cellular level, so that, therapeutic molecules could be developed to target underlying molecular defect. Additionally, the cellular and functional data on these mutations can improve CF genetic counseling. Recent advances of targeted molecular therapies and high throughput screening have resulted in multiple drug therapies that target many important mutations

in the CFTR protein (20).

In this manuscript, we provide the work done on CF at Postgraduate Institute of Medical Education and Research, Chandigarh with special reference to its diagnostic and molecular characterization of spectrum of mutations from both classical and non-classical forms of CF. Haplotype association have been used to trace the origin and age of different CF mutations worldwide (21). There is no information available in this regard from Indian subcontinent. Therefore, haplotype study was also carried out using associated intragenic and extragenic marker haplotypes. The study was also performed to investigate whether genetic modifiers of CF lung disease also predispose to CAVD in association with CFTR mutations. We also provide the latest results and current progress of CFTR modulators for the treatment of cystic fibrosis, focusing on potentiators of CFTR channel gating and *p.Phe508del* CFTR mutation. Special emphasis is placed on the molecular basis of understanding these new therapies.

### **Molecular Diagnosis of Cystic Fibrosis and its Underlying Pathogenesis**

The diagnosis of CF has vast implications for patients and their families. The broad spectrum of clinical disease and reports of over 2,000 different mutations have made the CF diagnosis difficult (22). The guidelines for CF diagnosis were established by the Cystic Fibrosis Foundation for diagnosis of both infants with positive newborn screening (NBS) findings and older patients presenting with an indistinct clinical picture. CF Foundation proposed the following diagnostic algorithm state: the diagnosis of CF should be based on the presence of one or more characteristic clinical features *viz.* respiratory, gastrointestinal or gastrourinary symptom, a history of CF in a sibling or a positive NBS test, plus laboratory evidence of an abnormality in the CFTR gene or protein (23, 24). Either biological evidence of channel dysfunction such as an abnormal sweat chloride

test or nasal potential difference and identification of CF disease causing mutation on each allele of the *CFTR* gene are acceptable evidence of a *CFTR* abnormality. Newborn screening depends on initial analysis of fetal blood for high values of immunoreactive trypsinogen (IRT) followed by genetic testing or repeat (25).

The sweat chloride test remains the initial test of choice and gold standard for CF diagnosis despite its limitations. Sweat chloride test was developed by Gibson-Cooke in 1959 (25). The test is performed *via* pilocarpine iontophoresis, which is used to stimulate sweat gland secretion. The sweat is collected and analyzed for chloride concentration. The underlying mechanism of elevated levels of sweat sodium was demonstrated by Roeve *et al* (26) (Fig. 2).

Sweat chloride concentration above 60 mmol per liter (>70 mmol/L in adolescent and adults) is suggestive of cystic fibrosis. In normal individuals and carriers of the CF gene, the mean sweat chloride concentrations are 30 mmol/L.

Cut-off value for infants is 30 mmol/L (27). A positive sweat test is diagnostic as long as it is performed on adequate amount of sweat (>100 mg) in CF. A second test for *CFTR* function such as nasal potential difference measurement or analysis of rectal mucosal biopsy is recommended if sweat test is equivocal (28).

DNA analysis in establishing CF diagnosis is most useful for those individuals with sweat chloride values in the intermediate range. Two or more disease causing *CFTR* mutations should be located on different alleles as CF is an autosomal recessive disease. CF Foundation recommends testing for the 23 CF mutation panel developed by the American College of Medical Genetics (ACMG). These mutations have been demonstrated to cause sufficient loss of *CFTR* function to confer CF disease and are therefore noted as conclusive genetic evidence for diagnosis of CF (23). Indirect non-invasive parameters available for assessing the pancreatic function test are serum immunoreactive trypsin (IRT), fecal chymotrypsin, stool immunoreactive human

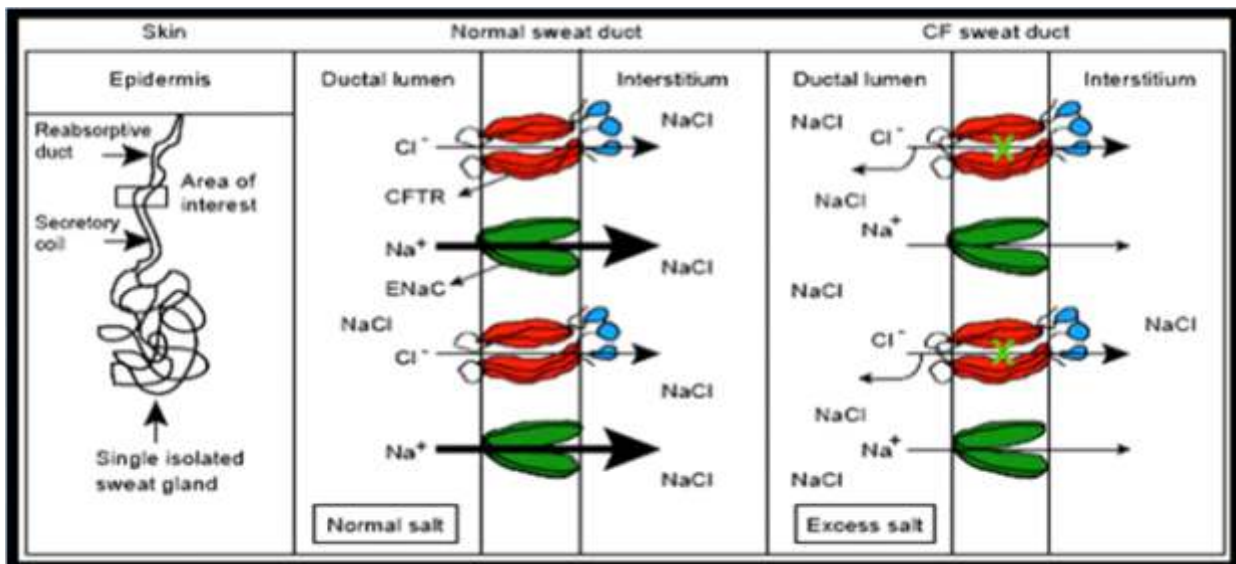


**Fig.2: Mechanism understanding elevated sodium and chloride levels in the sweat of CF patients.** Left panel shows cartoon of a sweat gland with sweat duct projecting out of the sweat gland through dermis into the epidermis. Middle panel shows role of CFTR and ENaC in maintaining normal salt concentration in sweat. Last panel shows dysfunctional CFTR leading to elevated salt concentration in sweat.

lipase and stool fat excretion as a gold standard (29).

### Spectrum of Mutations in Classical Cystic Fibrosis

A prospective cohort study was designed to establish a spectrum of mutations in *CFTR* gene. In this study, 1005 suspected CF subtypes were subjected for sweat chloride measurement. Notably, 45 subjects were diagnosed as CF on the basis of classical clinical phenotype and elevated sweat chloride. On the basis of clinical symptoms and autopsy reports that confirmed the diagnosis of CF in three patients with normal sweat chloride were also included. Besides, 2 infants with raised IRT were included as CF subjects.

Demographics and family history of CF subjects revealed that average age at diagnosis in CF subjects was 62.8 months compared to 9.3 months at age of presentation. Male to female ratio was 35.15. Notwithstanding, females had a higher median age at diagnosis (33 months) as compared to males (18 months). History of previous sib death due to respiratory or gastrointestinal problems was observed in 9 families. Consanguinity was noticed in three and history of similar gastrointestinal or respiratory complaints was recorded in another 4 families.

In 1 case, the patient's mother had a history of chronic pancreatitis and diabetes (30).

### Clinical Findings

The usual presentations include failure to thrive (94%), malabsorption (82%), chronic cough (90%), recurrent or persistent pneumonia (79%) and meconium ileus (10%). Mean Schwachman-Kidczyski score was  $57.34 \pm 12.07$ . The median age of CF patients with *P.aeruginosa* colonization was 39 months compared to 8 months with *S.aureus*. Pancreatic insufficiency was present in 37 patients (77%). Mean IRT levels in CF patients were  $176.43 \pm 141.23$  ug/L. Determination of fecal fat revealed steatorrhoea ( $7.36 \pm 4.56$  g/24h) in 8 patients out of 15 tested (53.33%). Notably, all patients with liver disease (n = 6) and meconium ileus (n = 5) had pancreatic insufficiency.

### Sweat Chloride

Median sweat chloride value in CF subjects was 86.25 mEq/L. All individual patient values were mean of two/three repeat sweat chloride estimation on different days. Amount of sweat chloride collected was more than 100 mg on each occasion ( $198 \pm 30$  mg). In 2 infants, adequate sweat could not be collected. Fig. 3 shows individual sweat chloride values of CF (n

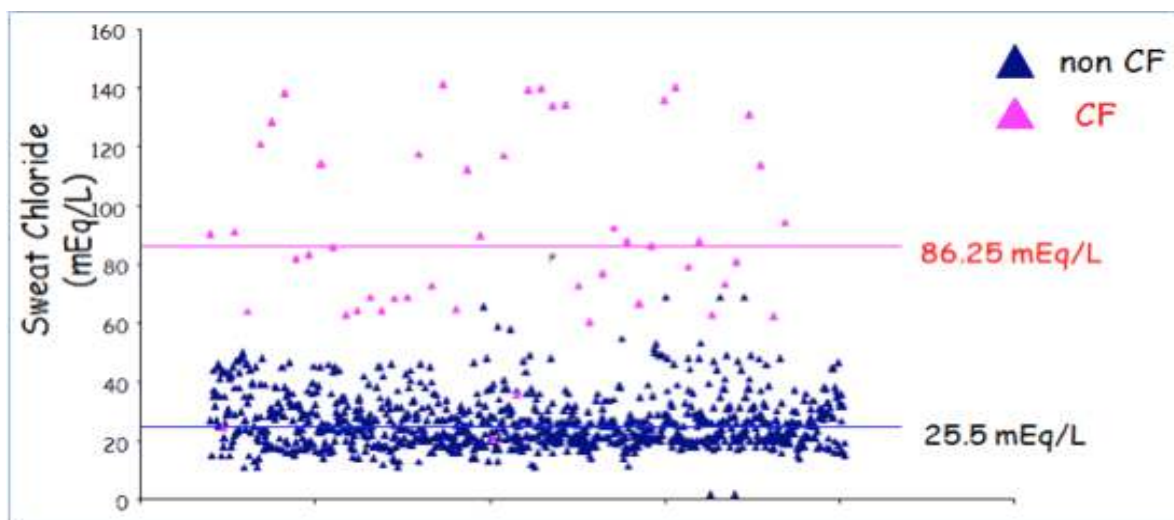


Fig.3: Comparison of sweat chloride values between CF and non-CF cases.

= 48) and non-CF (n = 956) subjects. Median sweat chloride value of 86.25 mEq/L in CF was significantly elevated as compared to 25.5 meq/L in non-CF individuals. In India, there are only few centers where sweat testing is performed.

### **Identification and Molecular Characterization of Mutations in the *CFTR* Gene from Classical CF**

The spectrum of mutations in *CFTR* gene from classical CF at PGI is listed in Table 1. In this study, 100 unrelated CF chromosomes were first analyzed for most common *delta F508* mutation, which was found with 27% of CF chromosomes. *R117H*, *R553X*, *N1303K* and *G551D* were identified by ARMS on a total of five chromosomes.

By restriction digestion, 3849+10 Kbc-T was found in 3 CF subjects with normal sweat chloride. Using SSCP and subsequently DNA sequencing, mutations were molecularly characterized in 31 of the remaining 65 CF chromosomes which include nine missense mutations, viz. *L69H*, *S158N*, *Q493L*, *Y517C*, *V520F*, *I530L*, *S549N*, *E1329Q* and *Y1381H*, one insertion mutation (1792 insA), three splice site mutations (*876-6del4*, *1525-1G-A*, *3120+1G-A*), two deletion mutation (*1161 delC*, *3986 delC*), and one nonsense mutation (*L218X*). *S549N* and *1525-1G-A* were the second most common mutations observed in our population (5% each). Among them, 8 novel mutations, viz. *L69H*, *Q493L*, *S158N*, *I530L*, *E1329Q*, *1792 InsA* and *3986-3987 delC* were identified in one patient each. Notably, none of novel mutation was found in 50 control subjects.

It is noteworthy here that output productions score for 3 novel mutation (*S158N*, *I530L* and *E1329Q*) was found 0.05, representing deleterious effects using molecular modeling and Bioinformatics CMMB. The most common CF mutation worldwide is the deletion of a phenylalanine residue at position 508. A review of all genotyped South Asian patients

showed that *delta 508* is identified in 19% to 44% CF alleles (31-33), which is lower than the reported frequency of 66% worldwide CF population. In our study, *delta F 508* represents only 27% of the analyzed and 41% of the identified CF allele (30). The striking characteristic of the mutation spectrum is absence of some mutations common in the Mediterranean and European population (34). *S549N* and *1525-1G-A* were the second most common mutations, followed by *3849+10 kbC-T*. This corroborates the study of Shastri *et al* (35) which has recommended testing Indian CF patient for *delta F508*, *1161 delC*, *3849+10 kbC-T* and *S549N*. Absolute linkage between *delta F508* and *KM.19-GATT -TUB9-M470V-T854T* haplotype (2-2-1-1-1) predicts a relatively recent appearance of *delta F508* in Indian CF patients (28). Low frequency of *delta F508* mutation and detection of eight novel and thirteen rare mutation imitate a heterogeneous spectrum of mutation in Indian CF patients. Notwithstanding, CF mutation frequencies and haplotypes vary widely among different populations and haplotype heterogeneity has been found to be greater in population with lower *delta F508* frequencies (36). We documented NBD1 and NBD2 as the hotspots identified in *CFTR* protein in CF patients at our institute (Table 1).

### **Identification and Molecular Characterization of Mutations in the *CFTR* Gene from Non-Classical CF (CAVD)**

#### ***Demographics and Clinical Variables***

At our center, we used the following algorithm: male CAVD patients comprising of bilateral absence of vas deferens, unilateral absence of vas deferens, absence of epididymis, and absence of seminal vesicle as well as renal agenesis. The median age of the CAVD patients at the time of enrollment was 28 years and most of the patient consulted an urologist only after the evaluation of their female partner by a gynecologist. Semen value (1.6±0.61) was much less in comparison to normal range (2-4 mL),

**Table 1: Frequency of CFTR mutaitons identified in Indian CF Patients. Total Chromosomes-100; known mutations - 66%, unknown mutaitons - 34%**

S.No	Mutation	Nucleotide change	Consequence	Exon/Int ron	Domain	Frequ ency
1	Delta F508	Deletion of 3bp (CTT or TTT) between 1652 and 1655	Deletion of Phe at 508	Exon 10	NBD1	27
2	1161 delC	Deletion of C at 1161	Frameshift	Exon 7	TM6 of MSD1	2
3	3986-3987 delC*	Deletion of C at 3986	Frameshift	Exon 20	NBD2	2
4	1792ins A*	Insertion of A at 1792	Frameshift	Exon 11	NBD1	2
5	R117H	G to A at 482	Argininie to Histidine at 117	Exon 4	Extracytoplasmic loop llinking Tm1-TM2	2
6	LC 9H*	T To A at 338	Leucine to Histidine at 70	Exon 3	NH2 terminal	1
7	S158N*	G To A at 605	Serine to Asparagine	Exon 4	Intracytoplamic loop llinking TM2-TM3	1
8	Q493L*	A to T at 1609	Glutamine to Leucine at 493	Exon 10	NBD1	1
9	Y517C	A To G at 1682	Tyrosien to Cystine at 517	Exon 10	NBD1	1
10	V520F	G To T at 1690	Valine to phenylalanine	Exon 10	NBD1	1
11	G551D*	A To C at 1 720	Isoleucine to leucine at 530	Exon 11	NBD1	2
12	S549N	G To A at 1778	Serine to Asparagine at 549	Exon 11	NBD1	5
13	G551D	G to A at 1784	Glycine to Asparatate at 551	Exon 11	NBD2	1
14	E1329Q*	G to C at 4117	Glutamate to Glutamine at 1329	Exon 22	NBD2	1
15	Y1381H	T To C at 4273	Tyrosine to Histidine at 1381	Exon 23	NBD2	2
16	N1303K	C To G at 4041	Asparagine to Lysine at 1303	Exon 21	Extracytoplasmic loop llinking Tm3-TM4	1
17	L218X	T To A at 785	Leucine to stop	Exon 6a	NBD1	1
18	R553X	C to T at 1789	Arginine to stop	Exon 11	-	1
19	876-6del4*	Deletion of 4 bp TACA from 876 -4	Splice site mutation	Intron 6a	-	2
20	1525-1G-A	G to A at 1525 -1	Splice site mutation	Intron 9	-	5
21	3120+1G-A	G To A at 3120 -1	mRNA splicing defect	Intron 16	-	2
22	3849+10kbC-T	C-T at 3849	Exon 9 skipping	Intron 19	-	3

\* denotes novel mutation; TM- transmembrane region; MSD - Membrane spanning domain; NBD - Nucleotide binding domain; Sharma et al (2008) Ann Human Genetics.

**Table 2: Spectrum of CFTR gene mutation in Indian CAVD males (n=110)**

Mutations	Nucleotide Change	Consequences	Exon/ Intron	No. of alleles
T5	Reduction of oligo T tract to 5T, c.1210-12T(5)	Aberrant splicing	Intron 8	59
F508del	c.1521_1523del CTT	Deletion of phenylalanine at 508	Exon 11	26
p.Gly480Ser	c.1438 G>A	Glycine to Serine at 480	Exon 11	1
p.Arg518Lys <sup>a</sup>	c.1553 G>A	Arginine to Lysine at 518	Exon 11	1
p.Arg117His	c. 350 G>A	Arginine to Histidine at 117	Exon 4	7
p.Gly126Cys <sup>a</sup>	c.376 G>T	Glycine to Cystine at 126	Exon 4	1
p.Ala141Gly <sup>a</sup>	c. 422 C>G	Alanine to Glycine at 141	Exon 4	1
p.His139Gln <sup>a</sup>	c.417 C>G	Histidine to Glutamine at 139	Exon 4	1
p.Ser118Pro <sup>a</sup>	c.352 T>C	Serine to Proline at 118	Exon 4	1
p.Arg170Cys	c.508 C>T	Arginine to Cystine at 170	Exon 5	1
p.Glu585Gln <sup>a</sup>	c.1753G>C	Glutamate to Glutamine at 585	Exon 13	1
p.Met281Arg <sup>a</sup>	c.842 T>G	Methionine to Arginine at 281	Exon 7	1
p.Arg933Thr <sup>a</sup>	c.2798 G>C	Arginine to Theronine at 933	Exon 17	1
p.Ser549Asn	c.1646 G>A	Serine to Asparagine at 549	Exon 12	1
p.Leu69His	c.338T > A	Leucine to histidine at 69	Exon 3	1
p.Phe87Ile	c.391T > A	Phenylalanine to isoleucine	Exon 3	1
p.Gly126Ser <sup>a</sup>	c.508G >A	Glycine to serine at 126	Exon 4	1
p.Phe157Cys <sup>a</sup>	c.602T > G	Phenylalanine to cystine at 157	Exon 4	1
p.Glu543Ala <sup>a</sup>	c.1760A> C	Glutamate to alanine at 543	Exon 11	1
p.Tyr852Phe <sup>a</sup>	c.2687A > T	Tyrosine to phenylalanine at 852	Exon 14a	1
3120 p 1 G-A	G >A 3120 p 1	Aberrant splicing	Intron 16	1
p.Pro1021Ser	c.3193C>T	Proline to serine at 1021	Exon 17a	1
p.Asp1270Glu <sup>a</sup>	c.3942T >A	Aspartate to glutamate at 1270	Exon 20	1

<sup>a</sup> Novel mutationsSharma *et al.*, 2009 (Human Reproduction) & Sharma *et al.*, 2014 (Molecular Human Reproduction)

however, the mean sweat chloride was in intermediate range (40-60 mEq/L). The mean serum hormone level of FSH, LH and testosterone were in normal range in CAVD patients.

### ***Spectrum of Mutations Identified in CAVD Patients***

Overall, 220 *CFTR* alleles were screened for mutation. We identified twenty three mutations (Table 2) (37-39). Two most common mutations, viz. *p. Phe 508 del* and *p. Arg 117H* is were found on 26 and 7 allele, respectively. Both of these mutations were found in the heterozygous conditions in all the patients. Another most common mild form of *CFTR* mutation, viz. *IVS8-T5 allele* observed on 59 alleles in infertile CAVD males. In 13% of CAVD, the mild mutation was present in both the alleles whereas in 15% of cases, *IVS8-T5* was detected in a compound heterozygous form with other mutation present in coding region of the *CFTR*. Other mutations were very rare. Among them, fourteen mutations were novel. All these novel mutations were subjected for determination of prediction score using SIFT (<http://blocks.fh.crc.org/sift/SIFT.html>) and confirmed by polyphen-2 (<http://genetics.bwh.harvard.edu/php>). Threshold for pathological mutations was 0.05. Among them, *Gly126Cys*, *Ser118Pro*, *Met281Arg*, *Arg933Thr*, *Lys69His*, *Glu543Ala* and *Asp1270Glu* were damaging mutation, which can perturb the protein structure (37-39).

Genetic analysis of the *CFTR* gene led to identification of the mutations in 81% of the Indian CAVD males and this detection was very similar to that of Caucasians, however, the spectrum of mutation in this study was different from that Caucasians (40-41). Notably, the allele frequency of *p. Phe508del* mutation in our population is similar to that of France (4) and Spain (5). The *5T allele* in our population was found with an allele frequency of 28% is very similar to that of Canada, Brazil (42, 43).

### **Association of Cystic Fibrosis Genetic Modifiers with Congenital Bilateral Absence of the Vas Deferens**

To investigate whether genetic modifiers of CF lung disease also predispose to CAVD in association with *CFTR* mutations, we tested the hypothesis that polymorphisms of TGF- $\beta$ 1 and *EDNRA* polymorphism might play a role in penetrance of CAVD. These polymorphisms have been reported to modify CF lung disease, and might also contribute as genetic modifiers of CAVD. Sixty CAVD subjects and fifty controls were investigated for candidate polymorphism *TGF- $\beta$ 1* or *EDNRA* associated with a more severe lung phenotype among CF disease. Importantly, CC genotype (SNP r5335) of *EDNRA* and TT genotype (SNP r51982073) *TGF- $\beta$ 1* were associated with CAVD to occur more frequently among CF individuals (37). TGF- $\beta$ 1 is the best described modifier of CF associated with pulmonary phenotype. In reference to our study, the human vas deferens, epididymis and seminal vesicles develop from the Wolffian duct. Notably, TGF- $\beta$ 1 and related signaling pathways play an important role in normal Wolffian duct development and differentiation (44, 45). On the other hand, other modifier of CF lung disease (*EDNRA*) is also associated with CAVD.

*EDNRA* has been implicated in normal formation of mammalian nervous system, the anorectum, and craniofacial structures such as mandible (46-48). *EDNRA* plays an important role during development of the vas deferens which could be due to loss of the vas in the setting of *CFTR* insufficiency. This is the first study in reference to the Indian population where we identify possible involvement of these pathways in an atypical CF-related condition, namely CAVD. Recently, it has been documented TGF- $\beta$ 1 receptor and P38 MAPK signaling reduce *CFTR* activity and probably enhance the effect associated with heterogeneous *CFTR* mutations and may result in male infertility (49).

### Functional Characterization and Pharmacological Correction of Novel and Rare Mutations

The striking characteristic of the identified mutations at our center were the presence of severe rare mutations but the absence of the most common mutations identified in the Mediterranean and European population, which clearly represented the heterogeneous spectrum of *CFTR* mutations at our Institute. These rare mutations are called *orphan mutation* because of their very low incidence. Moreover, rare familiar mutations cannot provide sufficient information on the phenotype due to these mutations, viz. *L69H*, *F87I*, *S118P*, *G126S*, *H139Q*, *F157C*, *F494L*, *E543A*, *S549N*, *Y852F* and *D1270E* from both classical CF patients and CAVD patients (40). It is noteworthy here that the cellular and function data on these mutations can improve CF genetic counseling. For functional characterization and therapeutic implications for these CF rare mutations, baby hamster kidney cells are an adherent cell line used for this study (50). Functional findings revealed that L69H was found as a novel class II CF mutation. The trafficking to the plasma membrane of L69H-*CFTR* is abnormal as corroborated by western blot analysis. Further confocal microscopic imaging showed the abundance of L69H mutated *CFTR* protein in the endoplasmic reticulum and absence on the plasma membrane. In view of above finding, the processing pathway of this variant is similar to that of F508 del-*CFTR* mutation which is the most common mutation worldwide. Misfolded F508 del-*CFTR* is retained by the ER and undergoes ubiquitination, thereby accelerating its proteome degradation and reducing F508 del-*CFTR* trafficking in the plasma membrane (51, 52). The model of 3D structure of *CFTR* which is predicted using the Sav1866 experimental 3D structure. L69H is studied in a short cytosolic  $\alpha$ -helix in the N-terminus of *CFTR* preceding the first transmembrane helix TMI of MSD that is called "elbow helix", which is conserved feature among the ABC exporter family. Possibly, L69H

mutation may perturb the network formed hydrophobic side chains of the cytosolic extension of MSD1TMI helices. MSDI-NBDI linker (1368) might thus play an important role for MSD1 folding and destabilization of this domain at the membrane. Another important S549N located in the LSGGQ signature motif of NBD1 and may alter the hydrolysis of ATP to regulate channel activity (53) as a result S549N classified as class III CF mutation (54). Normal maturation of S459 N-*CFTR* protein was observed in our study as reported by others (54). Further, the study was conducted to evaluate the effect of some potentiator viz Miglustat, Isolab and VX-809 to increase the activity of defective *CFTR* protein due to presence of these mutations. Ivacaftor (VX-770) is an investigational, orally bioavailable agent which was shown to augment the chloride transport activity of G551D-*CFTR* protein in vitro (54). In our study, the pharmacological corrector VX809 was found to activate L69H in BHK-21 cells in similar to that of delta F508 (50). The activation of L69H and delta F508 were both significantly corrected in terms of maturation and translocation of *CFTR* protein to cell membrane when cells were treated with VX809 potentiator. Whereas, S549N mutation classify as type III mutation was also corrected as its translocation to plasma membrane (50). It is noteworthy here that VX809 molecule is FDA approved, so that this potentiator can be used as a therapeutic molecule to rescue from type II and III mutations associated with Indian CF patients.

### Current Progress in Treatment of Basic Defects in CF

*CFTR* modulator therapies have been directed towards specific disease causing mutations and the molecules pathways that underlie these causes. *CFTR* mutations grouped into conservative classes have led to the development of specific approaches towards treating the molecular effect in CF (Table 3) (55-58). Non-sense mutations in *CFTR* have been shown to be rescued with application of a compound ataluren, derived from

**Table 3: CFTR based therapies completed or in progress towards treating the basic defect in CF**

CFTR mutation	Mutation Frequency (%)	Therapeutic approach	Status
G551D/other	4	Ivacaftor	FDA approved
Non-G551D gating/other	1	Ivacaftor	Phase II/III
R117H/other	5	Ivacaftor	Phase III
$\Delta$ F508/ $\Delta$ F508	49	Lumacaftor+ivacaftor VX-661+ivacaftor	phase III planned Phase II
PTC/other	10	Ataluren	Phase III

aminoglycoside antibiotic that can induce read-through of premature termination codons. This investigational drug is in phase III clinical trial (55). Two new molecules have been developed for correction, VX809 and potentiator, VX770, of the delta F508 mutations. Some of class III mutants respond to VX770 by increasing the chlorides transport. *CFTR* potentiator Ivacaftor (Kalydeco, VX-770, vertex pharmaceuticals, Boston, MA, USA) FDA and European regulatory authorities approved drug to treat CF patient with a class III G551D mutation (56-58). Recent advances of targeted molecular therapies and high throughput screening have resulted in multiple drug therapies that target many important mutations in the *CFTR* protein (59).

In summary, these findings represent an important milestone in the development of treatments designed to improve *CFTR* protein function as a means of addressing the underlying cause of cystic fibrosis.

### Future Directions

In Indian scenario, the diagnosis of CF is important since sweat chloride measurement using pilocarpine iontophoresis is limited to only few centers despite a large population in this country. Sweat chloride measurement technique facility is must at every district level to pick up the CF population. The most reliable is the sweat induction by pilocarpine iontophoresis, followed by sweat chloride

collection on a gauze or filter paper. Sweat chloride concentration in the CF patient is in intermediate range. In these cases, gene sequencing is essential to provide positive CF diagnosis as well as, mutations specific therapies which have become available recently (59, 60).

Other mechanisms of corrector therapy are being developed. Recently, the direct and indirect modulation of the nitric oxide (NO) pathway has been investigated as a possible corrector mechanism in delta F508-*CFTR* (58, 59). If future drug combinations are sufficiently robust to correct *CFTR* function in individuals with only one copy Phe508 del, this modulator will ideally provide clinical benefit to over 90% of all patients with CF. Thus, other approaches such as drugs that read through premature stop mutation and gene replacement or editing must continue (61).

### Acknowledgement

I am thankful to Prof. M. Singh, Prof. B. R. Thapa, Advance Pediatric Centre, PGIMER, Chandigarh, and Prof. S. K. Singh, Deptt. of Urology, PGIMER, Chandigarh who provided classical and non-classic form of CF patients. I am also thankful to Prof. Frederic Becq, Laboratoire Signalisation et Transports Ioniques Membranaires, Universite de Poitiers, CNRS, Poitiers France, who provided the facilities to carry out the work on functional characterization of novel mutations and use of potentiators as

therapeutic molecular. We are also thankful to Department of Science and Technology, New Delhi, and Indian Council of Medical Research, New Delhi as well as Charpak, Fellowship of France in India provided the funding to carry out this research work.

## References

1. Castellani C, Picci L, Tamanini A, Girardi P, Rizzotti P, Assael BM (2009). Association between carrier screening and incidence of cystic fibrosis. *JAMA* **302**: 2573-2579.
2. Prasad R, Sharma H, Kaur G (2010). Molecular basis of cystic fibrosis disease: an Indian perspective. *Indian J Clin Biochem* **25**: 335-341.
3. Bhakoo ON, Kumar R, Walia BNS (1968). Mucoviscidosis of the lung. Report of a case. *Indian J Pediatr* **35**: 183-185.
4. Prasad R, Marwaha RK, Kaur G, Walia BNS (1998). Spectrum of biochemical genetic diseases in North India. *Med Sci Res* **26**: 455-456.
5. Rowe SM, Miller S, Sorscher EJ (2005). Cystic fibrosis. *N Engl J Med* **352**: 1992-2001.
6. Chillón M, Casals T, Mercier B, *et al* (1995). Mutations in the cystic fibrosis gene in patients with congenital absence of the vas deferens. *N Engl J Med* **332**: 1475-1480.
7. Riordan JR, Rommens JM, Kerem B, *et al* (1989). Identification of the cystic fibrosis gene: cloning and characterization of complementary DNA. *Science* **245**: 1066-1073.
8. Rommens JM, Iannuzzi MC, Kerem B, *et al* (1989). Identification of the cystic fibrosis gene: chromosome walking and jumping. *Science* **245**: 1059-1065.
9. Zielenski J, Rozmahel R, Bozon D, *et al* (1991). Genomic DNA sequence of the cystic fibrosis transmembrane conductance regulator (CFTR) gene. *Genomics* **10**: 214-228.
10. Bear CE, Li CH, Kartner N, *et al* (1992). Purification and functional reconstitution of the cystic fibrosis transmembrane conductance regulator (CFTR). *Cell* **68**: 809-818.
11. Hyde SC, Emsley P, Hartshorn MJ, *et al* (1990). Structural model of ATP-binding proteins associated with cystic fibrosis, multidrug resistance and bacterial transport. *Nature* **346**: 362-365.
12. Short DB, Trotter KW, Reczek D, *et al* (1998). An apical PDZ protein anchors the cystic fibrosis transmembrane conductance regulator to the cytoskeleton. *J Biol Chem* **273**: 19797-19801.
13. Castellani C, Cuppens H, Macek M Jr, *et al* (2008). Consensus on the use and interpretation of cystic fibrosis mutation analysis in clinical practice. *J Cyst Fibros* **7**: 179-196.
14. Haardt M, Benharouga M, Lechardeur D, Kartner N, Lukacs GL (1999). C-terminal truncations destabilize the cystic fibrosis transmembrane conductance regulator without impairing its biogenesis. A novel class of mutation. *J Biol Chem* **274**: 21873-21877.
15. Anguiano A, Oates RD, Amos JA, *et al* (1992). Congenital bilateral absence of the vas deferens. A primarily genital form of cystic fibrosis. *JAMA* **267**: 1794-1797.
16. Chillón M, Casals T, Mercier B, *et al* (1995). Mutations in the cystic fibrosis gene in patients with congenital absence of the vas deferens. *N Engl J Med* **332**: 1475-1480.
17. Drumm ML, Konstan MW, Schluchter MD, *et al* (2005). Genetic modifiers of lung disease in cystic fibrosis. *N Engl J Med* **353**: 1443-1453.
18. Darrah R, McKone E, O'Connor C, *et al*

- (2010). EDNRA variants associate with smooth muscle mRNA levels, cell proliferation rates, and cystic fibrosis pulmonary disease severity. *Physiol Genomics* **41**: 71-77.
19. Goraca A (2002). New views on the role of endothelin (minireview). *Endocr Regul* **36**: 161-167.
  20. Solomon GM, Marshall SG, Ramsey BW, Rowe SM (2015). Breakthrough therapies: Cystic fibrosis (CF) potentiators and correctors. *Pediatr Pulmonol* **50**: S3-S13.
  21. Morral N, Nunes V, Casals T, *et al* (1993). Microsatellite haplotypes for cystic fibrosis: mutation frameworks and evolutionary tracers. *Hum Mol Genet* **2**: 1015-2102.
  22. Dodge JA (2015). A millennial view of cystic fibrosis. *Dev Period Med* **19**: 9-13.
  23. Farrell PM, Rosenstein BJ, White TB, *et al* (2008). Guidelines for diagnosis of cystic fibrosis in newborns through older adults: Cystic Fibrosis Foundation consensus report. *JPediatr* **153**: S4-S14.
  24. Rosenstein BJ, Cutting GR (1998). The diagnosis of cystic fibrosis: a consensus statement. Cystic Fibrosis Foundation Consensus Panel. *JPediatr* **132**: 589-595.
  25. Gibson LE, Cooke RE (1959). A test for concentration of electrolytes in sweat in cystic fibrosis of the pancreas utilizing pilocarpine by iontophoresis. *Pediatrics* **23**: 545-549.
  26. Rowe MS, Miller SBS, Sorcher EJ (2005). Cystic Fibrosis. *N Engl J Med* **352**: 1991-2001.
  27. Wallis C (1997). Diagnosing cystic fibrosis: blood, sweat, and tears. *Arch Dis Child* **76**: 85-88.
  28. Veeze HJ, Sinaasappel M, Bijman J, Bouquet J, de Jonge HR (1991). Ion transport abnormalities in rectal suction biopsies from children with cystic fibrosis. *Gastroenterology* **101**: 398-403.
  29. Walters MP, Kelleher J, Gilbert J, Littlewood JM (1990). Clinical monitoring of steatorrhoea in cystic fibrosis. *Arch Dis Child* **65**: 99-102.
  30. Sharma N, Singh M, Kaur G, Thapa BR, Prasad R (2009). Identification and characterization of CFTR gene mutations in Indian CF patients. *Ann Hum Genet* **73**: 26-33.
  31. Bowler IM, Estlin EJ, Littlewood JM (1993). Cystic fibrosis in Asians. *Arch Dis Child* **68**: 120-122.
  32. Kabra M, Kabra SK, Ghosh M, *et al* (2000). Is the spectrum of mutations in Indian patients with cystic fibrosis different? *Am J Med Genet* **93**: 161-163.
  33. Mei-Zahav M, Durie P, Zielenski J, *et al* (2005). The prevalence and clinical characteristics of cystic fibrosis in South Asian Canadian immigrants. *Arch Dis Child* **90**: 675-679.
  34. Morral N, Nunes V, Casals T, *et al* (1993). Microsatellite haplotypes for cystic fibrosis: mutation frameworks and evolutionary tracers. *Hum Mol Genet* **2**: 1015-1022.
  35. Shastri SS, Kabra M, Kabra SK, Pandey RM, Menon PS (2008). Characterisation of mutations and genotype-phenotype correlation in cystic fibrosis: experience from India. *J Cyst Fibros* **7**: 110-115.
  36. Kiliç MO, Niniş VN, Dağlı E, *et al* (2002). Highest heterogeneity for cystic fibrosis: 36 mutations account for 75% of all CF chromosomes in Turkish patients. *Am J Med Genet* **113**: 250-257.
  37. Sharma H, Mavuduru RS, Singh SK, Prasad R (2014). Heterogeneous spectrum of mutations in CFTR gene from Indian patients with congenital absence of the vas deferens and their association with cystic fibrosis genetic modifiers. *Mol Hum Reprod*

- 20: 827-835.
38. Sharma N, Singh M, Acharya N, *et al* (2008). Implication of the cystic fibrosis transmembrane conductance regulator gene in infertile family members of Indian CF patients. *Biochem Genet* **46**: 847-856.
  39. Sharma N, Acharya N, Singh SK, Singh M, Sharma U, Prasad R (2009). Heterogenous spectrum of CFTR gene mutations in Indian patients with congenital absence of vas deferens. *Hum Reprod* **24**: 1229-1236.
  40. Casals T, Bassas L, Egozcue S, *et al* (2000). Heterogeneity for mutations in the CFTR gene and clinical correlations in patients with congenital absence of the vas deferens. *Hum Reprod* **15**: 1476-8143.
  41. Castellani C, Cuppens H, Macek M Jr, *et al* (2008). Consensus on the use and interpretation of cystic fibrosis mutation analysis in clinical practice. *J Cyst Fibros* **7**: 179-196.
  42. Mak V, Zielenski J, Tsui LC, *et al* (1999). Proportion of cystic fibrosis gene mutations not detected by routine testing in men with obstructive azoospermia. *J Am Med Assoc* **281**: 2217-2224.
  43. Berinardino ALF, Lima CA, Zatz M (2003). Analysis of mutation in the cystic fibrosis transmembrane conductance regulator (CFTR) gene in patients with obstructive azoospermia. *Genet Mol Biol* **26**: 1-3.
  44. Blobel GC, Schiemann WP, Lodish HF (2000). Role of transforming growth factor beta in human disease. *N Engl J Med* **342**: 1350-1358.
  45. Hochar B, Schwarz A, Fagan KA, *et al* (2000). Pulmonary fibrosis and chronic lung inflammation in ET-1 transgenic mice. *Am J Respir Cell Mol Biol* **23**: 19-26.
  46. Ruest LB, Xiang X, Lim KC, Levi G, Clouthier DE (2004). Endothelin-A receptor -dependent and -independent signaling pathways in establishing mandibular identity. *Development* **131**: 4413-4423.
  47. Pla P, Larue L (2003). Involvement of endothelin receptors in normal and pathological development of neural crest cells. *Int J Dev Biol* **47**: 315-325.
  48. Moore SW, Zaahl MG (2007). Association of endothelin-beta receptor (EDNRB) gene variants in anorectal malformations. *J Pediatr Surg* **42**: 1266-1270.
  49. Yi S, Pierucci-Alves F, Schultz BD (2013). Transforming growth factor- $\beta$ 1 impairs CFTR-mediated anion secretion across cultured porcine vas deferens epithelial monolayer via the p38 MAPK pathway. *Am J Physiol Cell Physiol* **305**: C867-C876.
  50. Sharma H, Jollivet Souchet M, Callebaut I, Prasad R, Becq F (2015). Function, pharmacological correction and maturation of new Indian CFTR gene mutations. *J Cyst Fibros* **14**: 34-41.
  51. Cheng SH, Gregory RJ, Marshall J, *et al* (1990). Defective intracellular transport and processing of CFTR is the molecular basis of most cystic fibrosis. *Cell* **63**: 827-834.
  52. Ward CL, Omura S, Kopito RR (1995). Degradation of CFTR by the ubiquitin-proteasome pathway. *Cell* **83**: 121-127.
  53. Ramsey BW, Davies J, McElvaney NG, *et al* (2011). A CFTR potentiator in patients with cystic fibrosis and the G551D mutation. *N Engl J Med* **365**: 1663-1672.
  54. Yu H, Burton B, Huang CJ, *et al* (2012). Ivacaftor potentiation of multiple CFTR channels with gating mutations. *J Cyst Fibros* **11**: 237-245.
  55. Wilschanski M, Miller LL, Shoseyov D, *et al* (2011). Chronic ataluren (PTC124) treatment of nonsense mutation cystic fibrosis. *Eur Respir J* **38**: 59-69.
  56. Rowe SM, Borowitz DS, Burns JL, *et al* (2012). Progress in cystic fibrosis and the

- CF Therapeutics Development Network. *Thorax* **67**: 882-890.
57. Okiyoneda T, Veit G, Dekkers JF, *et al* (2013). Mechanism-based corrector combination restores  $\Delta F508$ -CFTR folding and function. *Nat Chem Biol* **9**: 444-454.
  58. Ramsey BW, Davies J, McElvaney NG, *et al* (2011). A CFTR potentiator in patients with cystic fibrosis and the G551D mutation. *N Engl J Med* **365**: 1663-1672.
  59. Solomon GM, Marshall SG, Ramsey BW, Rowe SM (2015). Breakthrough therapies: Cystic fibrosis (CF) potentiators and correctors. *Pediatr Pulmonol* **50**: S3-S13.
  60. De Boeck K, Vermeulen F, Dupont L (2017). The diagnosis of cystic fibrosis. *Presse Med* **46**: e97-e108.
  61. Fajac I, Wainwright CE (2017). New treatments targeting the basic defects in cystic fibrosis. *Presse Med* **46**: e165-e175.

# Phagocytes and the Leishmania Parasite: A Marriage of Convenience

*Mitali Chatterjee*

Department of Pharmacology,  
Institute of Post Graduate Medical Education and Research, Kolkata.

## ABSTRACT

The current drive by the Government of India to eliminate Leishmaniasis has pinpointed post-kala azar dermal leishmaniasis (PKDL) as the strongest contender for the disease reservoir. This emphasizes the necessity to consider the eradication of PKDL as top priority, and hinges on its early diagnosis and management. We undertook this challenge and have provided insights into *Leishmania* biology, by focusing our efforts in (i) delineating the immunopathogenesis of PKDL, a disease unique to South Asia (ii) developing diagnostic/prognostic tools for monitoring antileishmanial treatment in patients with visceral leishmaniasis and PKDL. In order to delineate the immunopathogenesis of PKDL, it was established that the parasite adopts multiple approaches to deviously manipulate host monocytes/macrophages, and thus facilitate parasite survival and disease progression. The parasite adopts a multipronged approach that includes attenuation of the oxidative burst within phagocytes, polarization of monocytes/ macrophages towards alternate activation, enhancement of CD8 T-cell exhaustion and a decreased presence of Langerhans cells. Identification of these immunological changes have allowed for development of biomarkers that have been exploited to develop diagnostic and prognostic markers for monitoring the disease progression, either in terms of antibody based markers, or quantification of the parasite load, the latter being the most definitive approach. Measurement of parasite load has proved to be an effective tool for monitoring the effectiveness of chemotherapy. Taken together, the identification of biomarkers and new chemotherapeutic modalities has helped in improved management and potential elimination of leishmaniasis.

**Keywords:** Leishmania biology, post-kala azar dermal leishmaniasis (PKDL), visceral leishmaniasis, Th-associated cytokines, Toll-like receptors, antimonials, miltefosine.

Leishmaniasis caused by the digenetic parasite *Leishmania* is a diverse group of neglected tropical diseases of poverty, that ranges from a self limiting cutaneous lesion to a fatal visceral form called kala-azar, and has a dermal sequel called post-kala azar dermal leishmaniasis (PKDL) (1). Its relevance to public health in India lies in the fact that over

60% of the world's cases of visceral leishmaniasis (VL) are reported from three countries, namely India, Nepal and Bangladesh, with an estimated 150 million people being at risk of VL in 109 districts (2). In India, the states of Bihar and adjoining areas of West Bengal, Jharkhand and Uttar Pradesh account for India's burden of VL.

---

**Correspondence:** Dr. Mitali Chatterjee, Department of Pharmacology, Institute of Postgraduate Medical Education & Research, 244 B Acharya JC Bose Road, Kolkata-700020. Tel: 91-33-2204 1428. Fax: 91-33-22234135.

DR. PRAN NATH CHHUTTANI ORATION delivered during the NAMSCON 2018 held at the Mahatma Gandhi Medical College & Research Institute, Puducherry.

In PKDL, the dermal sequel of VL, where *Leishmania* parasites remain restricted to the skin, manifest with nodular, papular, hypopigmented macular lesions, erythematous plaques and/or a mixed phenotype, termed as polymorphic (1-3) or a diffuse hypopigmentation considered as the macular variant. The etiopathogenesis of PKDL is still unclear and there is yet to emerge a consensus regarding possible causes for the generally viscerotropic *L. donovani* parasite to become dermatropic (4). An important limitation in PKDL is the absence of an animal model and therefore, information is derived solely from human studies, and understandably remains limited. In PKDL, similar to other leishmaniasis, *Leishmania* have developed several strategies to outmanoeuvre host immunity by subverting and/or suppressing macrophage microbicidal activities, thereby sustaining chronic infection (5).

A pivotal pathogenic event in Leishmaniasis is harboring of the causative *Leishmania* parasite within phagolysosomes of macrophages. To achieve this, the parasite deviously initiates mechanisms to modulate the macrophage microbicidal machinery (5). Additionally, as macrophages are sentinels of the immune system, establishment of infection critically hinges on the parasite's ability to modulate the hosts signaling systems, the end point being immunosuppression. Accordingly, the therapeutic armamentarium against *Leishmania* albeit limited, includes compounds that are directly parasitocidal and/or indirectly immunomodulatory with notable examples being antimonials, miltefosine, amphotericin B, and paromomycin (6).

It is universally accepted that monocytes-macrophages play a range of fundamental biological roles being inducers, regulators and effectors of innate and acquired immunity. Upon stimulation with Th1-associated cytokines, notably IFN $\gamma$ , they acquire a heightened effector function against intracellular pathogens, referred to as a

classically activated or M1 phenotype. Conversely, in the milieu of Th2 associated cytokines e.g. IL-4, IL-13, IL-33, TGF- $\beta$  and IL-10 or by microbial triggers, M2 polarization or alternative activation occurs (7). As M2 polarization requires a milieu comprising IL-4, IL-10 and IL-13, levels of these cytokines were estimated in patients with PKDL. The levels of IL-4 were significantly raised as compared to healthy individuals as was IL-10 and IL-13. Treatment caused a significant decrease in IL-10 reiterating its importance in leishmaniasis (8).

These M1 and M2 monocytes/macrophages are differentiated by cardinal genes regulated by inducible nitric oxide synthase (*iNOS*), arginase 1 (*ARG1*), mannose receptor (*CD206*) and *Fizz1* (9, 10). M2 macrophages can impede protective immunity to protozoan infection. In general, understanding of the phenotypic and functional complexity of M2 monocytes-macrophages is limited by a conspicuous discordance between data derived from murine vs. human systems (11). Unlike classically activated macrophages, where human and murine cells respond similarly, the molecular phenotype of alternatively activated macrophages in mice and humans have to date shown a limited overlap (12). Accordingly, we delineated the activation status of monocytes in peripheral blood and dermal macrophages of patients with PKDL, thus providing the first characterization of M2 polarized macrophages in human dermal leishmaniasis.

In PKDL, as compared to healthy controls, the frequency of CD14<sup>+</sup> monocytes expressing TLR-2<sup>+</sup> and TLR-4<sup>+</sup> was significantly reduced which was restored following treatment (Fig. 1A & B) (8). As attenuation of the oxidative burst, secondary to reduced phosphorylation of MAPKs occurred through the TLR-2 pathway or the CD40 signalosome, it was proposed that in PKDL, the decreased expression of TLR-2/4 translated into an impaired MAPK signalling, resulting in the intramonocytic redox imbalance tilting towards

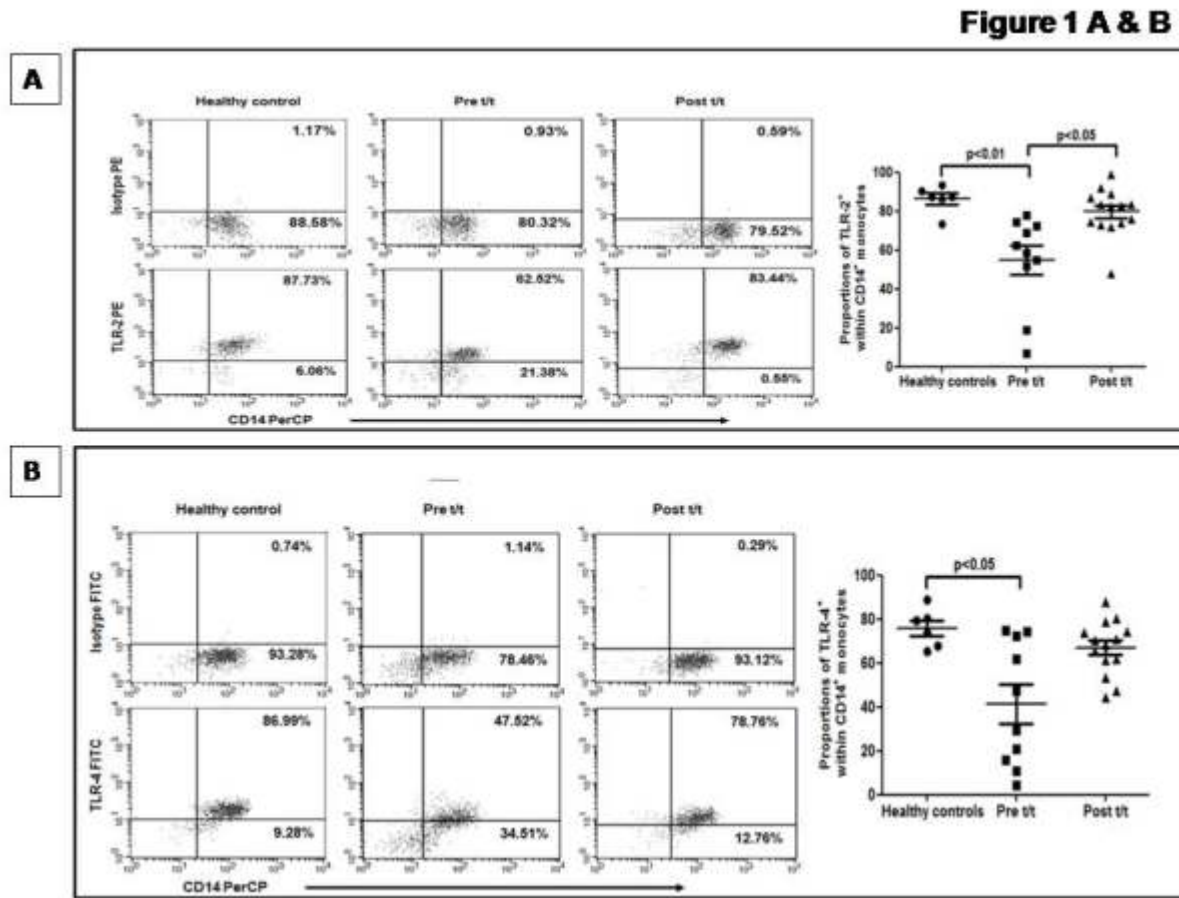


**Fig. 1: Decreased expression of TLR-2 and -4 and altered redox status within monocytes**  
**A-B:** Representative data showing expression of TLR-2 (A) and TLR-4 (B), within CD14<sup>+</sup> monocytes in a healthy control, a patient with PKDL pre (Pre t/t) and post treatment (Post t/t). Isotype control staining is also shown. \*Scatter plots showing frequency of CD14<sup>+</sup> monocytes expressing TLR-2 or TLR-4 in healthy controls (●), patients with PKDL (Pre t/t, ■) and post treatment (Post t/t, ▲). \*The proportion of CD14<sup>+</sup>TLR-2<sup>+</sup> and CD14<sup>+</sup>TLR-4<sup>+</sup> monocytes was calculated by dividing the percentages of upper right quadrant with the sum of upper and lower right quadrant.

an anti-inflammatory milieu (Fig. 2) (13). Alongside, the *ex-vivo* levels of NO in monocytes from PKDL patients was significantly diminished as compared to controls and following treatment, monocytes regained their ability to generate NO (Fig. 3A). Similarly, the generation of ROS was significantly attenuated at presentation *vis-a-vis* controls and treatment increased fluorescence, but remained lower than controls (Fig. 3B). These variations in the anti-oxidant status impacted on the redox

balance and impaired macrophage host defence functions, facilitating parasite survival (8).

Monocytes can differentiate into inflammatory or anti-inflammatory subsets, but their classification in relation to functional phenotypes remains to be precisely defined. Three subsets of blood monocytes, namely classical (CD14<sup>++</sup>CD16<sup>-</sup>), intermediate (CD14<sup>++</sup>CD16<sup>+</sup>), and non-classical (CD14<sup>+</sup>CD16<sup>++</sup>) have been described with

Figure 2

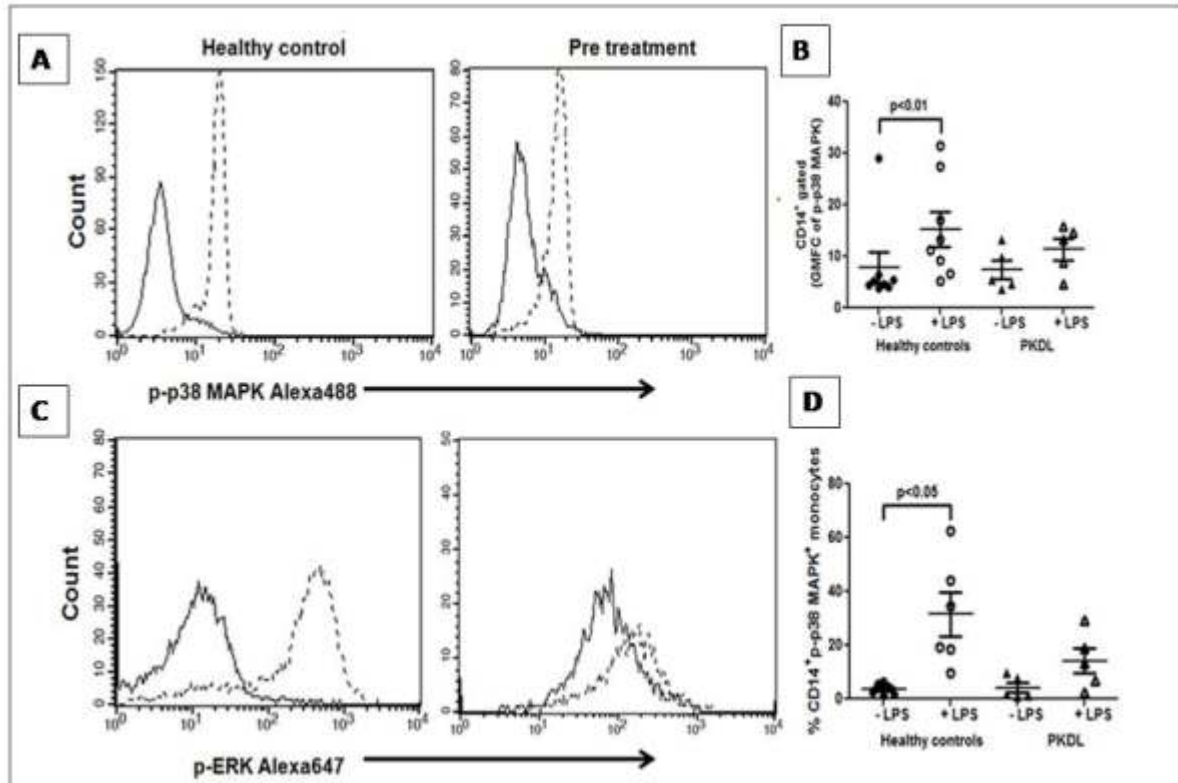


**Fig. 2: Intramonocytic phosphorylation status of p38 MAPK and ERK**

A. and C. Representative profile showing baseline (—) and LPS-stimulated (---) expression of p-p38 MAPK (A) and p-ERK (C) in monocytes from a healthy control and a patient with PKDL.

B and D. Scatter plots showing baseline and LPS-stimulated expression of p-p38 MAPK (B) and p-ERK (D) in healthy controls (●, ○) and patients with PKDL (▲, △).

discrete functions (14). In PKDL, at disease presentation, there was minimal decrease in classical (CD14<sup>++</sup>CD16<sup>-</sup>) monocytes whereas there was an increase in the intermediate variant (CD14<sup>++</sup>CD16<sup>+</sup>) and non-classical monocytes.

In mouse monocytes/macrophages, the intricate network of signalling molecules, associated transcription factors along with post transcriptional regulators mediating the different forms of activation are well delineated. IL-4 and IL-13 via STAT6 activation are known to skew the macrophage function towards the M2 phenotype leading to transcription of genes typical of M2 polarization, notably Mannose

receptor (*Mrc1*), Arginase (*Arg1*), PPAR and *Fizz1* among others (7). As decreased generation of reactive oxygen and nitrogen radicals suggested alternative activation (9, 10), monocytes from PKDL patients were examined for a M2 phenotype using a panel of robust markers. In circulating monocytes from PKDL cases, the mRNA expression of nuclear receptor *PPARG* which regulates oxidative metabolism in macrophages was increased ~50-fold, as was mRNA expression of *ARG1*. Confocal immunofluorescence confirmed localisation of arginase-1 within CD68<sup>+</sup> macrophages, which decreased post-treatment (Fig. 4A). The lesional 13.9 fold increase in *CD206* mRNA reinforced

**Figure 3 A & B**

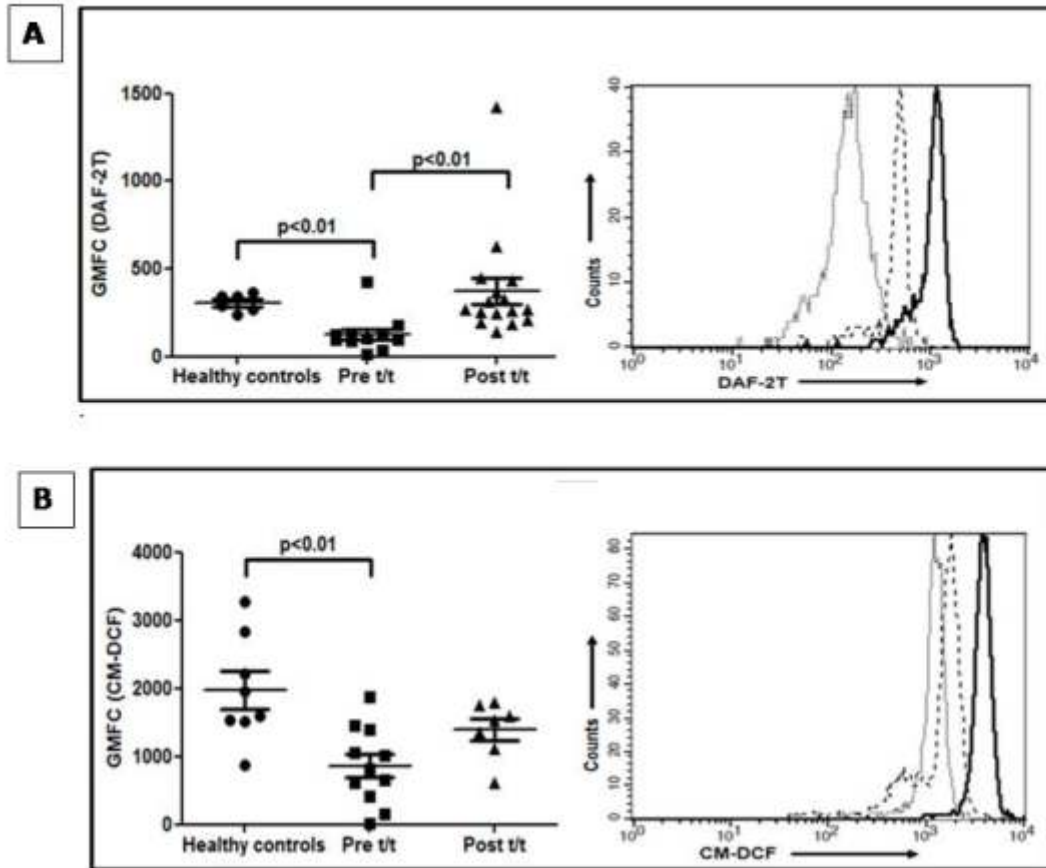


**Fig. 3: Production of reactive oxygen-/nitro-free radicals in circulating monocytes in healthy and patients with PKDL**

**A:** Scatter plots showing intracellular NO in circulating monocytes of healthy controls (●), patients with PKDL (Pre t/t, ■) and post treatment (Post t/t, ▲).

Representative histogram overlay showing DAF-2T fluorescence in monocytes from a healthy control (—), patient with PKDL (···) and on completion of treatment (---).

**B:** Scatter plots of intramonocytic generation of ROS as for C above. A representative histogram overlay showing CM-DCF fluorescence, as for D above.

the M2 polarized status (Fig. 4B) and was mirrored by raised protein expression evident via confocal microscopy (8).

As vitamin D receptor signaling has been linked to M2 polarization and generation of antimicrobial peptides (15), this pathway was examined as it may underlie the systemic and local M2 polarization in PKDL. Plasma  $1\alpha,25$ -dihydroxyvitamin  $D_3$  (1,25D3) was significantly raised during PKDL and in keeping with the

elevated plasma levels of 1,25D3, an increase in VDR, *CYP27B1* and LL-37 mRNA accumulation endorsed the upregulation of the vitamin D-related pathways.

In our efforts to delineate mechanisms that promote immunopathology, we evaluated the contribution of T-cells in PKDL by immunophenotyping in peripheral blood for T cells (CD3), T helper cells (CD3/CD4), cytotoxic T cells (CD3/CD8), NK cells (CD56),

**Figure 4 A & B**

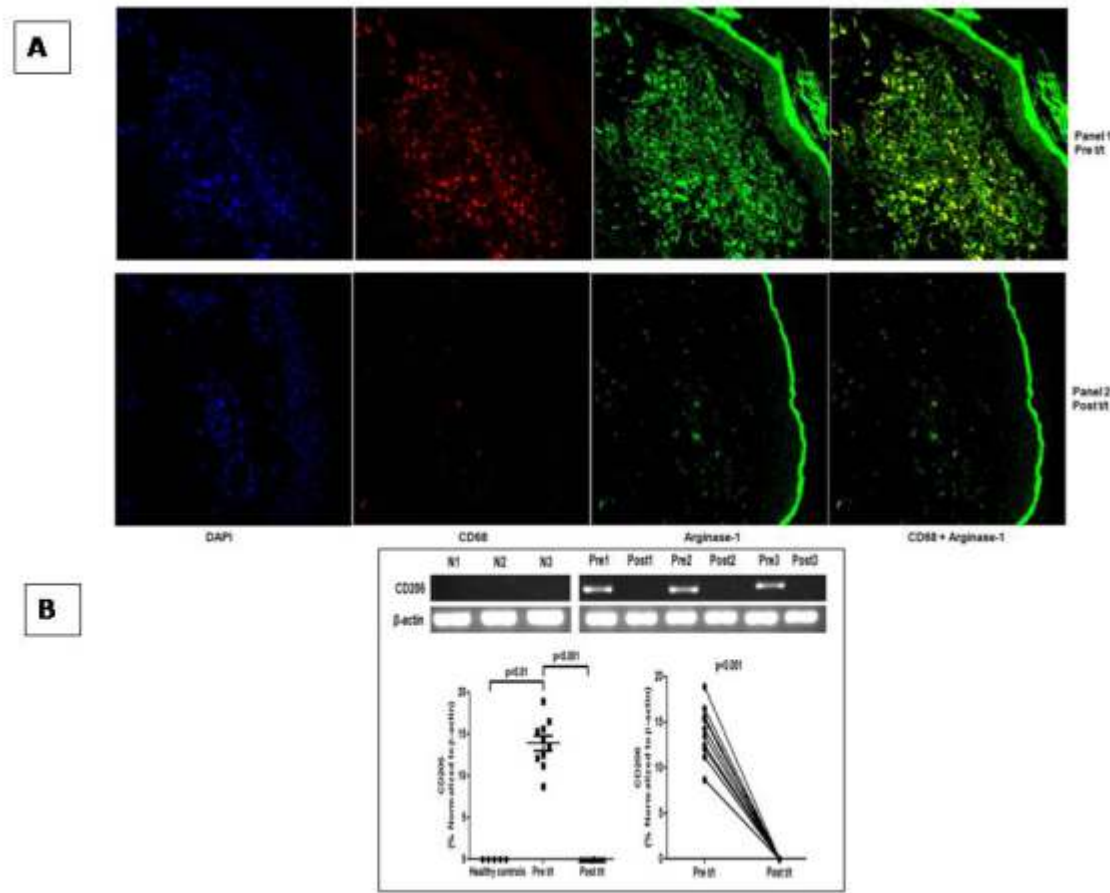


**Fig. 4: Lesional macrophages showed a raised expression of PPAR- $\gamma$ , arginase-1 and mannose receptor**

**A:** Expression of arginase-1 (green, panel 1 and 2 third from left) in CD68<sup>+</sup> macrophages (red, panel 1 and 2 second from left) at the lesional site of a patient with PKDL pre (Pre t/t) and post treatment (Post t/t). Nuclei are shown in blue (DAPI, panel 1 and 2, left most). Co-localization of macrophage and arginase-1 was shown in right most figure in each panel where co-localization of red and green appears as yellow. Figures were captured in 400X magnification.

**B:** Representative mRNA expression profile of CD206 in dermal lesions of healthy controls (N 1-3), and patients with PKDL pre (Pre 1-3) and post (Post 1-3) treatment; scatter plots are as in A-B, above.

NKT cells (CD3/CD56), T regulatory cells (CD4/CD25), B cells (CD19) and monocytes (CD14). In PKDL patients, both before and after treatment, the percentages of T lymphocytes, T helper cells, NK cells, NK T cells, T regulatory cells, B lymphocytes and monocytes were comparable with normal individuals (16). The only change reported from peripheral blood in PKDL patients was a small but significant

increase in the percentage of CD3/CD8 lymphocytes as compared to healthy controls which was retained even after treatment (16). Their responses to phytohemagglutinin was no different from healthy controls as the percentages of IFN- $\gamma$ , IL-2, IL-4 and IL-10 expressing lymphocytes was comparable to controls, and was in contrast to VL patients who demonstrated reduced proportions of IFN- $\gamma$  and

IL-2 expressing cells, along with an increase in IL-10 positive cells (16). The important difference in their T cell responses was in their response to *L. donovani* antigen as PKDL patients showed an 8 fold increase in the percentage of IL-10 expressing CD3/CD8 lymphocytes as compared to controls which decreased with treatment and accordingly, it was proposed that IL-10 producing CD3/CD8 lymphocytes are important protagonists in the immunopathogenesis of Indian PKDL (16).

Furthermore, our group reported that in patients with PKDL, there is an increased proportion of circulating CD8<sup>+</sup>CD28<sup>-</sup> and antigen-induced IL-10<sup>+</sup>CD3<sup>+</sup> lymphocytes which receded with treatment (17). Importantly, these CD8<sup>+</sup> lymphocytes demonstrated impaired proliferative responses to *Leishmania donovani* antigen and phytohemagglutinin, and were reinstated following treatment. At presentation, the upregulated lesional IFN- $\gamma$  and IL-10 mRNA, Foxp3 mRNA and protein was curtailed following treatment. Accordingly, it was proposed that the increased frequency of the CD8<sup>+</sup>CD28<sup>-</sup> phenotype, enhanced antigen-specific IL-10 production and accompanying anergy of circulating lymphocytes suggested their regulatory nature. This was endorsed by the elevated lesional expression of Foxp3 and their recruitment into the lesional site sustained disease pathology (17).

In peripheral blood, the functional status of CD8<sup>+</sup> T-cells was examined in terms of activation markers, CD127 and CD69 along with markers of cytotoxicity, perforin and granzyme. During active disease, the frequency of CD127 within CD8<sup>+</sup> T-cells was significantly decreased as compared to healthy controls and treatment translated into a significant increase (Chatterjee M, personal communication). However, the frequency of CD69, perforin and granzyme of CD8<sup>+</sup> T-cells remained unchanged, and was comparable with healthy controls suggesting that CD8<sup>+</sup> T-cells in peripheral blood remain immunocompetent. However, in dermal lesions, there was a conspicuous absence of

CD4<sup>+</sup> T-cells whereas there was an enhanced infiltration of CD8<sup>+</sup> T-cells. Importantly, these CD8<sup>+</sup> T-cells demonstrated an absence of perforin, granzyme and Zap-70. Concomitantly, dermal lesions showed an enhanced expression of PD-1 which suggested exhaustion of CD8<sup>+</sup> T-cells. In addition, lesions demonstrated an increased proportion of CD8<sup>+</sup>CCR4<sup>+</sup> T-cells and CCL17/CCL22 and it was proposed that dermal homing of anergic/exhausted CD8<sup>+</sup> T-cells was a feature of Indian PKDL (Chatterjee M, personal communication).

In the skin, dendritic cells (DCs) are the key immune sentinels, via their ability to respond to microbial signals and by subsequently activating naïve T-cells, play a pivotal role in initiating antimicrobial immunity (18). Accordingly, we delineated the lesional immunopathology in terms of tissue macrophages (M $\emptyset$ ), Langerhans cells, granuloma formation along with mRNA expression of IL-12p40 and IL-10. We collected lesional punch biopsies serially at disease presentation and completion of treatment. Immunohistochemical analysis was performed for M $\emptyset$  (CD68), while dermal dendritic cells (dDCs) and Langerhans cells (LCs) were identified using CD1a, CD207 and HLA-DR.

Despite the absence of a mature granuloma, there was heavy infiltration of CD68<sup>+</sup> M $\emptyset$  *vis-a-vis* healthy controls, which decreased with treatment (Fig. 5A). DCs in the epidermis were significantly decreased in PKDL when compared with healthy donors, and were morphologically altered, as demonstrated by loss of elongated cellular protrusions (Fig. 5B). These LCs did not migrate to the dermis as 6/9 patients showed a near total absence of dDCs (Fig. 5C), which remained unchanged with treatment (Fig. 5C) (19). The lesional mRNA expression of IL-10 during active disease was significantly upregulated as compared to healthy individuals and strengthened our proposition that in PKDL, this decrease in LCs along with increased IL-10 caused immune inactivation that allowed for disease sustenance,

**Figure 5 A-C**

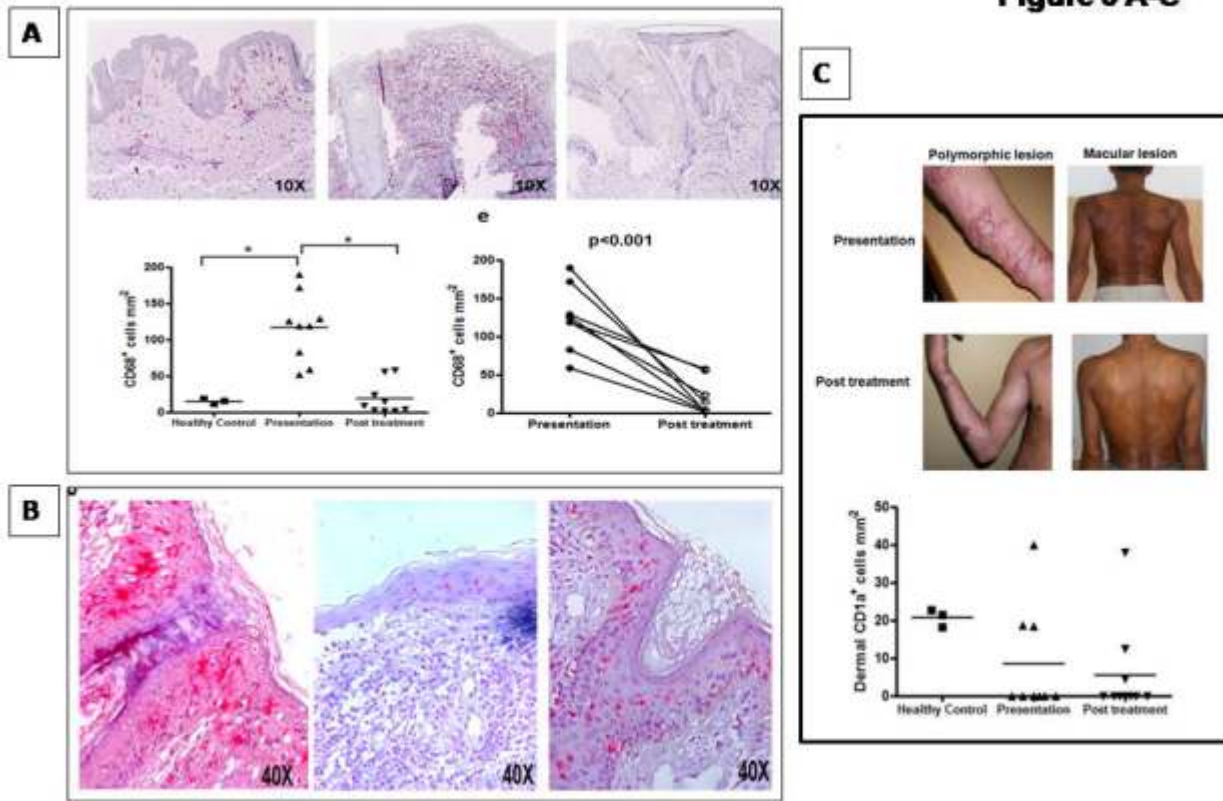


**Fig. 5: Dermal infiltration in patients with PKDL**

**A:** Representative IHC profile of CD68<sup>+</sup> cells in the dermal biopsy of a healthy control, a patient with PKDL at disease presentation and post treatment (magnification, 10X objective).

Comparison of CD68<sup>+</sup> cells of healthy controls (■), patients with PKDL at disease presentation (▲) and post treatment (▼), \*p<0.05. Each horizontal bar represents the median value.

**B:** Representative IHC profile showing distribution of CD207<sup>+</sup> cells in the dermal biopsy of a healthy control, patient with PKDL at disease presentation and post treatment under (magnification, 40X objective). Representative IHC profile showing distribution of CD1a<sup>+</sup> cells in the dermal biopsy of a healthy control, patient with PKDL at disease presentation and post treatment (magnification, 10X and 40X objectives).

**C:** Distribution of CD1a<sup>+</sup> cells in the epidermal and dermal compartment respectively of healthy controls (■), patients with PKDL at disease presentation (▲) and post treatment (▼), \*p<0.05. Each horizontal bar represents the median value.

emphasizing the importance of immunomodulation as a chemotherapeutic strategy against leishmaniasis.

This increasing incidence of unresponsiveness to antimonials (20) led to an invaluable spin off, as it saw the introduction of miltefosine, the first orally effective anti-leishmanial drug (21) along with amphotericin B

(22). Furthermore, in the backdrop of a strong political and administrative commitment the governments of India, Nepal, and Bangladesh, in collaboration with World Health Organization (WHO) and later joined by Bhutan and Thailand, developed a strategic framework to eliminate visceral leishmaniasis as a public health problem (23,24). The programme has three phases: attack (bring down cases to below 1/10,000 by 2017),

consolidation (case levels below 1/10,000 for three years, from 2017–2019), and maintenance (case levels below 1/10,000 beyond 2020) ([http://www.who.int/neglected\\_diseases/London\\_Declaration\\_NTDs.pdf](http://www.who.int/neglected_diseases/London_Declaration_NTDs.pdf)). Fortunately, it seems achievable as 2015 was the third year in a row that Nepal has been consistently below that target (25, 26), and in Bangladesh, only a few districts (*upazilas*) remain above the target (26). The Indian burden persists possibly attributable to the higher prevalence of the disease at the beginning.

The focused efforts in implementation of the VL elimination programme translated into a considerable reduction in the incidence by over 75% in the Indian subcontinent. However, in 2015, 90 of the 456 endemic blocks (20%) in India continue to remain endemic for VL and more importantly, new foci have emerged in non-endemic regions (26, 27). Additionally, a neglected component of the elimination programme has been PKDL, which is possibly the most intriguing clinically and scientifically, as it generally develops after apparent successful cure from VL (28, 29). PKDL is confined to South Asia and East Africa, mainly Sudan (1, 30), wherein the Sudanese variant presents with papular or nodular lesions while in South Asia, the polymorphic variant (co-existence of macules/patches along with papulo-nodules) is more prevalent. Although mortality from PKDL is minimal, it is a stigmatizing disease that carries a huge socio-economic burden, further amplified by a reluctance to obtain treatment or due to non compliance. Lesions, especially the papulo-nodules are parasite-rich, fuelling speculation that PKDL plays a pivotal role in the inter-epidemic transmission of VL and in South Asia where VL is anthroponotic, patients with PKDL are the strongest contenders to be the disease reservoir (31). Accordingly, PKDL has been recognised as a major barrier to the current VL elimination efforts and its elimination is now an essential component of the elimination programme currently targeted for 2020 (1).

Two critical factors that contributed

towards the reduction of VL cases were the prompt diagnosis by the rK-39 strip test along with the single dose treatment with liposomal amphotericin B, (LAmB) which revolutionized the chemotherapy of VL. However, the management of PKDL remained neglected by lack of a definitive test, as rK39 positivity can be attributed to a past infection with VL. Ideally, the demonstration of parasites in smears, culture or by PCR is logistically not feasible, but an even bigger hurdle is to motivate patients with PKDL to actively seek treatment, as the disease has practically no mortality and seeking treatment would be purely for cosmetic reasons. This has translated into a conspicuous absence of clinical trials. The treatment for PKDL is prolonged and as there is always a lurking danger of drug resistance, modalities to monitor the parasite load was the challenge we undertook. A treatment regimen for LAmB in PKDL was empirically set at 30 mg/kg b.w. for three weeks, we developed quantifiable approaches for measuring the parasite burden not merely at disease presentation but at the end of the treatment.

Our study population included 184 patients clinically diagnosed with PKDL whom we recruited via two types of surveillance (32) namely (i) *Passive surveillance* where patients presented at the dermatology outpatient departments of School of Tropical Medicine/Calcutta Medical College/Institute of PG Medical Education & Research, Kolkata, West Bengal or (ii) *Active surveillance* via field surveys conducted in endemic districts of West Bengal (Malda, Dakshin Dinajpur, Murshidabad and Birbhum) by a camp approach. This involved a house-to-house survey conducted by Kala azar technical supervisors using standard case definitions and defined risk factors e.g. living in an endemic area and having an epidemiological link (past history of VL). Subsequently, these cases were examined at medical camps wherein cases with hypopigmented macules were considered as macular PKDL, whereas an assortment of papules, nodules, macules, and/or plaques was

termed as polymorphic PKDL (29).

Irrespective of the type of surveillance, diagnosis of PKDL was confirmed by the rK39 strip test from blood along with an ITS-1 PCR (33). After confirmation by ITS-1 PCR, cases were randomly allocated to receive miltefosine (50 mg p.o. twice daily for 12 weeks) or LAmB (5 mg/kg body IV, twice weekly, for 3 weeks) as per recommended guidelines. Peripheral blood and a 4 mm skin biopsy were collected at three time points, namely disease presentation, on completion of treatment and six months later.

The clinical outcome was assessed by a dermatologist and they were considered cured based on total regression of papules/nodules, no new lesion(s) and considerable regression of macular lesions.

For measurement of parasite load, a standard curve was generated by adding a defined number of *Leishmania* parasites sourced from a *L. donovani* strain (ranging from 10 to  $1 \times 10^5$ ) to blood (180  $\mu$ l) from a healthy control (34) and DNA was eluted in 50 $\mu$ L of DNA elution buffer. Real-time PCR was performed using

**Figure 6 A-C**

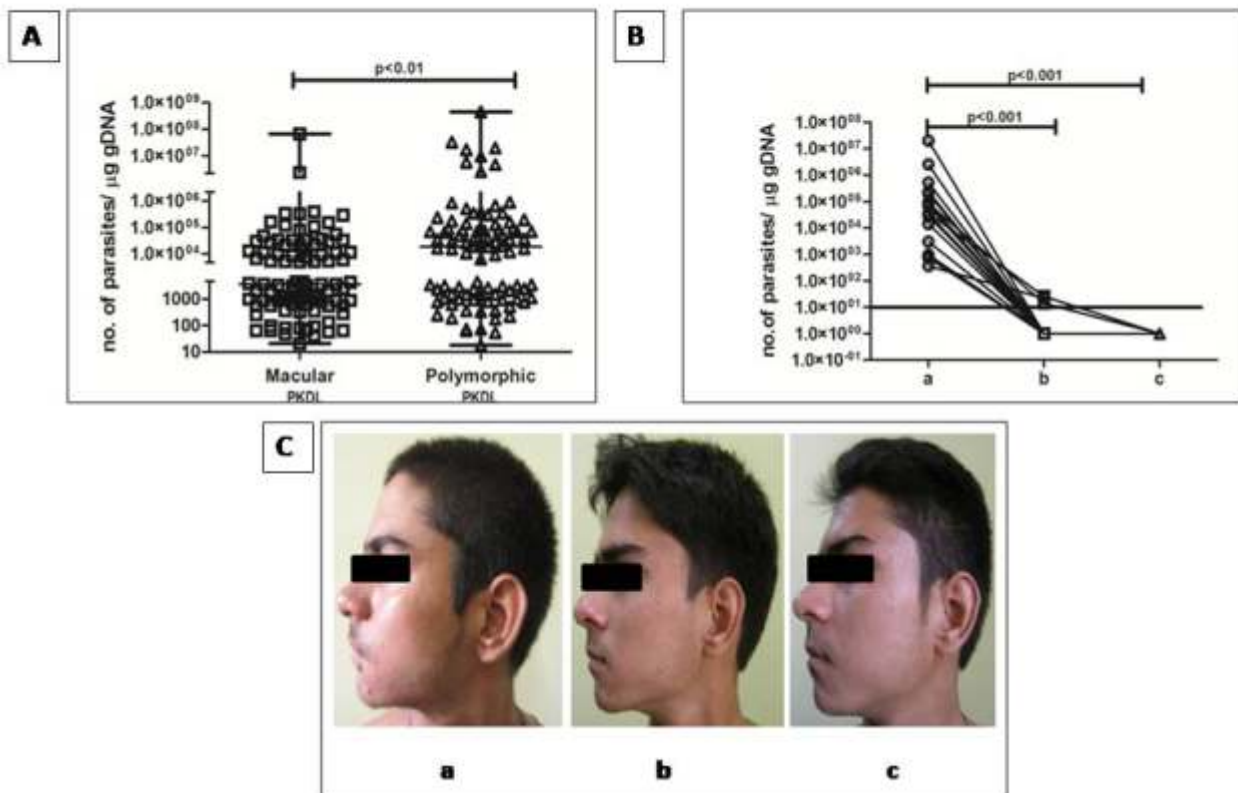


**Fig. 6: Status of parasite load in patients with PKDL**

**A:** Scatter plot showing the parasite load as median (range) in patients with PKDL on a lesional basis as macular (■, n=91) or polymorphic (▲, n=93).

**B:** Before after plots indicating the parasite load at disease presentation (●, n = 19, a), end of treatment with Miltefosine (■, n = 19, b) and six months later (▲, n = 6, c). The minimum detectable parasite number is indicated by a horizontal line.

**C:** Clinical features of a polymorphic PKDL case at disease presentation (a), following completion of treatment with Miltefosine (b), and six months later (c).

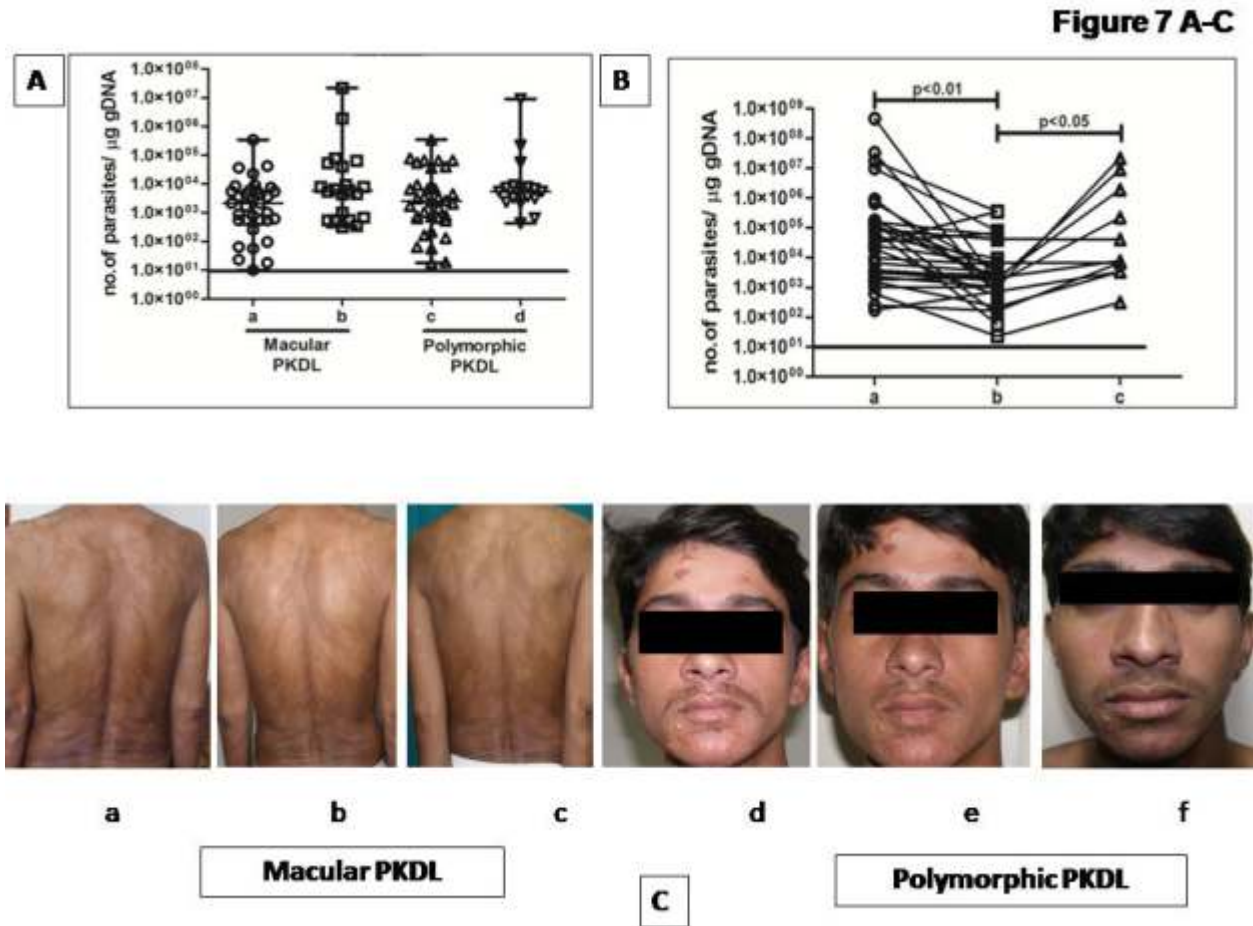


**Fig. 7: Effect of three-week treatment with LAmB on median parasite load, macular and polymorphic lesions profile**

**A:** Scatter plot indicating the median parasite load upon completion of three weeks treatment with LAmB presenting with macular lesions (●, n = 34, **a**) or polymorphic (▲, n = 36, **c**). They were again evaluated six months later and grouped based on their lesional profile, being macular (■, n= 21, **b**) or polymorphic (▼, n = 17, **d**). The minimum detectable parasite number is indicated by a horizontal line.

**B:** Before after plots indicating the parasite load at disease presentation (●, n = 31, **a**), end of treatment with LAmB (■, n = 31, **b**) and six months later (▲, n = 11, **c**). The minimum detectable parasite number is indicated by a horizontal line.

**C:** Representative clinical features of two PKDL patients, of macular and polymorphic variant at disease presentation (**a, d**), following completion of treatment with LAmB (**b, e**), and their evaluation six months later (**c, f**).

specific primers for minicircle kDNA; the number of parasites was extrapolated from the standard curve and final parasite load stated as the number/µg genomic DNA. The parasite number when <10 reported a C<sub>t</sub> value almost equivalent to NTC, and was accorded an arbitrary value of 1. Upon initial rK39 positivity, the ITS-1 PCR was performed and when positive

(n=184), the parasite burden was quantified by qPCR in macular (n=91) and polymorphic (n=93) PKDL. Their median (IQR) at disease presentation was 5229(896-50898). On examination on a lesional basis, the macular variant had a 5.1 fold lower parasite load as compared to the polymorphic cases being 3665 (615-21528) vs. 18620(1266-93934), p<0.01

(Fig. 6A).

Following ITS-1 PCR positivity, patients were randomly allocated to receive miltefosine or LAmB. Irrespective of the lesional variant, the repeat ITS-1 PCR at the end of treatment with miltefosine showed no product whereas following treatment with LAmB, a product was consistently obtained. Cases who returned at any time point six months later were examined, wherein patients who received miltefosine demonstrated no ITS-1 PCR product, while with LAmB, a product was always obtained.

In 19 cases that received miltefosine, the parasite load was serially monitored on completion of treatment and six months later. At presentation, their parasite load of 36500(963-197362) decreased significantly with treatment to 1(1-1),  $p < 0.001$  (Fig. 6B). Importantly, this decrease was sustained for at least six months as the parasite load remained negligible being 1(1-1),  $p < 0.001$  (Fig. 6B) and correlated with clinical features as total disappearance of dermal lesions was evident (Fig. 6C).

The story was less promising with LAmB, as there was a dramatic reduction in polymorphic cases, and less prominent in the macular variant (Fig. 7A). More importantly, in patients who reported six months later ( $n=38$ ), there was an alarming increase in the parasite load, both in macular and polymorphic cases (Fig. 7A). Additionally, the parasite burden was serially monitored in 31 patients who received LAmB. During active disease, the parasite load of 33257(3138-160727) decreased to 2128(731-9172),  $p < 0.01$  by 15.6 fold at the end of treatment (Fig. 7B). Eleven patients could be monitored six months later and all consistently showed a dramatic increase in their parasite load (Fig. 7B) and was reflected in persistence of their dermal lesions (Fig. 7C, a-f).

With considerable gains in our understanding of the nature and prevalence of NTDs, including leishmaniasis, especially with successes in improvement of chemotherapy

strategies and other health interventions (1), the NTDs continue to rank high among the world's greatest global health problems. Possibly a multipronged approach is necessary that should include improved drugs, sensitive diagnostic and monitoring tools along with vector control agents. This review has summarized some of the key challenges in translational science emphasizing on approaches to ensure success in our global efforts to eliminate leishmaniasis.

## References

1. Burza S, Croft SL, Boelaert M (2018). Leishmaniasis. *Lancet* **392**: 951-970.
2. World Health Organization (2005). Regional Technical Advisory Group on Kala-azar Elimination. Report of the first meeting, Manesar, Haryana, 20-23 December 2004. New Delhi: WHO Regional Office for South-East Asia.
3. Zijlstra EE, Alves F, Rijal S, Arana B, Alvar J (2017). Post-kala-azar dermal leishmaniasis in the Indian subcontinent: a threat to the South-East Asia Region Kala-azar Elimination Programme. *PLoS Negl Trop Dis* **11**: e0005877.
4. Mukhopadhyay D, Dalton JE, Kaye PM, Chatterjee M (2014). Post kala-azar dermal leishmaniasis: an unresolved mystery. *Trends Parasitol* **30**: 65-74.
5. Kaye P, Scott P (2011). Leishmaniasis: complexity at the host-pathogen interface. *Nat Rev Microbiol* **9**: 604-615.
6. Croft SL, Coombs GH (2003). Leishmaniasis current chemotherapy and recent advances in the search for novel drugs. *Trends Parasitol* **19**: 502-508.
7. Martinez FO, Helming L, Gordon S (2009). Alternative activation of macrophages: an immunologic functional perspective. *Annu Rev Immunol* **27**: 451-483.
8. Mukhopadhyay D, Mukherjee S, Roy S, *et al* (2015). M2 polarization of monocytes-macrophages is a hallmark of Indian post kala-azar dermal leishmaniasis. *PLoS Negl*

- Trop Dis* **9**:e0004145.
9. Gordon S (2003). Alternative activation of macrophages. *Nat Rev Immunol* **3**: 23-35.
  10. Sica A, Mantovani A (2012). Macrophage plasticity and polarization: in vivo veritas. *J Clin Invest* **122**: 787-795.
  11. Raes G, Van den Bergh R, De Baetselier P, *et al* (2005). Arginase-1 and Yml are markers for murine, but not human, alternatively activated myeloid cells. *J Immunol* **174**:6561.
  12. Martinez FO, Helming L, Milde R, *et al* (2013). Genetic programs expressed in resting and IL-4 alternatively activated mouse and human macrophages: similarities and differences. *Blood* **121**: e57-e69.
  13. Chatterjee M, Moulik S, Dey D, Mukhopadhyay D, Mukherjee S, Roy S (2018). Molecular regulation of macrophage class switching in Indian Post Kala-azar dermal Leishmaniasis (PKDL). In: Molecular Biology of Kinetoplastid Parasites. HK Majumder (ed). Caister Academic Press
  14. Ziegler-Heitbrock L, Ancuta P, Crowe S, *et al* (2010). Nomenclature of monocytes and dendritic cells in blood. *Blood* **116**: e74-e80.
  15. Griffin MD, Xing N, Kumar R (2003). Vitamin D and its analogs as regulators of immune activation and antigen presentation. *Annu Rev Nutr* **23**: 117-145.
  16. Ganguly S, Das NK, Panja M, *et al* (2008). Increased levels of IL-10 and IgG3 are hallmarks of Indian Post kala-azar dermal leishmaniasis. *J Infect Dis* **197**: 1762-1771.
  17. Ganguly S, Mukhopadhyay D, Das NK, *et al* (2010). Enhanced lesional Foxp3 expression and peripheral anergic lymphocytes indicate a role for regulatory T cells in Indian Post kala-azar dermal Leishmaniasis. *J Invest Dermatol* **130**:1013-1022.
  18. von Stebut E, Belkaid Y, Jakob T, *et al* (1998). Uptake of *Leishmania major* amastigotes results in activation and interleukin 12 release from murine skin derived dendritic cells: implications for the initiation of anti-Leishmania immunity. *J Exp Med* **188**: 1547-1552.
  19. Mukherjee S, Mukhopadhyay D, Braun C, *et al* (2015). Decreased presence of Langerhans cells is a critical determinant for Indian Post kala-azar dermal leishmaniasis. *Exp Dermatol* **24**: 232-234.
  20. Sundar S (2001). Drug resistance in Indian visceral Leishmaniasis. *Trop Med Int Health* **6**: 849-854.
  21. Sundar S, Jha TK, Thakur CP, Bhattacharya SK, Rai M (2002). Oral miltefosine for Indian visceral leishmaniasis. *N Engl J Med* **347**: 1739-1746.
  22. Sundar S, Chakravarty J, Agarwal D, Rai M, Murray HW (2010) Single-dose liposomal amphotericin B for visceral leishmaniasis in India. *N Engl J Med* **362**: 504- 512.
  23. World Health Organization (2004). Regional Strategic Framework for Elimination of Kala-azar from the South-East Asia Region (2005–2015). New Delhi: WHO Regional Office for South-East Asia.
  24. WHO (2007). Regional Technical Advisory Group on kala-azar elimination. Report of the Second Meeting, Kathmandu, Nepal, 20 October–2 November 2006. New Delhi: World Health Organization, Regional Office for South-East Asia. WHO Project: CCPCPC 050.
  25. Banjara MR, Gurung CK, Uranw S, Pandey K (2015). Internal Assessment of Visceral leishmaniasis Elimination Programme of Nepal. Public Health and Infectious Disease Research Center, Kathmandu, Nepal, 2015.

26. World Health Organization. Health Statistics (2015). [http://apps.who.int/iris/bitstream/10665/170250/1/9789240694439\\_eng.pdf?ua=1&ua=1](http://apps.who.int/iris/bitstream/10665/170250/1/9789240694439_eng.pdf?ua=1&ua=1)
27. Pandey BD, Pun SB, Kaneko O, Pandey K, Hirayama K (2011). Expansion of visceral leishmaniasis to the western hilly part of Nepal (Case report). *Am J Trop Med Hyg* **84**: 107-108.
28. Zijlstra EE, Musa AM, Khalil EA, el-Hassan IM, el-Hassan AM (2003). Post-kala-azar dermal leishmaniasis (Review). *Lancet Infect Dis* **3**:87-98.
29. Ganguly S, Das NK, Barbhuiya JN, Chatterjee M (2010). Post-kala-azar dermal leishmaniasis-an overview. *Int J Dermatol* **49**: 921-931.
30. Chappuis F, Sundar S, Hailu A, *et al* (2007). Visceral leishmaniasis: what are the needs for diagnosis, treatment and control? *Nat Rev Microbiol* **5**: 873-882.
31. Thakur CP (2016). Is elimination of kala-azar feasible by 2017? *Indian J Med Res* **144**: 799-802.
32. Moulik S, Chaudhuri SJ, Sardar B, *et al* (2018). Monitoring of parasite kinetics in Indian post kala azar dermal leishmaniasis. *Clin Inf Dis* **66**: 404-410.
33. Das NK, Singh SK, Ghosh S, *et al* (2011). Case series of misdiagnosis with rK39 strip test in Indian leishmaniasis. *Am J Trop Med Hyg* **84**: 688-691.
34. Ghosh S, Das NK, Mukherjee S, *et al* (2015). Inadequacy of 12-Week miltefosine treatment for Indian post-kala-azar dermal leishmaniasis. *Am J Trop Med Hyg* **93**: 767-769.

## **Instructions to Authors**

The Annals of the National Academy of Medical Sciences (India), appearing quarterly welcomes the submission of original contributions in all topics of biomedical sciences. Submission of a manuscript for publication in this journal implies that it has not been published and is not under consideration for publication elsewhere.

Review articles will be featured only by invitation. In the case of a multi-author submission, the contribution of each author must be clearly stated. The authors must declare conflict of interest, if any.

Three copies of the manuscript and a CD containing the manuscript complete with tables and figures should be submitted to: The Editor, Annals of the National Academy of Medical Sciences (India), NAMS House, Ansari Nagar, Mahatma Gandhi Marg, New Delhi-110 029.

### **Preparation of Manuscript**

Type the manuscript on one side of bond paper of standard A4 size with 2.5 cm margin all around in double spacing throughout, including the title page, text, acknowledgement, references, tables and legends for illustrations.

### **Title**

The title page should carry (1) the title of the article; (2) a short running title of not more than 10-12 words or 40 characters; (3) name of each author: first name, middle initial and surname; (4) name of the department(s) and institution(s) to which the work is attributed; (5) name and address of the author responsible for correspondence.

### **Text**

The second page should carry an abstract of not more than 150 words and should state the purpose of study, basic procedures, main findings and the principal conclusions. Below the Abstract three to ten keywords or short phrases that will assist indexers should be provided. The third page should begin with the main text which should usually, but not necessarily, be divided into sections with headings: Introduction, Methods, Results and Discussion. In Discussion, emphasis should be given to the new and important aspects of the study and conclusions. The data given in the Results should not be repeated. The Discussion should include the implications of the findings and their limitation and observations should be related to the other relevant studies. Conclusion(s) should be linked with the goals of the study but unqualified statements and conclusions not completely supported by the data should be avoided. At the end of the text under Acknowledgement(s), person(s) who have made substantial contribution(s) to the study may be acknowledged.

### **References**

References to literature cited should be numbered by arabic numerals in parenthesis in the text. At the end of the text on a new page the list of References by numbers as cited in the text should be provided. The style of the examples as given below should be used. The title of the journal(s) should be abbreviated according to the style used in Index Medicus and printed in its January issue each year. Some examples are given below:

## *Journals*

### *Standard journal article*

List all authors when six or less; when seven or more, list only first three and add *et al* after a comma, e.g.

Yan T, Chopp M, Ye X, *et al* (2012). Niaspan increases axonal remodeling after stroke in type 1 diabetes rats. *Neurobiol Dis* 46:157-164.

You CH, Lee KY, Chey WY, Menguy R (1980). Electrogastrographic study of patients with unexplained nausea, bloating and vomiting. *Gastroenterology* 78:311-314.

### *Corporate author*

The Royal Marsden Hospital Bone-Marrow Transplantation Team (1977). Failure of syngeneic bone-marrow graft without preconditioning in post hepatitis marrow aplasia. *Lancet* 2: 242-244.

### *No author given*

Anonymous (1981). Coffee drinking and cancer of the pancreas (Editorial). *Br Med J* 283: 628.

### *Books and Monographs*

#### *Personal author(s)*

Eisen HN (1974). *Immunology: An Introduction to Molecular and Cellular Principles of the Immune Response*, 5 edn. New York: Harper and Row, 406-416.

#### *Editor(s), compiler(s) as author*

Dausset J, Colombani J, eds. (1973). *Histo compatibility Testing 1972*. Copenhagen: Munksgaard, 12-18.

#### *Chapter in a book*

Weinstein L, Swartz MN (1974). Pathogenic properties of invading microorganisms. In: *Pathologic Physiology: Mechanisms of Disease*. Sodeman WA Jr, Sodeman WA, eds. Philadelphia: WB Saunders, 457-472.

Gutstein HB, Akil H (2001). Opioid analgesics. In: *Goodman and Gilman's The Pharmacological Basis of Therapeutics*, 10 edn. Hardman JG, Limbird LE, Goodman Gilman A, eds. New York: McGraw Hill, 569-619.

## **Legends for Illustrations**

Type legends for illustrations and Figures double spaced, starting on a separate page, with arabic numerals corresponding to the illustration. When symbols, arrows, numbers, or letters are used to identify parts of the illustration, identify and explain each one clearly in the legend. Explain internal scale and identify method of staining in photomicrographs.

*Reprints:* A maximum ten reprints of the article will be provided free of charge on request if there is only one author. If the article has two or more authors, maximum of twenty reprints will be provided on request free of charge. Request for further copies should be sent to the Editor, Annals of the NAMS (India).

Other details and information on online submission are available at : <http://annals-nams.in> at a link about the "Journal Section".

---

Printed and Published by Honorary Secretary, National Academy of Medical Sciences (India), New Delhi-110029.  
Tel. 011-26589289 & Printed at Kalakalp, 104, First Floor, Adeshwar Tower, Chopasni Road,  
Jodhpur - 342 003 Tel. : 0291-2640400, Mobile : 09414128128

**(Regd. No. R.N. 10690/65)**